



# LUND UNIVERSITY

## Application of Flamelet Chemistry Model to Vitiated Methane-Air Diffusion Flames

Tuovinen, Heimo

1992

[Link to publication](#)

*Citation for published version (APA):*

Tuovinen, H. (1992). *Application of Flamelet Chemistry Model to Vitiated Methane-Air Diffusion Flames*. (LUTVDG/TVBB--3065--SE; Vol. 3065). Department of Fire Safety Engineering and Systems Safety, Lund University.

*Total number of authors:*

1

**General rights**

Unless other specific re-use rights are stated the following general rights apply:

Copyright and moral rights for the publications made accessible in the public portal are retained by the authors and/or other copyright owners and it is a condition of accessing publications that users recognise and abide by the legal requirements associated with these rights.

- Users may download and print one copy of any publication from the public portal for the purpose of private study or research.
- You may not further distribute the material or use it for any profit-making activity or commercial gain
- You may freely distribute the URL identifying the publication in the public portal

Read more about Creative commons licenses: <https://creativecommons.org/licenses/>

**Take down policy**

If you believe that this document breaches copyright please contact us providing details, and we will remove access to the work immediately and investigate your claim.

LUND UNIVERSITY

PO Box 117  
221 00 Lund  
+46 46-222 00 00

**Lund University • Sweden**  
**Institute of Technology**  
**Department of Fire Safety Engineering**  
**ISSN 1102-8246**  
**ISRN LUTVDG/TVBB-3065-SE**

**Heimo Tuovinen**

**Application of Flamelet Chemistry Model  
to Vitiated Methane-Air Diffusion Flames**

**Lund, June 1992**



## **Abstract**

A laminar flamelet model has been used to calculate chemistry of methane-air flamelets in vitiated and non-vitiated environment.

The calculated results for temperature and stable species concentrations agree well with other models of the same kind. The present results also agree quite well with recent laboratory measurements of both laminar and turbulent diffusion flames. The largest discrepancy between measured and calculated results can be seen in CO-concentrations.



## Table of Contents

<b>Abstract . . . . .</b>	1
<b>1. Summary . . . . .</b>	3
<b>2. Introduction . . . . .</b>	5
<b>3. Flamelet model applied to turbulent diffusion flames . . . . .</b>	6
3.1 The conservation equations for turbulent diffusion flames . . . . .	6
3.2 Flamelet model and mixture fraction . . . . .	7
3.3 Determination of the statistical fluctuations in the mixture fraction . . . . .	11
3.4 The statistical properties of turbulent diffusion flame, PDFs of the mixture fraction . . . . .	14
3.5 The Beta function PDF . . . . .	15
3.6 The chemical model . . . . .	16
3.7 Transport properties . . . . .	19
3.7.1 Binary diffusion coefficient and the viscosity . . . . .	19
3.7.2 Multicomponent diffusion . . . . .	22
3.7.3 The heat flux . . . . .	25
3.7.4 Thermodynamic Properties . . . . .	27
<b>4. Solving of the differential equations . . . . .</b>	28
4.1 The SNECKS algorithm . . . . .	29
<b>5. The computer codes . . . . .</b>	31
5.1 The differences between the earlier version of SNECKS and the version with READCHKIN frontend . . . . .	31
5.2 Description of the READCHKIN - frontend and running advices . . . . .	31
5.3 Subprograms in READCHKIN . . . . .	34
5.3.1 Subroutines . . . . .	34
5.3.2 Functions . . . . .	35
<b>6. Results and discussions . . . . .</b>	36
6.1 Comparisons with other studies . . . . .	37
6.1.1 Comparison with theoretical models and Raman measurement . . . . .	37
6.1.2 Comparison with measurement in laminar and turbulent diffusion flames	39
6.2 Vitiated flamelets . . . . .	42
6.2.1 Temperature . . . . .	42
6.2.2 The stable species . . . . .	42
6.2.3 O <sub>2</sub> and H <sub>2</sub> concentrations . . . . .	43
6.2.4 Radicals . . . . .	43
6.2.5 The density, viscosity and enthalpy . . . . .	44
<b>7. Conclusions . . . . .</b>	45
<b>Nomenclature . . . . .</b>	46
<b>Acknowledgements . . . . .</b>	50
<b>Appendices</b>	54



# 1. Summary

This study presents theory and calculations with respect to methane-air flamelets in vitiated atmospheres. The laminar flamelet concept has been applied.

The present chemical model contains 13 elementary reaction steps involving 11 species. The chemical kinetics have been calculated using a modified SNECKS-code, which includes special codings for vitiation and a frontend package, READCHKIN.

The study gives a detailed mathematical background for the most relevant governing equations, such as equations for chemical source term and transport properties (molecular diffusion, heat transfer etc).

The computer code READCHKIN, which was coded in the present project, is described in detail.

The flamelet calculations were carried out for pure air and vitiated atmospheres. The vitiated environments included the dilution of oxidizer stream by main combustion products, CO<sub>2</sub> and H<sub>2</sub>O. Three different degrees of vitiation were treated to cover most configurations in turbulent flames in oxygen - poor environments: 20%, 40% and 60%. Both cold vitiation gas, 300 K, and hot gas, 1000 K, were used in computations.

The species concentrations, temperatures, viscosities, densities and enthalpies are given as a function of mixture fraction. These are shown in appendix E.

The results for non-vitiated flamelets have been compared with the latest results from other investigators.



## 2. Introduction

Most deaths in fires can be attributed to the poisonousness of carbon monoxide. Annually, fires in Sweden cause more than 100 deaths. About two thirds of the deaths are caused by CO. There is, therefore, a great need in fire research to understand the formation and spread of toxic products of combustion (such as CO) in fires.

The mechanism of formation of CO in fire is quite complicated and is largely dependent on fuel type, oxygen supply in surroundings, and how the fire develops. Many other factors such as fluid mechanics, heat transfer, turbulence, detailed reaction chemistry, etc also play a role.

To understand the formation of CO and other species in fires, one has to study the micro-structure of flames. Ignition, combustion and extinction occur in a real turbulent flame at the same time. In a given location these phenomena can have spatial separations of only a few millimeters. Locally the mixture can be diluted by complete or incomplete products of combustion, which can have considerable temperature variations. This influences the chemistry at that location. Thus at a given time, thousands of different states can exist at different points inside a large turbulent flame. These states at different locations in flames, interact with each other and contribute to the history of further development of the fire.

At some locations the chemistry can be treated as equilibrium chemistry, while at other locations the chemical reactions are far away from equilibrium. To predict the combustion in turbulent diffusion flames, the finite rate chemical kinetics must be modelled to account for the combustion efficiency, which varies considerably inside the same flame.

The present work is concerned with a special class of turbulent combustion, namely turbulent diffusion flames under influence of vitiation, i.e. fire gas recirculation. The laminar flamelet model is adopted. The modified version of Cranfield SNECKS-code (Solver for Non-Equilibrium Chemical-Kinetic Systems) is used to calculate the chemistry [1].

The model can be used with any flow field calculation model. It is used to some extent with the Fire Research Station's JASMINE-Code at Cranfield institute of Technology [2].



### 3. Flamelet model applied to turbulent diffusion flames

#### 3.1 The conservation equations for turbulent diffusion flames

The conservation equations for turbulent reacting flows are partial differential equations for conserving mass, momentum, energy and chemical species.

The overall continuity equation for conservation of mass is

$$\frac{\partial \rho}{\partial t} + \frac{\partial}{\partial x_j} (\rho u_j) = 0 \quad (1)$$

where  $t$  is time,  $\rho$  is mass density and  $u_j$  is the gas velocity component in  $x_j$ -direction in cartesian coordinate system.

The conservation of momentum is given by equation

$$\frac{\partial}{\partial t} (\rho u_j) + \frac{\partial}{\partial x_i} (\rho u_i u_j) = -\frac{\partial p}{\partial x_i} + \frac{\partial \tau_{ij}}{\partial x_j} \quad (2)$$

where  $p$  is the pressure of the gas and  $\tau_{ij}$  is the stress tensor defined as

$$\tau_{ij} = \left( \mu' - \frac{2}{3}\mu \right) \frac{\partial u_k}{\partial x_k} \delta_{ij} + \mu \left( \frac{\partial u_i}{\partial x_j} + \frac{\partial u_j}{\partial x_i} \right) \quad (3)$$

where  $\mu$  denotes the dynamic viscosity,  $\mu'$  the bulk viscosity of the fluid and  $\delta_{ij} = 1$  for  $i = j$ , and 0 for  $i \neq j$ . The terms on the left hand side of equation (2) are the increase in momentum and inertial forces. The first term on the right hand side is the pressure force and the second includes body forces and viscous forces.

The conservation of energy is given by the balance equation

$$\frac{\partial}{\partial t} (\rho h_i) + \frac{\partial}{\partial x_j} (\rho u_i h_i) = \frac{\partial p}{\partial t} + \frac{\partial}{\partial x_j} (u_i \tau_{ij} - q_j) \quad (4)$$

where the heat flux vector  $q_j$  is defined as minus the product of the heat conductivity  $\lambda$ , and the temperature gradient

$$q_j = -\lambda \frac{\partial T}{\partial x_j} \quad (5)$$

and the total enthalpy  $h_t$  is defined as

$$h_t = h + \frac{1}{2} u_i u_i \quad (6)$$

where  $h$  is the enthalpy per unit mass.

The first term on the left hand side of the equation of energy expresses the rate of accumulation of the internal and kinetic energy. The second term is the net rate of influx of the internal and kinetic energy by convection. The first term on the right hand side is the pressure work term. The last term can be divided into two parts: the dissipation of energy due to molecular friction and the transport of heat due to conduction.

The conservation of species is given by the equation

$$\frac{\partial Y_i}{\partial t} + u_i \frac{\partial Y_i}{\partial x_j} = \frac{\omega_i}{\rho} - \frac{\partial}{\partial x_j} (\rho Y_i V_i) / \rho \quad (7)$$

where  $Y_i$  is the mass fraction of species  $i$ ,  $\omega_i$  is the rate of production of species  $i$  by chemical reactions and  $V_i$  is the diffusion velocity of species  $i$ .

### 3.2 Flamelet model and mixture fraction

A first step in the modelling of the flamelet chemistry is to start from a laminar

diffusion flame, which provides unique relationships for chemical species, enthalpy, viscosity, temperature, soot concentration etc. in terms of a conserved scalar (mixture fraction) [3,4, 5]. A laminar diffusion flame also provides good opportunities for verifying these relationships by laboratory measurements, using, for example, a counterflow diffusion flame [6] or coflowing diffusion flame [1].

The next step is to assume that a turbulent flame consists of microscopic elements, which have the structure of an undisturbed laminar diffusion flame. The relationships for thermochemical variables (scalars) from a diffusion flame are then averaged for turbulent flames by using of an appropriate shape of the probability density function (PDF). The third step is to assume that chemical reactions are fast and occur mainly in these thin flamelets. These assumptions permit decoupling of the statistical uncertainties of a turbulent flow field from a complex multi-component reaction chemistry. As the reaction time is negligible compared to mixing time in turbulent flames, the instantaneous species concentration, thermochemical parameters and temperature are functions only of the conserved scalar [1]. Thus, the influence of turbulence is removed from the chemical reactions and the instantaneous local species concentrations and the temperature are directly related to the local value of the conserved scalar.

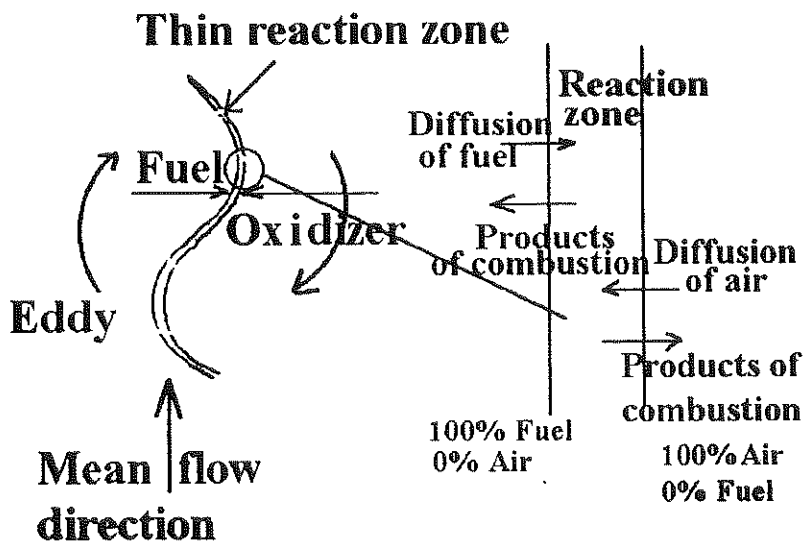


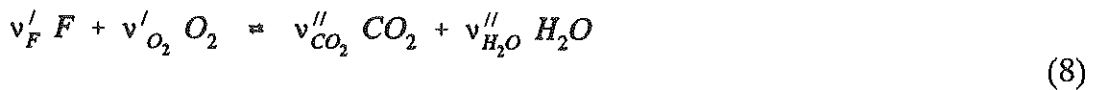
Figure 1. A sketch of a laminar flamelet travelling in a turbulent diffusion flame.

The oxidizer and fuel streams meet each other at the reaction zone. The mixing of the two streams is described by the mixture fraction  $\xi$ , so that  $\xi = 1$  for unmixed fuel stream and  $\xi = 0$  for unmixed oxidizer stream. Thus, the flamelet is bounded by mixture fraction values  $\xi = 0$  and  $\xi = 1$ . Between both streams the mixture fraction can have any value between 0 and 1.

In hydrocarbon-air diffusion flames there are four elements, which are conserved scalars, i.e. oxygen (O), hydrogen (H), carbon (C) and nitrogen (N) atoms. These can not be destroyed or created during combustion. Any of them can be used as a major parameter for describing the mixing of the two streams in a diffusion flame.

To illustrate the use of mixture fraction in characterizing mixing in diffusion flames, let us assume that the chemistry of any hydrocarbon can be described by a one-step overall reaction, and the entire reaction occurs at a reaction sheet as in a Burke-Schuman flame [6].

For a single-step overall chemical reaction, in which the hydrocarbon is directly converted to combustion products  $H_2O$  and  $CO_2$  according to the reaction formula:



where  $v'_\alpha$  and  $v''_\alpha$  are the stoichiometric coefficients of molecule  $\alpha$ , before and after the reaction respectively, the mixture fraction  $\xi$ , can be written as

$$\xi = \frac{v'_\alpha Y_F - Y_{O_2} + Y_{O_{2,2}}}{v'_\alpha Y_{F,1} + Y_{O_{2,2}}} \quad (9)$$

where the mass fraction of species  $\alpha$  is defined as the ratio of density of species  $\alpha$ ,  $\rho_\alpha$ , to the total mass density  $\rho$  of the mixture:

$$Y_\alpha = \frac{\rho_\alpha}{\rho} \quad (10)$$

The fuel is denoted by index F, indices 1 and 2 denote pure fuel and pure oxidizer streams and  $v_\alpha = v'_\alpha - v''_\alpha$  is the change of moles of species  $\alpha$  during the reaction. Because the flamelet is bounded between the mixture fractions  $\xi = 0$  and  $\xi = 1$ , there will always be some region in the flamelet where the mixture is stoichiometric. For a single-step reaction (8), the stoichiometric mixture fraction,  $\xi_{st}$  is given by

$$\xi_{st} = \left( 1 + \frac{v'_{O_2} M_{O_2} Y_{F,1}}{v'_F M_F Y_{O_{2,2}}} \right)^{-1} \quad (11)$$

where  $M_\alpha$  is the molecular weight of species  $\alpha$ . Sometimes one is interested in

expressing the mixture in terms of the equivalence ratio  $\phi$ , which is the ratio of the fuel to oxidizer ratio to the stoichiometric fuel to oxidizer ratio:

$$\phi = \frac{Y_F/F_{O_2}}{(Y_F/F_{O_2})_{st}} = \frac{\xi}{1-\xi} \cdot \frac{(1-\xi_{st})}{\xi_{st}} \quad (12)$$

The species-concentration profiles as a function of any hydrocarbon can have the shapes as plotted in figure 2.

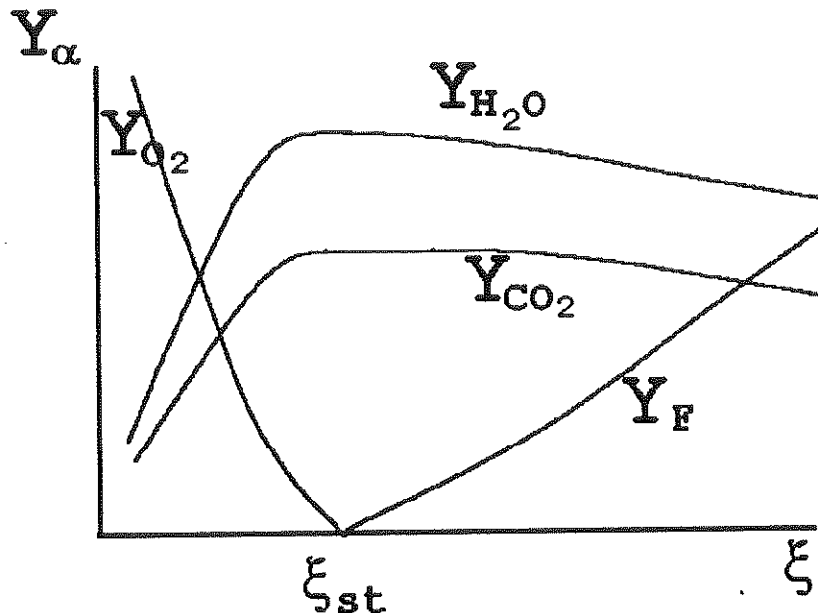


Figure 2. The species concentration  $Y_\alpha$ , as a function of mixture fraction for arbitrary hydrocarbon-oxidizer one-step chemical reaction

The adiabatic flame temperature as a function of mixture fraction can be obtained at the Burke-Schumann limit from equations:

$$T_b(\xi) = \begin{cases} T_u(\xi) + \frac{(-\Delta H)_{ref} Y_{F,1}}{c_p v'_F M_F} \xi; & \xi \leq \xi_{st} \\ T_u(\xi) + \frac{(-\Delta H)_{ref} Y_{O_2,2}}{c_p v'_{O_2} M_{O_2}} (1-\xi); & \xi > \xi_{st} \end{cases} \quad (13)$$

where  $(-\Delta H)_{ref}$  is the heat of combustion at reference atmospheric conditions, the indices b and u denote burned and unburned mixture respectively, and  $c_p$  is the heat capacititivity of air.

The unburned mixture temperature  $T_u(\xi)$ , which would give the "frozen" mixture temperature profile for pure mixing without chemical reactions, is related to the temperatures of originally unmixed fuel and oxidizer streams,  $T_F$  and  $T_{ox}$ , and mixture fraction through the linear expression of  $\xi$  [6]:

$$T_u(\xi) = T_{ox} + (T_F - T_{ox})\xi \quad (14)$$

The profile of the adiabatic flame temperature as a function of mixture fraction, at the Burke-Schumann limit, is plotted in figure 3 (eqs. (13)).

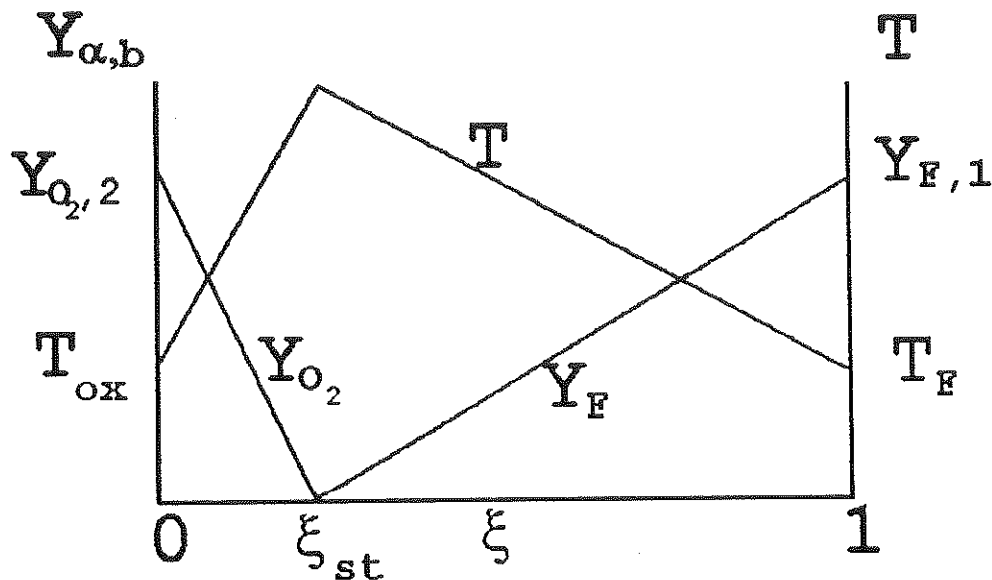


Figure 3. The adiabatic flame temperature  $T$  as a function of mixture fraction  $\xi$  for arbitrary hydrocarbon-oxidizer one-step chemical reaction.

### 3.3 Determination of the statistical fluctuations in the mixture fraction

A conserved scalar can not be created nor consumed, and hence has no chemical source term in its conservation equation. The balance equation for the mixture fraction as a conserved scalar can be written

$$\frac{\partial}{\partial t} (\rho \xi) + \frac{\partial}{\partial x_k} (\rho u_k \xi) = \frac{\partial}{\partial x_k} (\rho D \frac{\partial \xi}{\partial x_k}) \quad (15)$$

where  $u_k$  is the gas velocity in the  $x_k$ -direction in a Cartesian coordinate system,  $D$  is the mass diffusion coefficient and  $t$  is time.

The statistical fluctuation information for the mixture fraction is stored in the PDF, which depends on the Favre-averaged (mass weighted) first and second moments of the mixture fraction [2]. The modelled Favre-averaged mixture fraction  $\tilde{\xi}$ , the first moment of  $\xi$ , is obtained through solution of the Favre-averaged form of the balance equation, eq (15), given by Launder and Spalding [7]:

$$\frac{\partial}{\partial t} (\bar{\rho} \tilde{\xi}) + \frac{\partial}{\partial x_k} (\bar{\rho} \tilde{u}_k \tilde{\xi}) = \frac{\partial}{\partial x_k} \left\{ \left[ \frac{\mu_{lam}}{\sigma_{\xi lam}} + \frac{\mu_{tur}}{\sigma_{\xi tur}} \right] \frac{\partial \tilde{\xi}}{\partial x_k} \right\} \quad (16)$$

where

$\mu_{lam}$  and  $\mu_{tur}$  are laminar and turbulent viscosities, and  $\sigma_{\xi lam}$  and  $\sigma_{\xi tur}$  are the effective Prandtl/Schmidt numbers, respectively.

For stationary turbulent flow the first term in eq. (16) vanishes and for moderate to high Reynolds numbers

$$\left( \frac{\mu}{\sigma_{\xi}} \right)_{lam} \ll \left( \frac{\mu}{\sigma_{\xi}} \right)_{tur} \quad (17)$$

Thus, in turbulent flames, the laminar  $\mu/\sigma_{\xi}$  can be neglected and equation (16) can be simplified

$$\frac{\partial}{\partial x_k} (\bar{\rho} \tilde{u} \tilde{\xi}) = \frac{\partial}{\partial x_k} \left( \frac{\mu_{tur}}{\sigma_{\xi tur}} \frac{\partial \tilde{\xi}}{\partial x_k} \right) \quad (18)$$

Similarly, the Favre-averaged mixture fraction variance,  $\tilde{\xi}^{1/2}$ , the second moment of  $\xi$ , is obtained through solution of the balance equation:

$$\frac{\partial \bar{p} \tilde{\xi}^{1/2}}{\partial t} + \frac{\partial}{\partial x_k} (\bar{p} \tilde{u}_k \tilde{\xi}^{1/2}) = \frac{\partial}{\partial x_k} \left\{ \left[ \frac{\mu_{lam}}{\sigma_{\xi lam}} + \frac{\mu_{tur}}{\sigma_{\xi tur}} \right] \frac{\partial \tilde{\xi}^{1/2}}{\partial x_k} \right\} + c_{g1} \mu_i \left( \frac{\partial \tilde{\xi}}{\partial x_k} \right)^2 - c_{g2} \bar{p} \left( \frac{\tilde{\epsilon}}{\tilde{k}} \right) \tilde{\xi}^{1/2} \quad (19)$$

where  $\tilde{u}_k$  and  $\tilde{\xi}''$  are the Favre-averaged components of the velocity in  $x_k$ -direction and the mixture fraction fluctuation around its mean value, respectively.

The empirical constants  $c_{g1}$  and  $c_{g2}$  have values 2.8 and 2.0, respectively.  $\tilde{k}$  and  $\tilde{\epsilon}$  are the Favre-averaged turbulent kinetic energy and viscous dissipation terms, given by their balance equations.

$$\begin{aligned} \bar{p} \tilde{u}_k \frac{\partial k}{\partial x_k} &= \frac{\partial}{\partial x_k} \left\{ \left( \mu + \frac{\mu_{tur}}{\sigma_{k tur}} \right) \frac{\partial k}{\partial x_i} \right\} - \bar{p} \widetilde{u_i'' u_k''} \frac{\partial \tilde{u}_i}{\partial x_k} - \\ &- \frac{\mu_{tur}}{\bar{p}^2} \frac{\partial \bar{p}}{\partial x_i} \frac{\partial \bar{p}}{\partial x_i} - \bar{p} \epsilon \end{aligned} \quad (20)$$

$$\begin{aligned} \bar{p} \tilde{u}_k \frac{\partial \epsilon}{\partial x_k} &= \frac{\partial}{\partial x_k} \left\{ \left( \mu + \frac{\mu_{tur}}{\sigma_{\epsilon tur}} \right) \frac{\partial \epsilon}{\partial x_k} \right\} - \\ &c_{\epsilon 1} \frac{\epsilon}{k} \left( \bar{p} \widetilde{u_i'' u_k''} \frac{\partial \tilde{u}_i}{\partial x_k} + \frac{\mu_{tur}}{\bar{p}^2} \frac{\partial \bar{p}}{\partial x_i} \frac{\partial \bar{p}}{\partial x_i} \right) - c_{\epsilon 2} \bar{p} \frac{\epsilon^2}{k} \end{aligned} \quad (21)$$

where  $u_i''$  and  $u_k''$  are fluctuating parts of the velocities in  $x_i$ - and  $x_k$ -directions,  $\sigma_{k tur}$  and  $\sigma_{\epsilon tur}$  are turbulent Pandtl/Schmidt numbers for  $k$  and  $\epsilon$ ,  $\bar{p}$  is a conventional (Reynolds) mean value of pressure, and the emprical constants  $c_{\epsilon 1}$  and  $c_{\epsilon 2}$  have values 1.44 and 1.92, respectively.

### 3.4 The statistical properties of turbulent diffusion flame, PDFs of the mixture fraction

The probability density function of a mixture fraction is obtained from laboratory measurements of inert gas or fine particle concentration in the turbulent flow field [8]. There are not many results from measurements of mixture-fraction PDFs in turbulent reacting flows. The PDFs for temperature fluctuations have been measured in a wide range of non-reacting flows, e.g. jets, wakes, boundary layers etc [8]. The measured PDFs depend on the flow conditions. In reacting flows, the chemical heat release can have a large dependence on actual shapes of PDFs.

There are regions in the turbulent diffusion flame, which at some instants in time contain unmixed fuel and at other instants unmixed air. The PDF for such a region is simplest described by two Dirac delta functions, each at  $\xi = 0$  and  $\xi = 1$ .

For example, consider a large liquid-poolfire, where the rate of gasification of fuel, and air entrainment from the sides are high. At the position near the fire centre line and not far away from the fuel surface the flow consists of unmixed fuel, i.e. the PDF at this location can be represented by single  $\delta$ -function at  $\xi = 1$  in  $\xi$ -space. On the other hand, in the mixing layer region, where the air is entrained into the fire, the islands of unmixed air and unmixed fuel are travelling through a randomly chosen location. The PDF for a mixing layer, where concentration gradients between fuel and air regions are sharp, can be described as in figure 4.

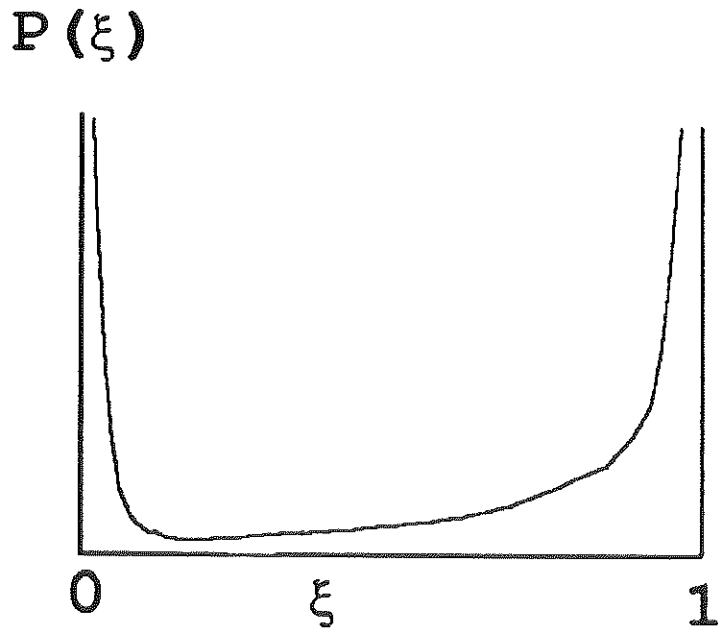


Figure 4. The possible shape of the probability density function (PDF) at mixing layer of a large diffusion flame.

Such a shape of a distribution function is easiest to describe using a so-called Beta-function [9]. It is quite cumbersome to treat mathematically, but the Beta-function seems to be the most realistic form of PDF to fit the wide range of statistical variations in turbulent flaming problems.

The other type of PDF is a clipped Gaussian distribution function. The physically unattainable tails of normal distribution are clipped and redistributed by Dirac delta functions.

There are several simpler forms of PDFs, e.g. triangular shape, combination triangular and delta function etc. Generally, there are no rules as to how the PDF should look, but it must fit the distribution of statistical variables at a given location.

### 3.5 The Beta function PDF

The Favre-averaged PDF of mixture fraction  $\tilde{P}(\xi)$  in the form of a Beta function can be written

$$\tilde{P}(\xi) = \frac{\xi^{\alpha-1} (1-\xi)^{\beta-1}}{\int_0^1 \xi^{\alpha-1} (1-\xi)^{\beta-1} d\xi} \quad (22)$$

where

$$\alpha = \tilde{\xi} \left\{ \frac{\tilde{\xi} (1-\tilde{\xi})}{\tilde{\xi}^{1/2}} - 1 \right\} \quad (23)$$

$$\beta = \frac{\alpha (1-\tilde{\xi})}{\tilde{\xi}} \quad (24)$$

The beta function is defined in the range (0,1). The integrals involved can readily be evaluated. When the Favre PDF of the mixture fraction  $\xi$  is known, the Favre mean of any scalar which depends on the mixture fraction can be obtained from the

integral:

$$\tilde{\phi} = \int_0^1 \phi(\xi) \tilde{P}(\xi) d\xi \quad (25)$$

and similarly the Favre variance of the scalar  $\tilde{\phi}^2$ , from

$$\tilde{\phi}^2 = \int_0^1 \phi^2(\xi) \tilde{P}(\xi) d\xi \quad (26)$$

The corresponding Reynolds (time averaged) mean quantities of the scalar's first two moments can then be evaluated if the instantaneous density  $\rho(\xi)$  is known

$$\bar{\phi} = \bar{\rho} \int_0^1 \frac{\phi(\xi)}{\rho(\xi)} \tilde{P}(\xi) d\xi \quad (27)$$

$$\bar{\phi}^2 = \bar{\rho} \int_0^1 \frac{\phi^2(\xi)}{\rho(\xi)} \tilde{P}(\xi) d\xi \quad (28)$$

### 3.6 The chemical model

The present chemical model for combustion of methane consists of 13 elementary reaction steps involving 11 species. The reaction scheme is shown in table A1 in Appendix A.

For multicomponent chemistry the reaction formula of form (8) can be generalized for a set of reversible chemical reactions



where  $\phi_i$  is a chemical symbol for species  $i$ ,  $v'_i$  and  $v''_i$  are stoichiometric coefficients of species  $i$  appearing as reactant and product respectively. Forward and backward reaction rates  $R_f$  and  $R_b$  are

$$R_f = k_f (\rho \sigma_m)^{\gamma_f} \prod_{i=1}^{NS} (\rho \sigma_i)^{v'_i} \quad (30a)$$

$$R_b = k_b (\rho \sigma_m)^{\gamma_b} \prod_{i=1}^{NS} (\rho \sigma_i)^{v''_i} \quad (30b)$$

where  $\sigma_m$  is the reciprocal of the mean molecular weight of the mixture, and  $\gamma_f$  and  $\gamma_b$  have values unity if the reactions occur on the third body, otherwise  $\gamma_f, \gamma_b = 0$ .

$\sigma_i$  is the number of species  $i$ ,  $k_f$  and  $k_b$  are the forward and backward rate constants respectively for the reaction according to Arrhenius expressions:

$$k_f = A_f T^{\beta_f} \exp\left(-\frac{E_f}{RT}\right) \quad (31a)$$

$$k_b = A_b T^{\beta_b} \exp\left(-\frac{E_b}{RT}\right) \quad (31b)$$

where  $E_f$  and  $E_b$  are the activation energies for forward and backward reactions, respectively,  $A_f$  and  $A_b$  are the Arrhenius preexponential factors, and  $\beta_f$  resp  $\beta_b$  the temperature exponents.

The quantities  $A_f T^{\beta_f}$  and  $A_b T^{\beta_b}$  represent the collision frequencies for forward and backward reactions. The exponential term is Boltzmann's factor. Thus the reaction rates are strongly dependent on the temperature and number of collisions per time unit.

The net changes of concentration of species  $\phi_i$  according to the reaction (29) can be calculated from equation:

$$\frac{dC_{\phi_i}}{dt} = (v''_i - v'_i) k_f \prod_{j=1}^N C_{\phi_j}^{v'_j} + (v'_i - v''_i) k_b \prod_{j=1}^N C_{\phi_j}^{v''_j} \quad (32)$$

At the equilibrium  $\frac{dC_{\phi_i}}{dt} = 0$

which defines the equilibrium constant  $K_c$

$$K_c = \frac{k_f}{k_b} = \prod_{j=1}^N (C_{\phi_{j,s}})^{(v_j'' - v_j')} \quad (33)$$

For conservation of chemical species, the chemical kinetic source term for species  $\phi_i$  in the reaction scheme (29), consisting of M elementary reaction steps involving N total number of chemical species, can be written

$$\omega_i = - \sum_{j=1}^M (v'_{ij} - v''_{ij}) (R_{fj} - R_{bj}) \quad i = 1, \dots, N \quad (34)$$

By using equations (30), (31), the ideal gas equation of state

$$p = \rho RT \sum_{i=1}^N \left( \frac{Y_i}{W_i} \right) \quad (35)$$

and the identity

$$X_i = \frac{(Y_i/W_i)}{\sum_{j=1}^N (Y_j/W_j)} \quad i = 1, \dots, N \quad (36)$$

the production of chemical species i (i.e. eq. (34)) can be written

$$\begin{aligned} \omega_i &= W_i \sum_{k=1}^M (v''_{ik} - v'_{ik}) B_k T^{\alpha_k} e^{-(E_k/RT)} \\ &\cdot \sum_{j=1}^N \left( \frac{x_j p}{RT} \right)^{v'_{jk}}; \quad i = 1, \dots, N \end{aligned} \quad (37)$$

where  $W_i$  is the molecular weight of molecule i,  $B_k$ ,  $\alpha_k$  and  $E_k$  are the Arrhenius preexponential factor, temperature exponent and activation energy respectively, for the k:th reaction.

### 3.7 Transport properties

The species transport properties are calculated from Chapman-Enskog expressions by using the Lennard-Jones parameters [1]. The Chapman-Enskog method is based on the three basic assumptions:

- a) molecular collisions are binary collisions
- b) translational energy is treated using classical mechanics
- c) spatial gradients of the macroscopic or continuum properties of the gas are assumed to be small.

The method proceeds from a series expansion of the velocity distribution function about the Maxwellian distribution in order to obtain explicit expressions for the transport vector in terms of the gradients of the dependent variables of fluid dynamics from the Boltzmann equation [6]. The result is a set of Navier-Stokes equations, which is applicable for large deviations from the equilibrium.

The Chapman-Enskog conditions a)-c) above, are best satisfied by monoatomic molecules. The flames easily satisfy this requirement except at very high pressures.

In order to be applicable to gases of polyatomic molecules the diffusional flux of internal energy and inelastic collisions must be taken into account. For each internal quantum state a separate distribution function must be defined in such case [10, 11, 12].

#### 3.7.1 Binary diffusion coefficient and the viscosity

Assuming the molecules  $i$  and  $j$  to be hard spheres having the radii  $r_i$  and  $r_j$ , the collision cross section  $\sigma_{ij}$ , is given by

$$\sigma_{ij} = \pi(r_i + r_j)^2 \quad (38)$$

which is illustrated in figure 5.

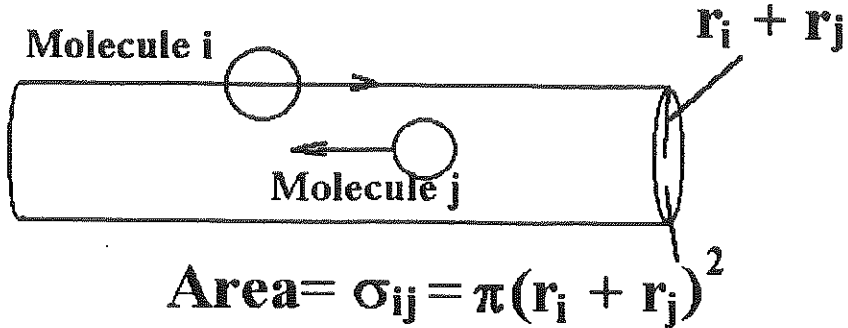


Figure 5. The definition of the collision cross section of two molecules approximated as hard spheres with radii  $r_i$  and  $r_j$ .

If the relative average velocity of molecules  $i$  and  $j$  is expressed as  $v_{ij}$ , then the individual molecule  $i$  will sweep through a volume  $\sigma_{ij} v_{ij}$  per unit time relative to the molecule  $j$ . The average number of molecules  $j$  in the volume  $\sigma_{ij} v_{ij}$  will be  $n_j$ . Then the average number of collisions of a molecule of type  $i$  with a molecule of type  $j$  will be  $n_j \sigma_{ij} v_{ij}$  per unit time. Because there are  $n_i$  molecules of type  $i$  inside this volume per unit time, the total number of collisions between molecules  $i$  and  $j$ , per unit time will be

$$v_{ij} = n_i n_j \sigma_{ij} v_{ij} \quad (39)$$

Expressed in the terms of molecular fraction of species  $i$  and  $j$

$$v_{ij} = n^2 X_i X_j \sigma_{ij} v_{ij} \quad (40)$$

where  $X_i$  and  $X_j$  are the molecule fractions of molecules  $i$  and  $j$ , respectively.

At equilibrium the relative average velocity of molecules  $i$  and  $j$  is given by the Maxwellian distribution of velocities

$$v_{ij} = \left\{ \frac{8k T}{\pi m_{ij}} \right\}^{1/2} \quad (41)$$

where  $k$  is the Boltzmann constant,  $T$  the temperature and  $m_{ij}$  is reduced mass for

collision of molecules i and j, defined as

$$m_{ij} = \frac{m_i m_j}{m_i + m_j} \quad (42)$$

The kinetic theory of gases has been utilized to derive equation (41).

The binary diffusion coefficient  $D_{ij}$  for the mixture of molecules i and j is defined [13]:

$$D_{ij} = \frac{X_i X_j p}{m_{ij} v_{ij}} \quad (43)$$

where p is the pressure.

By using equations (41) and (42), and the ideal gas law,  $p = nkT$ , the equation (43) can be written

$$D_{ij} = \frac{1}{\sigma_{ij} p} \left( \frac{\pi}{8 m_{ij}} \right)^{1/2} (kT)^{3/2} \quad (44)$$

Thus the binary diffusion coefficient is proportional to  $T^{3/2}/p$  when molecules are assumed to be hard spheres. For typical molecules the value of the temperature exponent lies between 3/2 and 2. In flames, the value 3/2 is reasonable. By expressing the reduced mass for collision in molecular weights of species i and j, and using the expression for the collision integral, the binary diffusion expression for  $D_{ij}$  becomes [1, 6]:

$$D_{ij} = \frac{1.86 \cdot 10^{-7} \left( \frac{W_i + W_j}{W_i W_j} \right)^{1/2} T^{3/2}}{p \sigma_{ij}^2 \Omega_{D_{ij}}^{(1,1)*}} \quad (45)$$

where  $W_i$  and  $W_j$  are molecular weights of species i and j, respectively and  $\Omega_{D_{ij}}^{(1,1)*}$  is the mass diffusivity collision integral.

The viscosities for individual species, except  $H_2O$ , are given as [1]:

$$\mu_j = \frac{2.6693 \cdot 10^{-6} (W_j T)^{1/2}}{\sigma_{ij}^2 \Omega_{\mu_j}^{(2,2)*}} \quad j \neq H_2O \quad (46)$$

where  $\Omega_{\mu_j}^{(2,2)*}$  is the thermal conductivity collision integral. The viscosity of  $H_2O$  is given by [1]:

$$\mu_{H_2O} = \begin{cases} \frac{2.5639 T^{1/2}}{1 + \frac{1371}{T} \cdot 10^{-37.4/T}} \times 10^{-6}; & T \leq 1300K \\ \frac{1.498 T^{1/2}}{1 + \frac{24.51}{T^2}} \times 10^{-6}; & T > 1300K \end{cases} \quad (47)$$

Both  $\Omega_{D_{ij}}^{(1,1)*}$  and  $\Omega_{\mu_j}^{(2,2)*}$  are functions of  $kT/\epsilon_{ij}$ . The quantity  $\epsilon_{ij}/k_{LJ}$  is the Lennard-Jones constant (unit = K). These are tabulated in appendix B for some of the species included in the study.

### 3.7.2 Multicomponent diffusion

The Chapman-Enskog expressions can be generalized for multicomponent diffusion [13]. The diffusion is driven by concentration gradients, pressure gradients, temperature gradients and external forces. The diffusion velocity  $\vec{V}_i$  for species i in a multicomponent mixture is given by the expression

$$\begin{aligned} \vec{V}_i = & \sum_j \frac{\tilde{D}_{ij}}{X_i X_j} Y_j (\nabla X_j + (X_j - Y_j) \frac{1}{p} \nabla p + \\ & + Y_i \frac{\rho}{p} (\vec{F} - \vec{F}_p)) - \frac{1}{\rho Y_i} D_{Ti} \frac{1}{T} \nabla T \end{aligned} \quad (48)$$

where  $\tilde{D}_{ij}$  are multicomponent diffusion coefficients and  $D_{Ti}$  is the multicomponent

thermal diffusion coefficient,  $\nabla p$  and  $\nabla T$  are the pressure and temperature gradients, respectively,  $\vec{F}$  is the total external force per unit mass of the mixture and  $\vec{F}_i$  the external force per unit mass on species i.

The last term, the temperature gradient effect, in equation (48) is small in most cases, so that it can be neglected. The quantity  $(1/p)\nabla p$  is also often negligible even though  $\nabla p$  may be large in flames. Diffusion due to concentration gradient is most pronounced for species with molecular masses differing from the mean molecular mass. The hydrogen molecule  $H_2$  having very low molecular mass diffuses very fast. That is the reason for difficulties in predicting  $H_2$ -concentration profiles across the flamelet.

In Stefan-Maxwell's modification of the Chapman-Enskog solution method diffusion is given by binary diffusion coefficients rather than multicomponent diffusion coefficients. The expression for the concentration gradient of species i by Stefan-Maxwell formulation is given by the equation:

$$\begin{aligned} \nabla X_i = & \sum_j \frac{X_i X_j}{D_{ij}} (\vec{V}_j - \vec{V}_i) + (Y_i - X_i) \frac{1}{p} \nabla p + \\ & + \frac{\rho}{p} \sum_j Y_i Y_j (\vec{F}_i - \vec{F}_j) + \\ & + \sum_j \left\{ \frac{X_i X_j}{\rho D_{ij}} \left( \frac{D_{Tj}}{Y_j} - \frac{D_{Ti}}{Y_i} \right) \right\} \frac{1}{T} \nabla T \end{aligned} \quad (49)$$

The ratio  $\nabla p/p$  and thermal diffusion (the Soret effect) are negligible and the body forces are nearly equal for all species in fires. The concentration gradient of species i can therefore be simplified to

$$\nabla X_i = \sum_j \frac{X_i X_j}{D_{ij}} (\vec{V}_j - \vec{V}_i) \quad (50)$$

Equation (50) is called the Stefan-Maxwell equation.

It is easy to derive Fick's law of diffusion starting from equation (50). For the sake of simplicity consider a two component mixture of species 1 and 2. Equation (50) becomes

$$\nabla X_1 = \frac{v_{12} m_{12}}{p} (\vec{V}_2 - \vec{V}_1) \quad (51)$$

where  $v_{12}$  is the collision frequency and  $m_{12}$  the reduced mass for collision of species 1 and 2 defined as in equation (42). The mole fraction of species 1 in the mixture can be expressed as the numbers of moles of species 1 and 2

$$X_1 = \frac{n_1}{n_1 + n_2} \quad (52)$$

where  $n_1$  and  $n_2$  are the numbers of moles of species 1 and 2. Expressed in terms of the molecular masses and the mass fractions of both species,  $n_1 = Y_1/m_1$  and  $n_2 = Y_2/m_2$ , respectively

$$X_1 = \frac{m_2 Y_1}{m_1 + (m_2 - m_1) Y_1} \quad (53)$$

and

$$\nabla X_1 = \frac{m_1 m_2}{(m_2 Y_1 + m_1 Y_2)^2} \nabla Y_1 \quad (54)$$

In equation (51)  $\vec{V}_2$  on the right hand side can be expressed in terms of  $\vec{V}_1$ , and by considering elastic collisions between molecules, so that the law of conservation of momentum can be written

$$Y_1 \vec{V}_1 + Y_2 \vec{V}_2 = 0 \quad (55)$$

and the sum of mass fractions of species equals unity

$$Y_1 + Y_2 = 1, \quad (56)$$

then the difference

$$\vec{V}_2 - \vec{V}_1 = - \left\{ \frac{Y_1}{Y_2} + 1 \right\} \vec{V}_1 = - \frac{1}{Y} \vec{V}_1 \quad (57)$$

Inserting equations (55) - (57) into equation (51) gives

$$\frac{m_1 m_2}{(m_2 Y_1 + m_1 Y_2)^2} \nabla Y_1 = - \frac{v_{12} m_{12}}{p} \frac{1}{Y_2} \vec{V}_1 \quad (58)$$

from which the Fick's law of diffusion is obtained for two-component mixture

$$Y_1 \vec{V}_1 = -D_{12} \nabla Y_1 \quad (59)$$

where

$$D_{12} = \frac{X_1 X_2 p}{m_{12} v_{12}} \quad (60)$$

The expression for Fick's law for a multicomponent mixture is obtained by generalisation of the above derivation (eqs (51) - (60)).

### 3.7.3 The heat flux

The expression for heat flux  $\vec{q}$ , in the form of the Stefan-Maxwell formulation of the Chapman-Enskog procedure is [13]

$$\vec{q} = -\lambda \nabla T + \rho \sum_i h_i Y_i \vec{V}_i + kT \sum_i \sum_j \left\{ \frac{X_j D_{Tl}}{m_l D_{ij}} \right\} (\vec{V}_i - \vec{V}_j) \quad (61)$$

The first term on the right hand side is the heat flux due to thermal conduction, whose driving force is the temperature gradient  $\nabla T$ . The heat conductivity  $\lambda$ , in binary and multicomponent gas mixtures is more complicated than in solids. In so-called Eucken formulae [6, 10, 13, 14] the detailed gas kinetics are used to express the heat conductivity of gases, thus taking into account the energy contained in internal degrees of freedom of molecules:

$$\lambda = \frac{\mu c_v (9\gamma - 5)}{4} \quad (62)$$

where  $\mu$  is the shear viscosity of gas and  $\gamma$  is the ratio of specific heats of gas at constant pressure and constant volume  $c_p/c_v$ . However, the empirical expressions for  $\lambda$  are recommended for both binary and ternary mixtures, due to uncertainties of internal energy in eq (62) [6].

The second term on the right hand side of equation (61) arises because  $\vec{q}$  has been defined as the energy flow relative to the mass-averaged velocity. The enthalpy  $h_i$  for species  $i$ , given in gas kinetics formulation by taking into account the internal degrees of freedom of the molecules, can be expressed

$$h_i = \frac{1}{m_i} \frac{5}{2} kT + u_i \quad (63)$$

where  $u_i$  is the average energy in internal degrees of freedom per unit mass of specie  $i$ .

The third term in the equation (61) is known as the so-called Dufour effect. This describes how the diffusion of species through the mixture can lead to a temperature gradient and to a flow of energy [13].

### 3.7.4 Thermodynamic Properties

For calculating heat capacities and enthalpies of species, the polynomial fit for temperature is used. The polynomial coefficients are stored in a data base. There are 14 coefficients for each species stored in the data base: seven coefficients for the temperature range 300 K to 1000 K and seven for the temperature range 1000 K to 5000 K. Five first coefficients for each range are used to fit the expression for heat capacity,  $c_{pk}$  for species k.

$$\frac{c_{pk}}{R} = \sum_{n=1}^5 a_{nk} T^{(n-1)} \quad (64)$$

where  $a_{nk}$  are coefficients for polynomial fit in the thermodynamical data base. Similarly the enthalpies  $h_k$  for individual species are fitted by using six coefficients from each range

$$\frac{h_k}{RT} = \sum_{n=1}^5 \frac{a_{nk} T^{(n-1)}}{n} + \frac{a_{6k}}{T} \quad (65)$$

The form of the data base is shown in appendix B.

## 4. Solving of the differential equations

The governing set of differential equations consists of one-dimensional unsteady, parabolic differential equations of the form [1]:

$$\frac{\partial \phi}{\partial t} = \frac{\partial}{\partial \psi} \left( \rho \Gamma_\phi \frac{\partial \phi}{\partial \psi} \right) + \frac{S_\phi}{\rho} \quad (66)$$

where  $\phi$  is a symbol for any atomic element or enthalpy,  $\Gamma_\phi$  is a transport coefficient,  $S_\phi$  is the source term (for chemical species same as in  $\omega_i$  in eq. (34)), and  $\psi$  is a stream function.

The set of the above differential equations is reduced to a set of algebraic equations by using finite difference technique. The calculations are performed by using a staggered finite-difference grid (Patankar-Spalding) [1,15], which is shown in fig (6).

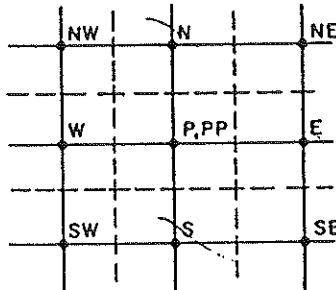


Figure 6. Conventional staggered finite-difference grid for calculation within a flow domain. Points H ("high") and L ("low") are above and below the plane of E-W-N-S-P. PP refers to conditions at P at the previous time step. [15]

The value of a dependent variable at each node in such grid is related to the values at neighbouring nodes. In this special grid the lines represent a constant time, which intersect the lines of constant nondimensional stream function.

The equation (66) integrated with respect to  $\phi$  over an appropriate control volume gives

$$D_t \phi_{i,D} = A_i \phi_{i+1,D} + B_i \phi_{i-1,D} + C_i + \frac{S_{\phi i}}{\rho} \left( \omega_{i+\frac{1}{2}} - \omega_{i-\frac{1}{2}} \right) \delta \quad (67)$$

where  $\phi_{i,D}$  is a value of a dependent variable at a "late" time node  $i$ , indices  $i+1$  and  $i-1$  denote the nodes  $i+1$  and  $i-1$ , respectively. The coefficients  $A_i$ ,  $B_i$ ,  $C_i$  and  $D_i$  contain the effect of diffusion and stretch,  $\omega$  is the non-dimensional stream function between 0 and 1.

The equations in the present model are solved by a code called SNECKS. SNECKS is an efficient procedure which is suitable for solving problems associated with chemically reacting flows. SNECKS is a modified version of CREK, Combustion Reaction Equilibrium and Kinetics [1,15]. The solution for chemical species is determined simultaneously point-by-point and coupled with temperature through some form of energy equation. The rapid convergence is achieved by using derivative information, which implies if local variation in the species concentrations or the temperatures are large. The solution procedure is as follows [1]:

- Set up the initial conditions.
- Assign the boundary conditions, planes of symmetry.
- Store the species values for the last time step.
- Point-by-point iteration.
- Solve a set of Newton-Raphson correction equations simultaneously and iteratively at the grid node until correction variables equal the pre-set values.
- Compute the local temperature and density.
- Compute the cross-section distance which varies in the presence of stretch.
- Calculate cross-stream profiles.
- Advance in time until a specified eddy time is reached.

#### 4.1 The SNECKS algorithm

Equation (67) written in the functional form is [1]

$$f_\phi = D_i(\phi_i - \phi_i^*) - \frac{S_{\phi i}}{\rho} (\omega_{i+\frac{1}{2}} - \omega_{i-\frac{1}{2}}) \delta t \quad (68)$$

where  $f_\phi$  is a Newton-Raphson function of species or enthalpy, and

$$\phi_i^* = \frac{A_i}{D_i} \phi_{i+1} + \frac{B_i}{D_i} \phi_{i-1} + \frac{C_i}{D_i} \quad (69)$$

The coefficients  $C_i$  and  $D_i$  do not include any contribution from the chemical source term  $S_{\phi i}$ , which may be highly nonlinear form. The species Newton-Raphson

correction equation set can be written

$$\sum_{k=1}^M \left( \frac{\partial f_{\phi_i}}{\partial \phi_k} \right) \Delta \log \phi_k = -f_{\phi_i} \quad i=1, \dots, M \quad (70)$$

which is solved by pivotal Gaussian elimination technique iteratively for all species until pre-set values of  $\Delta \log \phi_i$  are reached. The temperature is solved using a similar equation to (70). The computed new values of the dependent variables are

$$\log \phi_i^{(k+1)} = \log \phi_i^{(k)} + \eta (\Delta \log \phi_i)^{(k)} \quad (71)$$

where  $\eta$  is the under-relaxation or acceleration parameter, defined at each iteration step as [1]:

$$\eta = \min(1, \eta_1, \eta_2)$$

where

$\eta_1, \eta_2$  are defined for T,  $\sigma_n$  and species by

$$\frac{2}{\max \left\{ |\Delta \log T|, |\Delta \log \sigma_m|, |\Delta \log \sigma_i| \right\}}; \quad \frac{\sigma_j}{\sigma_m} > 10^{-8}; \quad \Delta \log \sigma_j > 0 \quad (72)$$

$$\eta_2 = \frac{\log(10^{-4}) - \log(\frac{\sigma_i}{\sigma_m})}{\Delta \log \sigma_i \cdot \Delta \log \sigma_m}; \quad \frac{\sigma_i}{\sigma_m} < 10^{-8}; \quad \Delta \log \sigma_i > 0 \quad (73)$$

For further details see ref [1].



## **5. The computer codes**

In the present work, a computer code, SNECKS, programmed by S.K. Liew at Cranfield Institute of Technology in the UK [1] has been used to calculate flamelet chemistry. The SNECKS - code is a derivative of CREK, originally coded as an interface program for GENMIX [15]. SNECKS has been modified by the users at Cranfield Institute of Technology, where it has been used since 1985 in combustion studies. The author of this report made the latest extension of the code in 1991 at Cranfield Institute of Technology by coding an interface program READCHKIN. READCHKIN makes it easier to run SNECKS, because this program reads most of the data automatically from databases. In the earlier version the user must type appropriate values into the code, which can be tiresome if the reaction scheme or fuel is to be changed.

### **5.1 The differences between the earlier version of SNECKS and the version with READCHKIN frontend**

The user's input to the earlier version of SNECKS goes via editing of FORTRAN-DATA lines. These are initial values of physical parameters, constants and coefficients for thermodynamic properties, Lennard-Jones parameters, species molecular weights, number of atoms of different kinds in molecules, Arrhenius parameters for chemical kinetics etc.

In the recent version with the READCHKIN frontend the input of thermodynamic properties, chemical kinetic parameters, Lennard-Jones parameters, chemical reaction formulas and atomic weights are read automatically from data bases. Only a few parameters need to be edited when running SNECKS by the latest version of READCHKIN in connection with, for example, changing initial values such as grid parameters, number of steps, step length etc. READCHKIN also echoes the read input files and, writes some information and error messages to output file.

### **5.2 Description of the READCHKIN - frontend and running advices**

Two source codes SNECKS.FOR and READCHKIN.FOR are needed to run the current version of SNECKS. In the present work the codes were tested for methane and it is easy to change to other fuels. The following files must be in the user's directory when running the code:

READCHKIN.FOR  
SNE\_IN.DAT  
SNE\_OUT.DAT  
ATOMIC\_W.DAT  
NASACHON.DAT  
LENNARD\_JONES.DAT

READCHKIN.FOR and SNECKS.FOR must be compiled and linked. The easiest way of running this version of SNECKS is to use a command procedure, SNEC.COM (if a VAX-computer is used), which compiles, links and runs the codes. A coding of SNEC.COM which was used in current work at Cranfield Institute of Technology is shown in Appendix C.

To make running as easy as possible, all input to READCHKIN goes through input files (ASCII-format): SNE\_IN.DAT, ATOMIC\_W.DAT, NASACHON.DAT and LENNARD\_JONES.DAT.

SNE\_IN.DAT contains the chemical model, i.e. elements, species, reaction formulas and Arrhenius parameters for reaction rates. ATOMIC\_W.DAT contains the atomic weights of all atoms. The collision coefficients and Lennard-Jones parameters for the 16 species of interest in the present study are written in LENNARD\_JONES.DAT. The parameters for additional species are easy to write in the file when needed. The thermodynamic data base NASACHON.DAT contains 14 coefficients, (7 for low temperature range (300-1000 K) and 7 for high temperature range (1000 - 5000 K)) for calculating individual heat capacities and enthalpies for species according to equations (64) and (65). The structures of all input files are shown in Appendix B.

READCHKIN creates one output file, SNE\_OUT.DAT where all data read from SNE\_IN.DAT are echoed and the results from any calculation (e.g. molecular weights) are written. If READCHKIN encounters any errors in the input files, warnings are written in the SNE\_OUT.DAT-file. During an interactive run the warnings are also written to the terminal, so that the user can take immediate action. The file structure of SNE\_OUT.DAT is shown in Appendix D.

The different chemical models can be stored in separate files, which should be renamed to SNE\_IN.DAT before running the code. The user can write comments in the chemical model files by inserting them between (. and .). Comments and blank lines can be removed by running COM\_Rem (the COM\_Rem was originally coded by Göran Olson at the Institute of Atomic Physics, University of Lund), which is then ready to use by READCHKIN. It is recommended that a single file contains

a database of all possible reactions which are inserted as comments as described above. Specific cases can then be run by uncommenting the appropriate reactions. The preprocessor COM\_Rem extracts the selected mechanism and writes it into SNE\_IN.DAT.

In SNE\_IN.DAT the symbols of elements (atoms) are listed on lines between texts ELEMENTS and END; for example:

ELEMENTS

N

C

H

O

END

When READCHKIN encounters the word ELEMENTS, the reading of elements from the following line starts and will continue until the word END is encountered. Similarly the species and reactions are read from SNE\_IN.DAT after the words SPECIES and REACTIONS, respectively, are read and the reading is terminated when END is read.

The chemical element symbols are recognized as their universal symbols. The first letter must always be an upper-case letter and for two-letter symbols the second character must be a lower-case letter, e.g. Al, Cl, Ca (not AL, CL, CA).

In the current version, species symbols are restricted to 12 characters. Brackets are not allowed in the species formula. For example,  $\text{Cl}_2\text{C}(\text{NO}_2)_2$  (dichlorodinitromethane) should be written as  $\text{Cl}_2\text{CN}_2\text{O}_4$ .

Reactions are stored in character variables with length 38 characters. The first 39 positions of each line in the reaction scheme are reserved for specifications of reactions. Arrhenius parameters for the forward reaction rate must begin at position 40 and for the reverse reaction rate at position 70. If Arrhenius parameters are lacking for some reactions or if they do not start at the 40th and 70th positions, an error warning is given. The error warnings are also given if the thermodynamic data and Lennard-Jones parameter are not written in the files NASACHON.DAT and LENNARD\_JONES.DAT-files, respectively.

## 5.3 Subprograms in READCHKIN

### 5.3.1 Subroutines

Subroutine PRINTOUT prints the output data into file SNE\_OUT.DAT. It writes information about the reaction scheme, number of elements, species and reactions, and specifies whether the reactions are irreversible or reversible.

The elements are written together with their atomic weights and English names, which are read from the file ATOMIC\_W.DAT. The species are listed together with their molecular weights, which are calculated automatically from atomic weights of the elements involved.

Reactions with Arrhenius parameters are written in a way that is similar to the way in which they are stored in the input file SNE\_IN.DAT, except that the reactions are numbered in SNE\_OUT.DAT. The PRINTOUT also writes information about stoichiometric coefficients, the number of each atom in the species and species indices (i.e. the species number in the species list). The correct input to SNECKS can therefore be verified. The subroutine PRINTOUT also writes thermodynamic data and Lennard-Jones parameters for involved species in SNE\_OUT.DAT.

Subroutine SIRS identifies the chemical species in each reaction step. It simply checks if the character string RE\*38 in which reaction is stored contains substrings equal to species symbols which are in the species list.

Subroutine REACTYPE checks whether the reaction is irreversible or reversible and whether the species in the reaction formulas are on the left hand side or on the right hand side. Reversible reactions are indicated by an equal sign (=) and irreversible reactions by a minus sign (-) between reactants and products in the reaction formulas. Species symbols and '+', '-' and '=' signs must always be separated by at least one blank character in SNE\_IN.DAT.

Subroutine SPIN picks up the species indices for all species involved in the reaction steps. Unknown species are returned by index 0. Unidentified species are thus detected.

Subroutine READSTOIC reads the stoichiometric coefficients in the chemical reaction formulas. If there is no stoichiometric coefficient in front of a species then the stoichiometric coefficient of this species is set equal to 1. The stoichiometric coefficients in the current version of the program must be of type INTEGER, i.e. fractional coefficients are not allowed. No spaces are allowed between the

stoichiometric coefficients and species symbols.

Subroutine ATOMWGT is used for picking up the atomic weights of the elements which are written in file ATOMIC\_W.DAT.

Subroutine MOLWGT calculates the molecular weights of species in the reaction scheme by using atomic weights of atoms involved read by subroutine ATOMWGT. This also calculates the numbers of different atoms in each species.

Subroutine READTHERMO reads the thermodynamic database NASACHON.DAT. The database should be written in "NASA-format", where every item of species data is written in four lines. This current version of the program accepts the standard NASA-type file that is used as input to the Gordon and McBride equilibrium code. The data following the species names in the lines numbered as 1 are not used. These areas can therefore be used to write comments, eg. reference, date, etc; see Appendix B.

Subroutine LENJONES reads the Lennard-Jones parameter form input file LENNARD\_JONES.DAT.

### 5.3.2 Functions

Function NUMERIC converts a number in a character string to a corresponding numeric value. Here, this function is used for the identification of atom indices and stoichiometric coefficients.

Function IVALUE converts the whole part of numeric characters to a corresponding numeric value. This function works together with function NUMERIC.



## 6. Results and discussions

In the present work the flamelet chemistry was calculated for methane-air diffusion flames in both non-vitiated and vitiated atmospheres. The influence of vitiating, i.e. recirculation of combustion products back to the flame was simulated by replacing the air stream by the mixture of air + combustion products. For the sake of simplicity the combustion products were assumed to consist only of H<sub>2</sub>O and CO<sub>2</sub>. The vitiated oxidizer stream temperature was treated in two different ways:

1. Recirculating combustion products at about 1000 K.
2. Recirculating combustion products at 300 K.

Three degrees of vitiating were used: the oxidizer stream was diluted by 20%, 40% and 60% of combustion products. The temperature of the combustion products + air mixture, when using hot combustion products, was calculated as the arithmetic mean values of hot gas at 1000 K and air at 300 K, (equal heat capacities for hot gas and air were assumed). The temperatures of oxidizer streams for different degrees of vitiating together with file name specifications are shown in table 1.

File specification	Vitiating (%)	Temperature of oxidizer stream (K)
CH4VIT-00	0	300
CH4VIT-20	20	300
CH4VIT-40	40	300
CH4VIT-60	60	300
CH4VTR-00	0	300
CH4VTR-20	20	450
CH4VTR-40	40	570
CH4VTR-60	60	680

Table 1: The temperature of recirculating combustion products + air mixtures at different degrees of vitiating. The temperature of the fuel stream was 300 K in each case.

Equation (11) is also valid for the vitiating environment. Due to dilution, the stoichiometric mixture fraction is shifted towards the lower values. The only

parameter, which varies due to vitiation in equation (11) is  $Y_{O_2,2}$ . The fuel stream  $Y_{F,1}$ , is assumed to be unaffected by vitiation and thus always equals unity. The stoichiometric coefficients  $v'_{O_2}$  and  $v'_{F}$  for oxygen and fuel are unchanged,  $v'_{O_2} = 2$  and  $v'_{F} = 1$ , respectively. The molecular weights of  $O_2$  and  $CH_4$  are approximately 32 and 16, respectively. Thus, the stoichiometric mixture fraction for vitiated oxidizer stream can be calculated from a simple formula

$$\xi_{st,vit} \approx \left( 1 + \frac{4}{Y_{O_2,2}} \right)^{-1} \quad (74)$$

By introducing a vitiation factor  $\Psi_{vit}$ , the  $O_2$ -massfraction in the oxidizer stream can be expressed as a function of  $\Psi_{vit}$ :

$$Y_{O_2,2} = \frac{v'_{O_2} M_{O_2}}{v'_{O_2} M_{O_2} + v'_{N_2} M_{N_2}} (1 - \Psi_{vit}); \quad 0 \leq \Psi_{vit} \leq 1; \quad (75)$$

The stoichiometric mixture fraction  $\xi_{st,vit}$  and the oxygen mass fraction  $Y_{O_2,2}$  in the oxidizer stream for  $\Psi_{vit} = 0.00, 0.20, 0.40$  and  $0.60$  are shown in table 2.

Vitiation factor ( $\Psi_{vit}$ )	Oxygen mass frac- tion $Y_{O_2,2}$	Stoichiometric mix- ture fraction $\xi_{st, vit}$
0.00	0.233	0.055
0.20	0.186	0.045
0.40	0.140	0.034
0.60	0.093	0.023

Table 2: Variation of stoichiometric mixture fraction  $\xi_{st,vit}$  and oxygen mass fraction  $Y_{O_2,2}$  with different degree of vitiation.

All the simulated results from the present calculations are presented in figures E1 - E42 in Appendix E.

## 6.1 Comparisons with other studies

### 6.1.1 Comparison between theoretical models and Raman measurements

The temperatures and major species concentrations calculated in the present study agree well with earlier calculations by Peters and Kee [16-19]. They used a four-step, reduced reaction mechanism to calculate the parameters of stretched laminar methane-air diffusion flames. Peters and Kee's work includes the calculation of different strain rates. Figure 7 shows a comparison of the present calculations with those of Peters and Kee for strain rates of  $450 \text{ s}^{-1}$ ,  $300 \text{ s}^{-1}$  and  $100 \text{ s}^{-1}$ . Figure 7 also shows the scatter plot data from laser Raman experiments on high-momentum flames, with a  $41 \text{ m/s}$  central jet velocity, at the point  $x/D = 20$  and  $r/D = 1.14$  and  $1.55$ , where  $x$  and  $r$  are the distances from burner top and the axis of symmetry, respectively, and  $D$  is the burner exit diameter [17]. Peters and Kee used a pulsed dye laser (COUMARIN 521) with a wavelength,  $\lambda$  of  $532 \text{ nm}$ ,  $\Delta\lambda$  of  $0.3 \text{ nm}$ , a pulse energy  $0.75 \text{ J}$  and a pulse length of  $3 \mu\text{s}$  during which the gas movements are so small that measured values can be considered as instantaneous. The laser beam was focused to a  $300 \mu\text{m}$  waist diameter.

The temperatures predicted in the present study do not differ very much from Peters and Kee's study near  $\xi = \xi_{st}$ . For  $\xi > 0.4$  the temperature is about  $100-150 \text{ K}$  lower in the present study.

The concentration of  $\text{CO}_2$  at  $\xi = \xi_{st}$  predicted by the present work is about the same as Peters and Kee's calculation for a strain rate of  $100 \text{ s}^{-1}$ . For higher values of  $\xi$  the  $\text{CO}_2$  concentration in the present study moves towards the  $300 \text{ s}^{-1}$  curve, see figure 7b. This indicates that, according to current model, the combustion is more incomplete for rich mixtures than in Peters and Kee's model.

The concentration of  $\text{H}_2\text{O}$  follows the same pattern as that of  $\text{CO}_2$  and comparisons with the present results are therefore omitted.

Predicted values of CO mass fractions are compared in figure 7c. In the present study, somewhat higher concentrations of CO were found compared with Peters and Kee's calculations. There is a large discrepancy in CO concentrations between the calculated results and those measured with Raman methods. In the blue regions of hydrocarbon flames the laser signals are contaminated by fluorescence, the intensity of which is of the same order as the Raman signals. As the source molecules for this fluorescence are not fully known, this can lead to a large uncertainty in measured species concentrations. Discrepancies in CO concentrations between measured and calculated results can be attributed to this fluorescence.

Figure 7a. Joint pdf scatter plot for temperature versus mixture fraction. Lines denote predictions by Peters and Kee (17)

— Peters and Kee,  
strain rate  $450 \text{ s}^{-1}$   
—·— Peters and Kee,  
strain rate  $300 \text{ s}^{-1}$   
----- Peters and Kee,  
strain rate  $100 \text{ s}^{-1}$   
—··— Current work

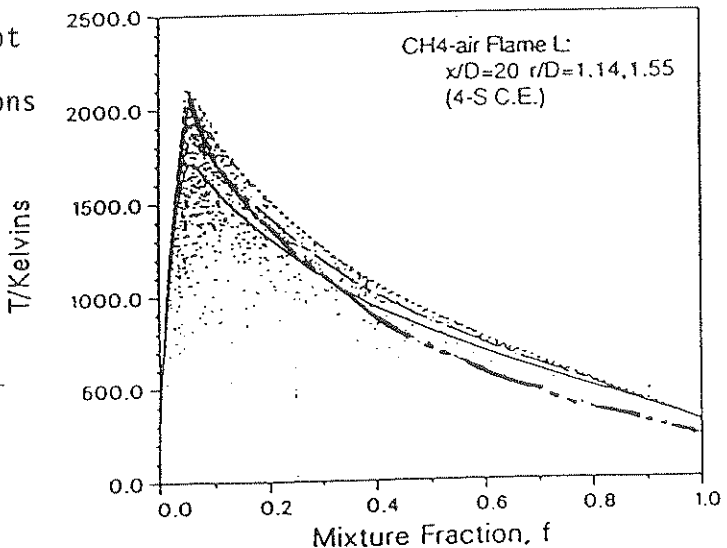


Figure 7b. Joint pdf scatter plot for  $\text{CO}_2$  versus mixture fraction. Lines denote predictions by Peters and Kee (17)

— Peters and Kee,  
strain rate  $450 \text{ s}^{-1}$   
—·— Peters and Kee,  
strain rate  $300 \text{ s}^{-1}$   
----- Peters and Kee,  
strain rate  $100 \text{ s}^{-1}$   
—··— Current work

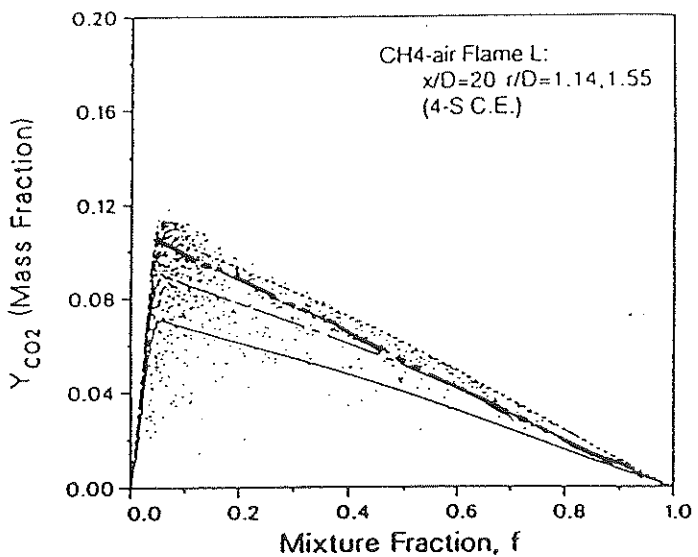
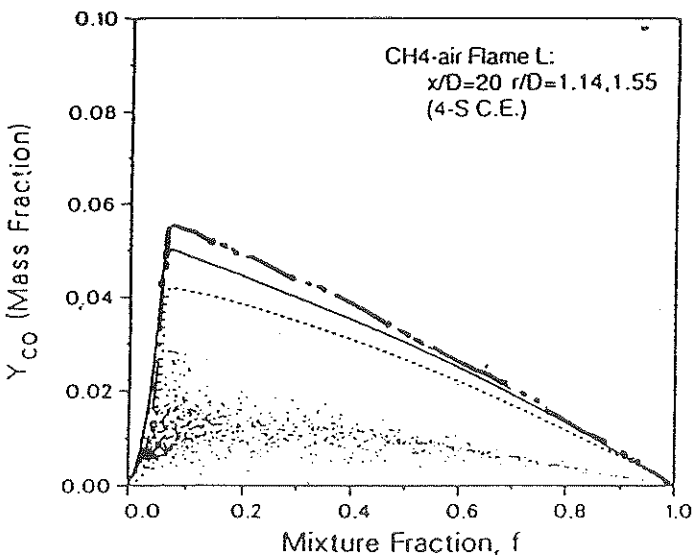


Figure 7c. Joint pdf scatter plot for  $\text{CO}$  versus mixture fraction. Lines denote predictions by Peters and Kee (17)

— Peters and Kee,  
strain rate  $450 \text{ s}^{-1}$   
—·— Peters and Kee,  
strain rate  $300 \text{ s}^{-1}$   
----- Peters and Kee,  
strain rate  $100 \text{ s}^{-1}$   
—··— Current work



### 6.1.2 Comparison with measurements in laminar and turbulent diffusion flames

Smith and Cox [20] have made detailed measurements of time-averaged concentrations of major species produced in several sizes of turbulent diffusion flames of natural gas (94% methane). A 0.3 x 0.3 m square, porous refractory burner was used in their experiments which included flames with theoretical heat release rates between 18 and 111 kW. The concentrations of fuel, CO<sub>2</sub>, CO and H<sub>2</sub>O were measured directly using infra-red absorption techniques, and the O<sub>2</sub> concentration was measured using a parametric susceptibility analyser. All species measurements were time-averaged over a period of at least 10 min. Smith and Cox's measurements of turbulent diffusion flames yield curves which show generally the same behaviour as those from laminar diffusion flames measured by Mitchell et al. [21] and Tsuji and Yamaoka [4], but there are some significant differences. Peak values of temperature, CO and CO<sub>2</sub> concentrations occur further beyond the fuel-rich side of the stoichiometric mean mixture fraction than in laminar diffusion flames. As expected, the time averaging of the species fluctuations in the turbulent flames causes the reduction of peak values of concentrations [20].

Mitchell et al. [21] used a cylindrical diffusion flame burner, which consisted of two concentric tubes. Fuel was injected through the inner tube of radius 0.633 cm and air through the outer tube of radius 2.54 cm. Temperatures were measured using a silica-coated, 3 mil (76.2  $\mu$ m) Pt/Pt - 13% Rh thermocouple. Radiation and conduction correlations were made to the thermocouple bead temperature to determine the unperturbed gas temperature at the bead location. A constant emissivity of 0.22 was used for the thermocouple bead when making radiation corrections. Species concentrations were investigated using a quartz microprobe. Samples withdrawn from the flame were continuously directed to two Fisher-Hamilton gas partitioners where analyses were performed for CO, CO<sub>2</sub>, CH<sub>4</sub>, H<sub>2</sub>, N<sub>2</sub> and O<sub>2</sub>-Ar content.

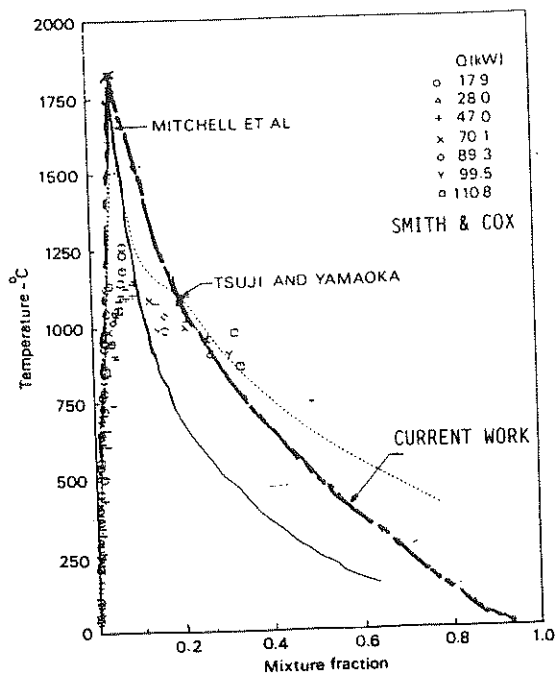
Tsuji and Yamaoka [4] used a rectangular combustion chamber with a cross section of 3 x 12 cm and an uncooled porous (sintered bronze) cylinder, length 3 cm and diameter 6 cm. The air was supplied by a blower through a settling chamber and a converging nozzle to the combustion chamber. The fuel was supplied to the porous cylinder through a capillary flowmeter or an orifice. For temperature measurements a Pt/Pt-Rh-thermocouple with a wire diameter of 0.1 mm and a junction 0.2 mm diameter sphere were used. Stable species concentrations were determined using a micropore sampling technique and gas chromatography.

Tsuji and Yamaoka did not make any radiation corrections to the thermocouple bead temperature. The effect of neglecting the radiation correction is that the peak

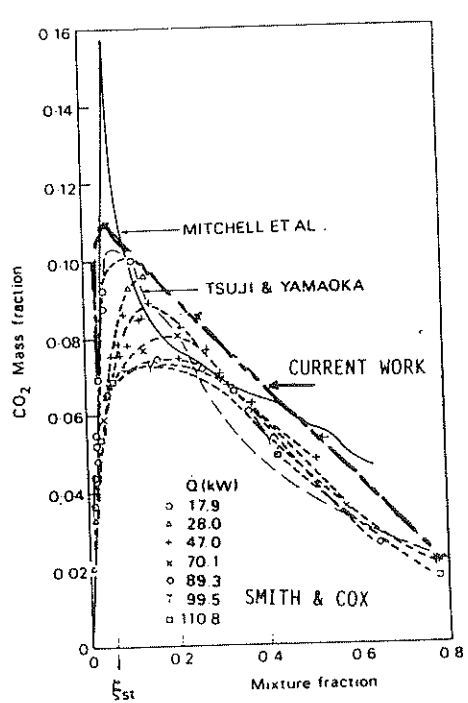
value of the measured temperature will be considerably lower than the actual value, as can be seen in figure 8.

At  $\xi = \xi_{st}$  the results from laminar flames obtained by Mitchell et al. yielded the same results for temperature and CO concentrations (fig. 8a, c) as computed with the present model. For  $\xi > \xi_{st}$  calculated values of temperature are about 200-300°C higher and CO concentration about 25-40% higher. The temperatures measured by Tsuji and Yamaoka agree well with calculated results for  $\xi > \xi_{st}$ . At stoichiometry, Tsuji and Yamaoka measured considerably lower values of temperature, CO and  $\text{CO}_2$  concentration than Mitchell et al. For  $\xi > 0.2$  the temperatures measured by Tsuji and Yamaoka are higher than those calculated.

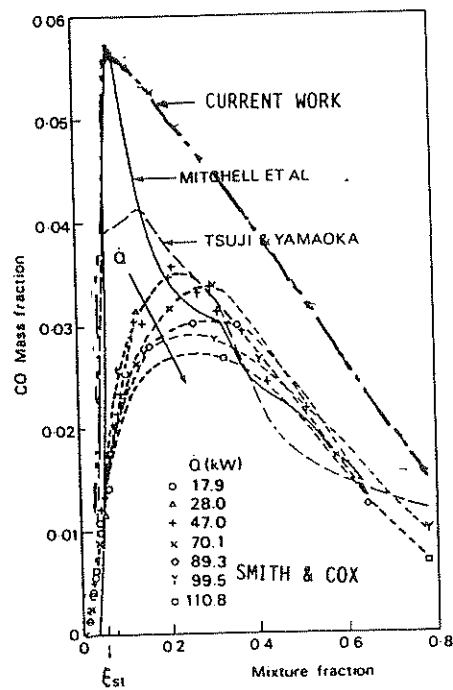
The radiation energy losses are omitted in the present calculation model which would shift the temperature to somewhat lower values and would increase the concentration of CO slightly.



a)



b)



c)

Figure 8. Comparison of current calculations with measured centreline mean temperature (a) and mean mass fractions of  $\text{CO}_2$  and  $\text{CO}$  (b) and c)) as functions of mean mixture fraction.  
 Mitchell et al and Tsuji & Yamaoka: laminar flames  
 Smith & Cox; turbulent flames (20)

## 6.2 Vitiated flamelets

The effect of vitiation by hot combustion products in scalars as a function of mixture fraction are shown in figures E1 to E21 and the corresponding effect of cold combustion products in figures E22 to E42 in Appendix E. At the time this study was made there were no publications found in literature concerning flamelet problems in vitiated atmosphere.

### 6.2.1 Temperature

Figures E1a - d and E2a - d show the temperature variation as a function of mixture fraction for  $\psi_{vit} = 0, 0.2, 0.4$  and  $0.6$ . As expected, the temperature decreases with the increase in  $\psi_{vit}$ . The peak temperature decreases approximately 100 K for every 10 % increase in vitiation factor, in the case of hot gas vitiation. The temperature for  $\xi = \xi_{st}$  is about 2000 K for  $\psi_{vit} = 0$ , while it is less than 1400 K for  $\psi_{vit} = 0.6$ . In the case when cold gas is used as vitiating gas the temperature decrease is slightly larger with increase in vitiation. For  $\psi_{vit} = 0.6$  the spreading of results between timesteps is large when cold vitiation is used, indicating that the mixture is near the limit of flammability, see figures E22-23.

### 6.2.2 The stable species

The concentrations of  $\text{CO}_2$  and  $\text{H}_2\text{O}$  behave in similar manner with vitiation. For hot gas as vitiating gas, the concentration of  $\text{CO}_2$  increases slightly with increased vitiation, while in the case of cold vitiation, the  $\text{CO}_2$  - concentration is nearly constant for rich mixtures, see figures E3 - E4, E24 - E25. The  $\text{H}_2\text{O}$  - concentration seems to be unaffected by whether the vitiation gas is cold or hot for the rich side of stoichiometry. See figures E5 - E6 and E26 - E27.

The CO-concentrations are presented in figures E7 - E8 (hot vitiation) and E28 - E29 (cold vitiation). There are considerable differences in CO concentration between, when the vitiated gas is hot and when it is cold. In the case of hot vitiation the peak-value of the CO-mass fraction (at  $\xi = \xi_{st}$ ) decreases from 0.052 to about 0.032 when  $\psi_{vit}$  is increased from 0 to 0.6. In the case of cold vitiation, the peak concentration of CO is almost constant at 0.052, for  $\psi_{vit}$  between 0 and 0.6.

### 6.2.3 O<sub>2</sub> and H<sub>2</sub> concentrations

The mass fractions of O<sub>2</sub> decrease from initial values in oxidizer streams at  $\xi = 0$  to zero at  $\xi_{st, vit}$ . The decrease is a linear function of  $\xi$  for  $\xi > \xi_{st, vit}$  at which the concentration of O<sub>2</sub> is zero indicating that O<sub>2</sub> is consumed totally.

The maximum H<sub>2</sub>-mass fractions occur at about the range  $\xi = 0.1$  to  $0.15$ , as figures E10-E11 and E31-E32 indicate. The temperature has a significant effect on H<sub>2</sub>-concentration. For hot gas vitiation the mass fraction of H<sub>2</sub> is 0.0035 for  $\Psi_{vit} = 0$  and  $\xi = 0.1$  to  $0.2$ . For  $\Psi_{vit} = 0.6$  the H<sub>2</sub>-mass fraction is about 0.0025. For cold vitiation the  $Y_{H_2}$  is about 0.0043 for all  $\Psi_{vit}$ , except for  $\Psi_{vit} = 0.6$  where the mass fraction of H<sub>2</sub> is about 0.004. The peak value of H<sub>2</sub> is also shifted slightly towards the richer mixture fraction when the vitiating gas is cold.

### 6.2.4 Radicals

O-radicals exist only within a narrow band at the lean side of stoichiometry. At  $\xi = \xi_{st}$  ( $\xi = \xi_{st, vit}$  in vitiating cases) the O-concentration has almost vanished. The peak values of O-concentrations occur at  $\xi \approx 0.95 \xi_{st}$ . The mass fraction of O at that point is about 0.0015 for  $\Psi_{vit} = 0$  and 0.00039 for  $\Psi_{vit} = 0.60$ . The cold vitiation gas raises these values slightly for  $\Psi_{vit} < 0.4$ , and lowers them for  $\Psi_{vit} = 0.60$ . See figures E12 and E33.

H-radical mass fractions  $Y_H$  are plotted in figures E13 - E14 and E34 - E35 for the two different cases of vitiation. As expected, the H-radicals exist on the rich side of stoichiometry in the flamelet where methane molecules lose their first H-atoms due to heat from the flame, exactly as O<sub>2</sub> begins to dissociate on the lean side of stoichiometry for the same reason. According to calculations, the H-radical concentration vanishes at about  $\xi = 0.8$ , having at  $\xi = 0.5$  about 1/5 of its maximum value, which occurs at about  $\xi = 1.05 \xi_{st}$ . The increases in vitiating gas temperature lower the H-radical concentration.

OH-radical concentrations in the flamelets follow the same pattern as O-radical concentrations, except that the peak occurs at  $\xi = \xi_{st}$ . The peak concentration levels are about 2 to 3 times those of O-radical levels. OH-concentrations vanish at about  $\xi = 0.2$  (figures E15 and E36).

HO<sub>2</sub>-radicals exist only on the lean side of stoichiometry. The peak concentrations  $\sim 1 \cdot 10^{-5}$  are located at the oxidizer boundary of flamelet  $\xi \approx 0$ . At the mixture fraction  $\xi = \xi_{st}$  the HO<sub>2</sub> concentration is zero. See figures E16 and E37.

### 6.2.5 The density, viscosity and enthalpy

The mean density of the mixture is an inverse function of the gas temperature, having its minimum at the point of highest temperature, i.e. at  $\xi = \xi_{st}$ , Fig E17-E18 and E38-E39. The viscosity is proportional to temperature. The viscosities as a function of  $\xi$  are shown in figures E19-E20 and E40-E41. Figures E21 and E42 show enthalpies of mixture as a function of  $\xi$ . The peculiar behaviour, which is seen most remarkably in the density graphs in figures E17-E18 and E38-E39, depends on numeric errors of rich mixtures  $\xi \geq 0.8$ .

## 7. Conclusions

The stable species concentrations and the temperatures calculated using the present thirteen-step reaction model agree well with the earlier calculations of Peters and Kee using a four-step, reduced-reaction mechanism. Near stoichiometry the agreement is also quite good with recent measurements on laminar diffusion flames. The largest discrepancy is found to be in CO concentrations. For  $\xi \geq 0.2$  the calculated CO concentrations are overestimated by 30%.

The agreement of the present model with turbulent diffusion flames is also quite good, except that measured peak values of temperature, CO and CO<sub>2</sub> concentrations, due to time averaging, are considerably lower and occur further on the rich side of the stoichiometry.

Vitiation affects the temperature and hence the chemistry. In case of hot vitiation the temperature is reduced approximately 100 K for every 10% increase of vitiation. In case of cold vitiation the temperature effect is larger.

As it can be seen in figure E8, the peak concentration of CO is reduced by nearly 40% when the vitiation factor is increased from 0 to 60% in case of hot vitiation. Notice, that this does not mean that combustion is more complete. Due to vitiation the oxidizer stream contains less O<sub>2</sub>, the stoichiometric mixture fraction is shifted towards lower values. Because the stoichiometric combustion is defined as all the O<sub>2</sub> is consumed in the mixture and because the relation fuel-oxygen is still the same, the more total mass of oxidizer gas is needed for combustion of a certain portion (for example one mole) of fuel. Because the species concentrations, and so CO concentrations in figure E8 is presented in fraction of total mass in the mixture, there actually is about 35% increase of CO concentration per combusted CH<sub>4</sub> when vitiation is increased from 0 to 60%. In case of cold gas vitiation the increase of CO production is 150% calculated in that way.



## Nomenclature

$a_{nk}$	= polynomical coefficient in enthalpy equations and heat capacity equation
$c_{g1}$	= empirical constant (value 2.8)
$c_{g2}$	= empirical constant (value (2.0)
$c_{ei}$	= empirical constant (value 1.44)
$c_{e2}$	= empirical constant (value 1.92)
$c_p$	= heat capacity of air
$c_v$	= specific heat at constant volume
$f_\phi$	= Newton - Raphson function of species or enthalpy $\phi$
$h$	= enthalpy of gas
$h_t$	= total enthalpy
$k$	= turbulent kinetic energy
$k$	= Boltzmann constant
$k_b$	= rate constant for backward reaction
$k_f$	= rate constant for forward reaction
$\tilde{k}$	= Favre averaged turbulent kinetic energy
$m_{ij}$	= reduced mass for collision of molecules with masses $m_i$ and $m_j$
$n_i, n_j$	= number of molecules i and j
$p$	= gas pressure
$\bar{p}$	= mean pressure
$\tilde{P}(\xi)$	= Favre - PDF of $\xi$
$q$	= heat flux
$r_i, r_j$	= radii of molecules i and j
$t$	= time
$u$	= gas velocity
$u_i$	= the average internal energy
$u_k''$	= fluctuating part of velocity $u_k$
$\tilde{u}_k$	= Favre averaged velocity in x - direction
$v_{ij}$	= relative average velocity of molecules i and j
$x$	= room coordinate
$A_f, A_b$	= Arrhenius pre-exponential factor in forward and backward reaction rates

$A_i, B_i, C_i, D_i$	= polynomical coefficients in eq (67)
$B_k$	= Arrhenius pre-exponential factor
$C_{\phi_i}$	= concentration of species $\phi_i$
$D$	= mass diffusion coefficient
$D_{ij}$	= binary diffusion coefficient of molecules i and j
$D_{Ti}$	= thermal diffusion coefficient
$\tilde{D}_{ij}$	= multicomponent diffusion coefficient
$E_f, E_b$	= activation energies in forward and backward reactions
$\vec{F}$	= external force vector per unit mass
$\vec{F}_i$	= external force per unit mass on species i
$K_c$	= equilibrium constant
$M$	= number of elementary reaction steps
$M_\alpha$	= molecular weight of species $\alpha$
$N$	= number of chemical reactions
$NS$	= total number of species
PDF	= Probability chemistry function
$\nabla p$	= pressure gradient
$R$	= universal gas constant
$R_b$	= backward reaction rate
$R_f$	= forward reaction rate
$S_\phi$	= chemical source term
$T$	= gas temperature
$T_b$	= temperature of burned mixture
$T_F$	= temperature of fuel stream
$T_{ox}$	= temperature of oxidizer stream
$T_u$	= temperature of unburned mixture
$\nabla T$	= temperature gradient
$V_i$	= diffusion velocity of species i
$\vec{V}_i$	= diffusion velocity vector for species i
$X_i$	= mole fraction of species i
$\nabla X_i$	= concentration gradient of species i
$Y_i$	= mass fraction of species i
$Y_{F,1}$	= fuel stream
$Y_{o_2,2}$	= oxidizer stream

$W$	= molecular weight of species i
$(-\Delta H)_{ref}$	= heat of combustion at reference atmospheric conditions
$\frac{\epsilon_{ij}}{k_{LJ}}$	= Lennard-Jones constant
$\alpha, \beta$	= exponent in Beta function
$\beta_f, \beta_b$	= temperature exponents in forward and backward reaction rates
$\gamma$	= ratio of species heats at constant pressure and constant volume $c_p/c_v$
$\gamma_p, \gamma_b$	= third body reaction exponents
$\delta_{ij}$	= Kroneches delta function
$\epsilon$	= dissipation of turbulent kinetic energy
$\tilde{\epsilon}$	= Favre averaged dissipation of turbulent kinetic energy
$\eta$	= under-relaxation or acceleration parameter
$\lambda$	= heat conductivity
$\mu$	= dynamic viscosity
$\mu$	= shear viscosity
$\mu'$	= bulk viscosity
$\mu_{lam}$	= laminar viscosity
$\mu_{tur}$	= turbulent viscosity
$v_{ij}$	= collision frequency
$v_\alpha$	= change of mass of species $\alpha$ in chemical reaction
$v'_\alpha$	= stoichiometric coefficient of reactant $\alpha$
$v''_\alpha$	= stoichiometric coefficient of product $\alpha$
$\xi$	= mixture fraction
$\xi_{st}$	= stoichiometric mixture fraction
$\xi_{st, vit}$	= stoichiometric mixture fraction in vitiated atmosphere
$\tilde{\xi}$	= Favre averaged mixture fraction (mass weighted)
$\tilde{\xi}^{/\!/ 2}$	= Favre averaged mixture fraction variance
$\rho$	= mass density of gas
$\bar{\rho}$	= mean density
$\sigma_m$	= reciprocal of the mixture mean molecular weight
$\sigma_{ij}$	= collision cross section of molecules i and j
$\sigma_{\xi lam}$	= the effective laminar Prandtl/Schmidt number

$\sigma_{\xi \text{fur}}$	= the effective turbulent Prandtl/Schmidt number
$\tau_{ij}$	= stress tensor
$\phi$	= scalar (i.e. temperature, viscosity or enthalpy)
$\phi$	= equivalence ratio
$\phi$	= atomic element symbol
$\bar{\phi}$	= time averaged (Reynolds mean) of $\phi$
$\overline{\phi}^2$	= Reynolds variance of $\phi$
$\tilde{\phi}$	= Favre-average $\phi$
$\tilde{\phi}^{/\!/ 2}$	= variance of $\tilde{\phi}$ (second moment of $\phi$ )
$\psi$	= stream function
$\psi_{\text{vit}}$	= vitiation factor
$\omega$	= nondimensional stream function
$\omega_i$	= rate of productivity of species i
$\Omega_{D_y}^{(1,1)*}$	= mass diffusivity collision integral
$\Omega_{\mu_j}^{(2,2)*}$	= thermal conductivity collision integral
$\Gamma_\phi$	= transport coefficient

## **Acknowledgements**

This work was supported by NUTEK and Brandforsk which are gratefully acknowledged. The author would like to thank Göran Holmstedt for his sustained interest in this work and many helpful discussions.

Acknowledgement is also given to the School of Mechanical Engineering at the Cranfield Institute of Technology in the UK, where all the calculations in this study were performed.



## References

- [1] Liew, S.K., Flamelet Models of Turbulent Non-Premixed Combustion. Phd thesis, Department of Aeronautics and Astronautics, The University, Highfield, Southampton, UK.
- [2] Syed, K.J., Moss, J.B., Flamelet Chemistry in JASMINE. Progress Report on Research under Building Research Establishment (Fire Research Station), School of Mechanical Engineering, Cranfield Institute of Technology, England.
- [3] Bilger, R.W. (1977), Reaction rates in diffusion flames. Combustion and Flame 30, 277-284.
- [4] Tsuji, H, Yamaoka, I (1970), Structure analysis of counterflow diffusion flames in the forward stagnation region of a porous cylinder. Thirteenth Symposium (International on Combustion, pp 723-731, Pittsburgh, Penn., Combustion Institute
- [5] Michel, R.E., Sarofin, A.F. and Clomberg, L.A. (1980), Experimental and numerical investigation of confined laminar diffusion flames. Combustion and Flame, 37, 227-244.
- [6] Williams, F.A., Combustion Theory. Princeton University, The Benjamin/Cummings Publishing Company, Inc.
- [7] Launder, B.E., Spalding, D.B., Mathematical models of turbulence. Academic press.
- [8] Kuo, K.K.(1989), Principles of Combustion. John Wiley & Sons, USA.
- [9] Syed, K.J., Moss, J.B., Flamelet Modelling of Species Concentration in Fires. School of Mechanical Engineering, Cranfield Institute of Technology, Bedford, England (1991).
- [10] Hirschfelder, J.O., Curtiss, C.F., Bird, R.B., Molecular theory of gases and liquids. Wiley (1954).

- [11] Dixon-Lewis, G., Flame Structure and Flame Reaction Kinetics II. Transport Phenomena in Multicomponent systems, Proc. Roy. Soc. A307, pp 11-135 (1968).
- [12] Wolfrum, J., Chemical Kinetics in Combustion Systems: the Specific Effect of Energy, Collisions and Transport Processes. Twentieth Symposium (International) on Combustion, The Combustion Institute (1984) pp 559-573.
- [13] Burden, A., Lecture Notes, Combustion Physics. A course given at Lund University.
- [14] Ferziger, J.H., Kaper, H.G., Mathematical theory of transport processes in gases. North-Holland (1972).
- [15] Pratt, D.T., Calculation of Chemically Reacting Flows with Complex Chemistry. Studies in Convection, 2, Launder B.E. (ed.), Academic Press (1977).
- [16] Peters, N., Kee, R.J., The computation of stretched laminar methane-air diffusion flames using a reduced four-step mechanism. Combustion and Flame 68 (1987).
- [17] Chen, J-Y., Kollmann, W., Dibble, R.W., Pdf Modelling of Turbulent Nonpremixed Methane Jet Flames. Combustion Research Facility, Sandia National Laboratories, Livermore, CA 94551, SAND89-8403 (1989).
- [18] Masri, A.R., Bilger, R.W., Dibble, R.W., Turbulent Nonpremixed Flames of Methane Near Extinction: Probability Density Functions. Combustion and Flame 73: 261-285 (1988).
- [19] Masri, A.R., Bilger, R.W., Dibble, R.W., Conditional Probability Density Functions Measured in Turbulent Nonpremixed Flames of Methane Near Extinction. Combustion and Flame 74: 267-284 (1988).
- [20] Smith, D.A., Cox, G., Major Chemical Species in Buoyant Turbulent Diffusion Flames. Combustion and Flame 91:226-238 (1992).

- [21] Mitchell, R.E., Sarofim, A.F., Clomberg, L.A., Experimental and Numerical Investigation of Confined Laminar Diffusion Flames. Combustion and Flame 37:227-249 (1980).



# **Appendices**

**A. Chemical model**

**B. Input files to SNECKS**

- B:1** The structure of SNE.IN.DAT
- B:2** The structure of ATOMIC\_W.DAT
- B:3** The structure of NASACHON.DAT
- B:4** The structure of LENNARD\_JONES.DAT

**C. The example of VAX/VMS-command procedure for running the SNECKS**

**D. Output file from SNECKS.SNE\_OUT.DAT**

**E. The plots of computed results**



## Appendix A

**Table A1**

		Forward rate			Backward rate		
1.	O+H <sub>2</sub> O=OH+OH	1.76x10 <sup>10</sup>	-0.02	16747.3	1.55x10 <sup>9</sup>	0.0	0.0
2.	H+H=H <sub>2</sub>	1.00x10 <sup>12</sup>	-1.0	0.0	7.15x10 <sup>4</sup>	-0.82	103328.3
3.	O+O=O <sub>2</sub>	6.00x10 <sup>2</sup>	0.0	0.0	5.83x10 <sup>10</sup>	-1.0	119837.0
4.	H+H=H <sub>2</sub> O	2.00x10 <sup>17</sup>	-2.0	0.0	2.20x10 <sup>13</sup>	0.0	105217.9
5.	H+O <sup>2</sup> =OH+O	2.00x10 <sup>11</sup>	0.0	16665.8	1.65x10 <sup>9</sup>	0.27	0.0
6.	O+H <sub>2</sub> =OH+H	6.00x10 <sup>10</sup>	0.0	10008.6	1.94x10 <sup>10</sup>	-0.03	8059.4
7.	O <sub>2</sub> +H=HO <sub>2</sub>	15.0x10 <sup>9</sup>	0.0	994.5	2.10x10 <sup>12</sup>	0.0	46039.3
8.	H+HO <sub>2</sub> =OH+OH	1.59x10 <sup>11</sup>	0.0	1080.0	1.26x10 <sup>10</sup>	0.0	39873.4
9.	CO+OH=CO <sub>2</sub> +H	1.50x10 <sup>8</sup>	0.0	100.5	1.50x10 <sup>10</sup>	0.0	23519.9
10.	H <sub>2</sub> +OH=H <sub>2</sub> O+1	1.50x10 <sup>10</sup>	0.0	5004.3	5.55x10 <sup>10</sup>	-0.01	19802.4
11.	CO+O=CO <sub>2</sub>	6.00x10 <sup>7</sup>	0.0	0.0	1.31x10 <sup>10</sup>	-0.58	125843.7
12.	H+O=OH	3.00x10 <sup>8</sup>	0.0	0.0	6.96x10 <sup>10</sup>	0.21	101379.1
13.	2CH <sub>4</sub> +O <sub>2</sub> -2CO+4H <sub>2</sub>	1.75x10 <sup>7</sup>	1.0	24265.7			



## Appendix B

### B:1. The structure of SNE\_IN.DAT

```

ELEMENTS
O
C
H
N
END
SPECIES
N2
H
OH
O
HO2
CO
CO2
H2O
O2
CH4
H2
END
REACTIONS
O + H2O = OH + OH      1.76E+10 -0.02 16747.3 1.55E+09
0.0      0.0
H + H    = H2           1.00E+12 -1.0   0.0   7.15E+04 -
0.82 103328.3
O + O    = O2           6.00E+02 0.0   0.0   5.83E+10 -
1.0 119837.0
H + OH   = H2O          2.00E+17 -2.0   0.0   2.20E+13
0.0 105217.9
H + O2   = OH + O       2.00E+11 0.0   16665.8 1.65E+09
0.27 0.0
O + H2   = OH + H       6.00E+10 0.0   10008.6 1.94E+10 -
0.03 8059.4
O2 + H   = HO2          1.50E+09 0.0   994.5  2.10E+12
0.0 46039.3
H + HO2  = OH + OH     1.59E+11 0.0   1080.0  1.26E+10
0.0 39873.4
CO + OH  = CO2 + H     1.50E+08 0.0   1000.5  1.50E+10
0.0 23519.9
H2 + OH  = H2O + H     1.50E+10 0.0   5004.3  5.55E+10 -
0.01 19802.4
CO + O   = CO2          6.00E+07 0.0   0.0   1.31E+10 -
0.58 125843.7
H + O   = OH            3.00E+08 0.0   0.0   6.96E+10
0.21 101379.1
2CH4 + O2  - 2CO + 4H2 1.75E+07 1.0   24265.7
END

```

B:2. The structure of ATOMIC\_W.DAT

ATOMIC WEIGHTS OF THE ELEMENTS

SOURCE: HANDBOOK OF CHEMISTRY AND PHYSICS, 54 EDITION, CRC-PRESS

SYMBOL	NAME	ATOMIC WEIGHT
H	HYDROGEN	1.008
He	HELIUM	4.00260
Li	LITHIUM	6.94
Be	BERYLLIUM	9.01218
B	BORON	10.81
C	CARBON	12.011
N	NITROGEN	14.0067
O	OXYGEN	15.9994
F	FLUORINE	18.9984
Ne	NEON	20.17
Na	SODIUM	22.9898
Mg	MAGNESIUM	24.305
Al	ALUMINIUM	26.9815
Si	SILICON	28.086
P	PHOSPHORUS	30.9738
S	SULPHUR	32.06
Cl	CHLORINE	35.453
Ar	ARGON	39.948
K	POTASSIUM	39.102
Ca	CALCIUM	40.08
Sc	SCANDIUM	44.9559
Ti	TITANIUM	47.90
V	VANADIUM	50.941
Cr	CHROMIUM	51.996
Mn	MANGANESE	54.9380
Fe	IRON	55.847
Co	COBALT	58.9332
Ni	NICKEL	58.71
Cu	COPPER	63.546
Zn	ZINC	65.37
Ga	GALLIUM	69.72
Ge	GERMANIUM	72.59
As	ARSENIC	74.9216
Se	SELENIUM	78.96
Br	BROMINE	79.904
Kr	KRYPTON	83.80
Rb	RUBIDIUM	85.467
Sr	STRONTIUM	87.62
Y	YTTRIUM	88.9059
Zr	ZIRCONIUM	91.22
Nb	NIOBIUM	92.9064
Mo	MOLYBDENUM	95.94
Tc	TECHNETIUM	98.9062
Ru	RUTHEHIMUM	101.07
Rh	RHODIUM	102.9055
Pd	PALLADIUM	106.4
Ag	SILVER	107.868
Cd	CADMİUM	112.40
In	INDIUM	114.82
Sn	TIN	118.69
Sb	ANTIMONY	121.75
Te	TELLURIUN	127.60
I	IODINE	126.9045
Xe	XENON	131.30
Cs	CESIUM	132.9055
Ba	BARIUM	137.34

Nd	NEODYMIUM	144.24
Pm	PROMETHIUM	145.
Sm	SAMARIUM	150.4
Eu	EUROPIUM	151.96
Gd	GADOLINIUM	157.25
Tb	TERBIUM	158.9254
Dy	DYSPROSIUM	162.50
Ho	HOLMIUM	164.9303
Er	ERBIUM	167.26
Tm	THULIUM	168.9342
Yb	YTTERBIUM	173.04
Lu	LUTETIUM	174.97
Hf	HAFNIUM	178.49
Ta	TANTALUM	180.947
W	TUNGSTEN	183.85
Re	RHENIUM	186.2
Os	OSMIUM	190.2
Ir	IRIDIUM	192.22
Pt	PLATINUM	195.09
Au	GOLD	196.9665
Hg	MERCURY	200.59
Tl	THALLIUM	204.37
Pb	LEAD	207.2
Bi	BISMUTH	208.9806
Po	POLONIUM	209.
At	ASTATINE	210.
Rn	RADON	222.
Fr	FRANCINUM	223.
Ra	RADIUM	226.
Ac	ACTINIUM	227.
Th	THORIUM	232.0381
Pa	PROTOACTIUM	231.0359
U	URANIUM	238.028
Np	NEPTUNIUM	237.0482
Pu	PLUTONIUM	244.
Am	AMERICIUM	243.
Cm	CURIUM	247.
Bk	BERKELIUM	247.
Cf	CALIFORNIUM	251.
Es	EINSTENIUM	254.
Fm	FERMIUM	257.
Md	MENDELEVIUM	256.
No	NOBELIUM	254.

END

B:3. The structure of NASACHON.DAT

300.000	1000.000	5000.000		
Ar	L 5/66AR	100 000 000 OG	300.000 5000.000	1
0.25000000E 01	0.	0.	0.	2
-0.74537502E 03	0.43660006E 01	0.25000000E 01	0.	3
0.	0.	-0.74537498E 03	0.43660006E 01	4
Ar+	L12/66AR	1E -100 000 OG	300.000 5000.000	1
0.28420672E 01	-0.87648603E-04	-0.26463209E-07	0.12240311E-10 -0.11885139E-14	2
0.18272563E 06	0.36720201E 01	0.24857001E 01	-0.55682660E-03 0.33194849E-05	3
-0.39236795E-08	0.14143279E-11	0.18290215E 06	0.5880154E 01	4
C	J 3/61C	100 000 000 OG	300.000 5000.000	1
0.25810663E 01	-0.14696202E-03	0.74388084E-07	-0.79481079E-11 0.58900977E-16	2
0.85216294E 05	0.43128879E 01	0.25328705E 01	-0.15887641E-03 0.30682082E-06	3
-0.26770064E-09	0.87488827E-13	0.85240422E 05	0.46062374E 01	4
C+	L12/66C	1E -100 000 OG	300.000 5000.000	1
0.25118274E 01	-0.17359784E-04	0.95042676E-08	-0.22188518E-11 0.18621892E-15	2
0.21667721E 06	0.42861298E 01	0.25953840E 01	-0.40686645E-03 0.68923669E-06	3
-0.52664878E-09	0.15083377E-12	0.21666281E 06	0.38957298E 01	4
C-	J 9/65C	1E 100 000 OG	300.000 5000.000	1
0.24470591E 01	0.11286428E-03	-0.78591462E-07	0.19778614E-10 -0.11105555E-14	2
0.69972969E 05	0.42356992E 01	0.24925640E 01	0.53153068E-04 -0.13307994E-06	3
0.13951379E-09	-0.52150992E-13	0.69955757E 05	0.39811657E 01	4
CH	J12/67C	1H 10 00 OG	300.000 5000.000	1
0.22673116E 01	0.22043000E-02	-0.62250191E-06	0.69689940E-10 -0.21274952E-14	2
0.70838037E 05	0.87889352E 01	0.35632752E 01	-0.20031372E-03 -0.40129814E-06	3
0.18226922E-08	-0.86768311E-12	0.70405506E 05	0.17628023E 01	4
CH+	J12/71C	1H 1E -1 OG	300.000 5000.000	1
0.27466401E+01	0.15496991E-02	-0.52858324E-06	0.86132075E-10 -0.50909775E-14	2
0.19483672E+06	0.46994695E+01	0.35601593E+01	-0.22478101E-03 -0.26341623E-06	3
0.16716214E-08	-0.89478626E-12	0.19460363E+06	0.41570213E+00	4
CH2	J12/72C	1H 2 0 OG	300.000 5000.000	1
0.27525479E+01	0.39782047E-02	-0.14921731E-05	0.25956899E-09 -0.17110673E-13	2
0.45547759E+05	0.66534799E+01	0.35883347E+01	0.21724137E-02 -0.13323408E-05	3
0.19469445E-08	-0.89431394E-12	0.45315188E+05	0.22627869E+01	4
CH2O	J 3/61C	1H 20 10 OG	300.000 5000.000	1
0.28364249E 01	0.68605298E-02	-0.26882647E-05	0.47971258E-09 -0.32118406E-13	2
-0.15236031E 05	0.78531169E 01	0.37963783E 01	-0.25701785E-02 0.18548815E-04	3
-0.17869177E-07	0.55504451E-11	-0.15088947E 05	0.47548163E 01	4
CH3	J 6/69C	1H 30 00 OG	300.000 5000.000	1
0.28400327E 01	0.60869086E-02	-0.21740338E-05	0.36042576E-09 -0.22725300E-13	2
0.16449813E 05	0.55056751E 01	0.34666350E 01	0.38301845E-02 0.10116802E-05	3
-0.18859236E-08	0.66803182E-12	0.16313104E 05	0.24172192E 01	4
CH4	J 3/61C	1H 400 000 OG	300.000 5000.000	1
0.15027072E 01	0.10416798E-01	-0.39181522E-05	0.67777899E-09 -0.44283706E-13	2
-0.99787078E 04	0.10707143E 02	0.38261932E 01	-0.39794581E-02 0.24558340E-04	3
-0.22732926E-07	0.69626957E-11	-0.10144950E 05	0.86690073E 00	4
CN	J 6/69C	1N 10 00 OG	300.000 5000.000	1
0.36036285E 01	0.33644390E-03	0.10028933E-06	-0.16318166E-10 -0.36286722E-15	2
0.51159833E 05	0.35454505E 01	0.37386307E 01	-0.19239224E-02 0.47035189E-05	3
-0.31113000E-08	0.61675318E-12	0.51270927E 05	0.34490218E 01	4
CN+	J12/70C	1N 1E -10 OG	300.000 5000.000	1
0.36522919E+01	0.81427579E-03	-0.20853348E-06	0.29071604E-10 -0.17865094E-14	2
0.21560182E+06	0.43916910E+01	0.36175018E+01	-0.20179550E-02 0.79359855E-05	3
-0.77300616E-08	0.24798477E-11	0.21578134E+06	0.53579527E+01	4
CN-	J12/70C	1N 1E 10 OG	300.000 5000.000	1
0.29471725E+01	0.14988427E-02	-0.57579547E-06	0.10177789E-09 -0.67478503E-14	2
0.63644338E+04	0.63743952E+01	0.37034310E+01	-0.14896426E-02 0.31864701E-05	3
-0.14831305E-08	0.48121663E-13	0.62335826E+04	0.27722843E+01	4
CNN	J 6/66C	1N 200 000 OG	300.000 5000.000	1
0.48209077E 01	0.24790014E-02	-0.94644109E-06	0.16548764E-09 -0.10899129E-13	2
0.68685948E 05	-0.48484039E 00	0.35077779E 01	0.72023958E-02 -0.75574589E-05	3
0.42979217E-08	-0.94257935E-12	0.68994281E 05	0.60234964E 01	4
CN2	J12/70C	1N 20 00 OG	300.000 5000.000	1
0.55626268E+01	0.20860606E-02	-0.88123724E-06	0.16505783E-09 -0.11366697E-13	2
0.54897907E+05	-0.55989355E+01	0.32524003E+01	0.70010737E-02 -0.22653599E-05	3
-0.28939808E-08	0.18270077E-11	0.55609085E+05	0.66966778E+01	4

CO	J 9/65C	10	100	000	OG	300.000	5000.000	1
	0.29840696E 01	0.14891390E-02	-0.57899684E-06	0.10364577E-09	-0.69353550E-14			2
	-0.14245228E 05	0.63479156E 01	0.37100928E 01	-0.16190964E-02	0.36923594E-05			3
	-0.20319674E-08	0.23953344E-12	-0.14356310E 05	0.29555351E 01				4
CO2	J 9/65C	10	200	000	OG	300.000	5000.000	1
	0.44608041E 01	0.30981719E-02	-0.12392571E-05	0.22741325E-09	-0.15525954E-13			2
	-0.48961442E 05	-0.98635982E 00	0.24007797E 01	0.87350957E-02	-0.66070878E-05			3
	0.20021861E-08	0.63274039E-15	-0.48377527E 05	0.96951457E 01				4
CO2-	J 12/66C	10	2E	100	OG	300.000	5000.000	1
	0.45454640E 01	0.26054316E-02	-0.10928732E-05	0.20454421E-09	-0.14184542E-13			2
	-0.54761968E 05	0.18317369E 01	0.34743737E 01	0.16913805E-02	0.73533803E-05			3
	-0.99554255E-08	0.36846719E-11	-0.54249049E 05	0.83834329E 01				4
C2	J 12/69C	20	00	00	OG	300.000	5000.000	1
	0.40435359E 01	0.20573654E-03	0.10907575E-06	-0.36427874E-10	0.34127865E-14			2
	0.99709486E 05	0.12775158E 01	0.74518140E 01	-0.10144686E-01	0.85879735E-05			3
	0.87321100E-09	-0.24429792E-11	0.98911989E 05	-0.15846678E 02				4
C2-	J 12/69C	2E	10	00	OG	300.000	5000.000	1
	0.36926257E 01	0.41576040E-03	0.11654211E-07	0.23755880E-11	-0.14585314E-14			2
	0.52118953E 05	0.22470173E 01	0.37342914E 01	-0.23034649E-02	0.68417833E-05			3
	-0.58120827E-08	0.16604296E-11	0.52281427E 05	0.27860423E 01				4
C2H	J 3/67C	2H	100	000	OG	300.000	5000.000	1
	0.44207650E 01	0.22119303E-02	-0.59294945E-06	0.94195775E-10	-0.68527594E-14			2
	0.55835444E 05	-0.11588093E 01	0.26499400E 01	0.84919515E-02	-0.98165375E-05			3
	0.65373629E-08	-0.17356273E-11	0.56275751E 05	0.76898609E 01				4
C2H2	J 3/61C	2H	200	000	OG	300.000	5000.000	1
	0.45751083E 01	0.51238358E-02	-0.17452354E-05	0.28673065E-09	-0.17951426E-13			2
	0.25607428E 05	-0.35737940E 01	0.14102768E 01	0.19057275E-01	-0.24501390E-04			3
	0.16390872E-07	-0.41345447E-11	0.26188208E 05	0.11393827E 02				4
C2H4	J 9/65C	2H	400	000	OG	300.000	5000.000	1
	0.34552152E 01	0.11491803E-01	-0.43651750E-05	0.76155095E-09	-0.50123200E-13			2
	0.44773119E 04	0.26987959E 01	0.14256821E 01	0.11383140E-01	0.79890006E-05			3
	-0.16253679E-07	0.67491256E-11	0.53370755E 04	0.14621819E 02				4
C2H6	L 5/72C	2H	6	0	OG	300.000	1500.000	1
	0.21555281E+01	0.14779861E-01	0.23352804E-05	-0.64146428E-08	0.19036925E-11			2
	-0.11524517E+05	0.10776316E+02	0.21415788E+01	0.10529720E-01	0.18730274E-04			3
	-0.26691187E-07	0.10049332E-10	-0.11410486E+05	0.11647757E+02				4
C2N	J 3/67C	2N	100	000	OG	300.000	5000.000	1
	0.61931308E 01	0.14327539E-02	-0.61255161E-06	0.11578707E-09	-0.80401339E-14			2
	0.64818372E 05	-0.84132298E 01	0.32670394E 01	0.98211307E-02	-0.83284733E-05			3
	0.17650559E-08	0.59632768E-12	0.65589057E 05	0.65682304E 01				4
C2N2	J 3/61C	2N	200	000	OG	300.000	5000.000	1
	0.65968935E 01	0.38694131E-02	-0.15516161E-05	0.28141546E-09	-0.19069442E-13			2
	0.34883726E 05	-0.10001801E 02	0.39141782E 01	0.14011008E-01	-0.17404350E-04			3
	0.12012779E-07	0.33565772E-11	0.35514550E 05	0.32384353E 01				4
C2O	J 9/66C	2O	100	000	OG	300.000	5000.000	1
	0.48990313E 01	0.28430384E-02	-0.10209669E-05	0.16112165E-09	-0.95542914E-14			2
	0.32800545E 05	-0.91382280E 00	0.35364815E 01	0.69543872E-02	-0.53071374E-05			3
	0.17030470E-08	-0.14108072E-13	0.33151572E 05	0.60172370E 01				4
C3	J 12/69C	30	00	00	OG	300.000	5000.000	1
	0.36815361E 01	0.24165236E-02	-0.84348112E-06	0.14508198E-09	-0.95697300E-14			2
	0.97413955E 05	0.68377802E 01	0.57408464E 01	-0.84281238E-02	0.18620198E-04			3
	-0.14510529E-07	0.39676977E-11	0.97157524E 05	-0.23837376E 01				4
C3H8	J 5/85C	3H	800	00	OG	300.000	5000.000	1
	0.30340000E 01	0.25370000E-01	-0.91790000E-05	0.14840000E-08	-0.88740000E-13			2
	-0.14520000E 05	0.77030000E 01	0.32120000E 01	0.16420000E-01	0.16790000E-04			3
	-0.21560000E-07	0.57540000E-11	-0.14290000E 05	0.86560000E 01				4
C3H8O	S27/86C	3H	80	100	OG	300.000	5000.000	1
	0.19830000E 02	0.43830000E-02	-0.19390000E-05	0.35280000E-09	-0.22810000E-13			2
	-0.40170000E 05	-0.81630000E 02	0.54170000E 01	-0.88930000E-02	0.11760000E-03			3
	-0.14940000E-06	0.57910000E-10	-0.33100000E 05	0.68730000E 01				4
C3O2	J 6/68C	3O	20	00	OG	300.000	5000.000	1
	0.81435964E 01	0.54395018E-02	-0.22192869E-05	0.40778627E-09	-0.27915974E-13			2
	-0.14230013E 05	-0.15456769E 02	0.37161005E 01	0.19872164E-01	-0.20935751E-04			3
	0.11750112E-07	-0.26589416E-11	0.13089402E 05	0.69298412E 01				4
C4	J 12/69C	40	00	00	OG	300.000	5000.000	1
	0.65602101E 01	0.40985234E-02	-0.17000471E-05	0.31615228E-09	-0.21842144E-13			2
	0.11430434E 06	-0.11820311E 02	0.18432021E 01	0.19343592E-01	-0.20627502E-04			3
	0.10822626E-07	-0.21289203E-11	0.11550276E 06	0.12006898E 02				4
C5	J 12/69C	50	00	00	OG	300.000	5000.000	1
	0.82067016E 01	0.54889888E-02	-0.22694876E-05	0.42073365E-09	-0.28981924E-13			2
	0.11463647E 06	-0.20246108E 02	0.11012446E 01	0.29513421E-01	-0.33754342E-04			3
	0.19056534E-07	-0.40989018E-11	0.11637970E 06	0.15360193E 02				4

H	J 9/65H	100	000	000	OG	300.000	5000.000	1
0.25000000E	01 0.	0.	0.	0.	0.	0.	0.	2
0.25471627E	05-0.46011763E	00	0.25000000E	01 0.	0.	0.	0.	3
0.	0.	0.25471627E	05-0.46011762E	00				4
H+	J 6/66H	1E	-100	000	OG	300.000	5000.000	1
0.25000000E	01 0.	0.	0.	0.	0.	0.	0.	2
0.18403344E	06-0.11538620E	01	0.25000000E	01 0.	0.	0.	0.	3
0.	0.	0.18403344E	06-0.11538621E	01				4
H-	J 9/65H	1E	100	000	OG	300.000	5000.000	1
0.25000000E	01 0.	0.	0.	0.	0.	0.	0.	2
0.15961045E	05-0.11524488E	01	0.25000000E	01 0.	0.	0.	0.	3
0.	0.	0.15961045E	05-0.11524486E	01				4
HCN	L12/69H	1C	1N	10	OG	300.000	5000.000	1
0.37068121E	01 0.33382803E	-02-0.11913320E	-05	0.19992917E	-09-0.12826452E	-13		2
0.14962636E	05 0.20794904E	01 0.24513556E	01 0.87208371E	-02-0.10094203E	-04			3
0.67255698E	-08-0.17626959E	-11 0.15213002E	05 0.80830085E	01				4
HCO	J12/70H	1C	10	10	OG	300.000	5000.000	1
0.34738348E	+01 0.34370227E	-02-0.13632664E	-05 0.24928645E	-09-0.17044331E	-13			2
0.39594005E	+04 0.60453340E	+01 0.38840192E	+01-0.82974448E	-03 0.77900809E	-05			3
-0.70616962E	-08 0.19971730E	-11 0.40563860E	+04 0.48354133E	+01				4
HCO+	J12/70H	1C	10	1E	-1G	300.000	5000.000	1
0.37411880E	+01 0.33441517E	-02-0.12397121E	-05 0.21189388E	-09-0.13704150E	-13			2
0.98884078E	+05 0.20654768E	+01 0.24739736E	+01 0.86715590E	-02-0.10031500E	-04			3
0.67170527E	-08-0.17872674E	-11 0.99146608E	+05 0.81625751E	+01				4
HNCO	J12/70H	1N	1C	10	1G	300.000	5000.000	1
0.51300390E	+01 0.43551371E	-02-0.16269022E	-05 0.28035605E	-09-0.18276037E	-13			2
-0.14101787E	+05-0.22010995E	+01 0.23722164E	+01 0.13664040E	-01-0.13323158E	-04			3
0.64475457E	-08-0.10402894E	-11-0.13437059E	+05 0.11588263E	+02				4
HNO	J 3/63H	1N	10	10	OG	300.000	5000.000	1
0.35548619E	01 0.32713182E	-02-0.12734071E	-05 0.22602046E	-09-0.15064827E	-13			2
0.10693734E	05 0.51684901E	01 0.37412008E	01-0.20067061E	-03 0.75409300E	-05			3
-0.79105713E	-08 0.25928389E	-11 0.10817845E	05 0.50063473E	01				4
HNO2	J 6/63H	1N	10	2	OG	300.000	5000.000	1
0.55144941E	+01 0.41394403E	-02-0.15878702E	-05 0.27977639E	-09-0.18584209E	-13			2
-0.11276885E	+05-0.31425253E	+01 0.25098874E	+01 0.12171605E	-01-0.78618375E	-05			3
0.35351571E	-09 0.11540858E	-11-0.10450008E	+05 0.12399634E	+02				4
HNO3	J 6/63H	1N	10	3	OG	300.000	5000.000	1
0.70591100E	+01 0.567694446E	-02-0.22348863E	-05 0.40155529E	-09-0.27080510E	-13			2
-0.18920009E	+05-0.10778285E	+02 0.14377135E	+01 0.20903552E	-01-0.14574553E	-04			3
0.11972023E	-08 0.19117285E	-11-0.17385368E	+05 0.18246253E	+02				4
HO2	J 3/64H	10	200	000	OG	300.000	5000.000	1
0.37866280E	01 0.27885404E	-02-0.10168708E	-05 0.17183946E	-09-0.11021852E	-13			2
0.11888500E	04 0.48147611E	01 0.35094850E	01 0.11499670E	-02 0.58784259E	-05			3
-0.77795519E	-08 0.29607883E	-11 0.13803331E	04 0.68276325E	01				4
H2	J 3/61H	20	00	00	OG	300.000	5000.000	1
0.31001901E	01 0.51119464E	-03 0.52644210E	-07-0.34909973E	-10 0.36945345E	-14			2
-0.87738042E	03-0.19629421E	01 0.30574451E	01 0.26765200E	-02-0.58099162E	-05			3
0.55210391E	-08-0.18122739E	-11-0.98890474E	03-0.22997056E	01				4
H2O(S)	L11/65H	20	100	000	OS	200.000	273.150	1
0.	0.	0.	0.	0.	0.	0.	0.	2
0.	0.	-0.39269330E	-01 0.16920420E	-01 0.				3
0.	0.	-0.35949581E	05 0.56933784E	00				4
H2O(L)	L11/65H	20	100	000	OL	300.000	1000.0	1
0.	0.	0.	0.	0.	0.	0.	0.	2
0.	0.	0.12712782E	02-0.17662790E	-01-0.22556661E	-04			3
0.20820908E	-06-0.24078614E	-09-0.37483200E	05-0.59115345E	02				4
H2O	J 3/61H	20	100	000	OG	300.000	5000.000	1
0.27167633E	01 0.29451374E	-02-0.80224374E	-06 0.10226682E	-09-0.48472145E	-14			2
-0.29905826E	05 0.66305671E	01 0.40701275E	01-0.11084499E	-02 0.41521180E	-05			3
-0.29637404E	-08 0.80702103E	-12-0.30279722E	05-0.32270046E	00				4
H2O2	L 2/69H	20	20	00	OG	300.000	5000.000	1
0.45731667E	01 0.43361363E	-02-0.14746888E	-05 0.23489037E	-09-0.14316536E	-13			2
-0.18006961E	05 0.50113696E	00 0.33887536E	01 0.65692260E	-02-0.14850126E	-06			3
-0.46258055E	-08 0.24715147E	-11-0.17663147E	05 0.67853631E	01				4
N	J 3/61N	100	000	000	OG	300.000	5000.000	1
0.24502682E	01 0.10661458E	-03-0.74653373E	-07 0.18796524E	-10-0.10259839E	-14			2
0.56116040E	05 0.44487581E	01 0.25030714E	01-0.21800181E	-04 0.54205287E	-07			3
-0.56475602E	-10 0.20999044E	-13 0.56098904E	05 0.41675764E	01				4
NCO	J12/70N	1C	10	10	OG	300.000	5000.000	1
0.49964357E	+01 0.26250880E	-02-0.10928387E	-05 0.20309111E	-09-0.13915195E	-13			2
0.17379356E	+05-0.17325320E	+01 0.31092021E	+01 0.66201022E	-02-0.26070086E	-05			3
-0.14966380E	-08 0.10922032E	-11 0.17977514E	+05 0.83561334E	+01				4

NH	J12/71N	1H	1	0	OG	300.000	5000.000	1	
0.27789900E+01	0.13266349E-02-0.41101218E-06	0.69414505E-10-0.44536190E-14						2	
0.44567973E+05	0.57593434E+01	0.34936318E+01	0.24529034E-03-0.12578521E-05					3	
0.22011922E-08-0.92288834E-12	0.44326826E+05	0.18451723E+01						4	
NH2	J12/65N	1H	200	000	OG	300.000	5000.000	1	
0.25769524E 01	0.35896090E-02-0.12276328E-05	0.19549576E-09-0.11873401E-13						2	
0.19335912E 05	0.79074890E 01	0.40385791E 01-0.10098163E-02	0.40120903E-05					3	
-0.23085312E-08	0.39022887E-12	0.18973010E 05	0.52464285E 00					4	
NH3	J 9/65N	1H	300	000	OG	300.000	5000.000	1	
0.24165177E 01	0.61871211E-02-0.21785136E-05	0.37599090E-09-0.24448856E-13						2	
-0.64747177E 04	0.77043482E 01	0.35912768E 01	0.49388668E-03 0.83449322E-05					3	
-0.83833385E-08	0.27299092E-11-0.66717143E 04	0.22520966E 01						4	
NO	J 6/63N	1O	100	000	OG	300.000	5000.000	1	
0.31890000E 01	0.13382281E-02-0.52899318E-06	0.95919332E-10-0.64847932E-14						2	
0.98283290E 04	0.67458126E 01	0.40459521E 01-0.34181783E-02	0.79819190E-05					3	
-0.61139316E-08	0.15919076E-11	0.97453934E 04	0.29974988E 01					4	
NO+	J 6/66N	1O	1E	-100	OG	300.000	5000.000	1	
0.28885488E 01	0.15217119E-02-0.57531241E-06	0.10051081E-09-0.66044294E-14						2	
0.11819245E 06	0.70027197E 01	0.36685056E 01-0.11544580E-02	0.21755608E-05					3	
-0.48227472E-09-0.27847906E-12	0.11803369E 06	0.31779324E 01						4	
NO2	J 9/64N	1O	200	000	OG	300.000	5000.000	1	
0.46240771E 01	0.25260332E-02-0.10609498E-05	0.19879239E-09-0.13799384E-13						2	
0.22899900E 04	0.13324138E 01	0.34589236E 01	0.20647064E-02 0.66866067E-05					3	
-0.95556725E-08	0.36195881E-11	0.28152265E 04	0.83116983E 01					4	
NO2-	J 6/72N	1O	2E	1	OG	300.000	5000.000	1	
0.50160903E+01	0.21884463E-02-0.94586144E-06	0.17939789E-09-0.12052428E-13						2	
-0.26200160E+05-0.12861447E+01	0.29818036E+01	0.49398681E-02 0.28557293E-05						3	
-0.78905297E-08	0.35391483E-11-0.25501540E+05	0.99161680E+01						4	
NO3	J12/64N	1O	3	0	OG	300.000	5000.000	1	
0.72033289E+01	0.30908791E-02-0.13329045E-05	0.25461601E-09-0.17939047E-13						2	
0.58244016E+04-0.12608119E+02	0.76867377E+00	0.21181075E-01-0.16980256E-04						3	
0.22963836E-08	0.19321041E-11	0.75292921E+04	0.20406284E+02					4	
N2	J 9/65N	2O	00	00	OG	300.000	5000.000	1	
0.28963194E 01	0.15154866E-02-0.57235277E-06	0.99807393E-10-0.65223555E-14						2	
-0.90586184E 03	0.61615148E 01	0.36748261E 01-0.12081500E-02	0.23240102E-05					3	
-0.63217559E-09-0.22577253E-12-0.10611588E 04	0.23580424E 01							4	
N2H4	J12/65N	2H	400	000	OG	300.000	5000.000	1	
0.50947770E 01	0.93296138E-02-0.33626986E-05	0.56308304E-09-0.35859661E-13						2	
0.92996644E 04-0.35950952E 01	0.79803836E 00	0.21788097E-01-0.13456754E-04						3	
-0.12698753E-09	0.25865213E-11	0.10379887E 05	0.18248696E 02					4	
N2O	J12/64N	2O	100	000	OG	300.000	5000.000	1	
0.47306679E 01	0.28258267E-02-0.11558115E-05	0.21263683E-09-0.14564087E-13						2	
0.81617682E 04-0.17151073E 01	0.26189196E 01	0.86439616E-02-0.68110624E-05						3	
0.22275877E-08-0.80650330E-13	0.87590123E 04	0.92266952E 01						4	
N2O+	J12/70N	2O	1E	-10	OG	300.000	5000.000	1	
0.53926946E+01	0.22337196E-02-0.93548832E-06	0.17466166E-09-0.12059043E-13						2	
0.15847633E+06-0.36920186E+01	0.34273064E+01	0.63787690E-02-0.22585149E-05						3	
-0.20421800E-08	0.13481477E-11	0.15909237E+06	0.67997616E+01					4	
N2O4	J 9/64N	2O	400	000	OG	300.000	5000.000	1	
0.10506637E 02	0.58723267E-02-0.24766296E-05	0.46556024E-09-0.32402082E-13						2	
-0.28609096E 04-0.26252230E 02	0.36662865E 01	0.23491748E-01-0.16007297E-04						3	
0.11845939E-08	0.20001618E-11-0.90631797E 03	0.93973337E 01						4	
N2O5	J12/64N	2O	5	0	OG	300.000	5000.000	1	
0.14413736E+02	0.40494080E-02-0.17661640E-05	0.33912224E-09-0.23926356E-13						2	
-0.38366062E+04-0.43313433E+02	0.32144535E+01	0.37992511E-01-0.36847600E-04						3	
0.12409293E-07	0.24351911E-12-0.98609506E+03	0.13555831E+02						4	
N3	J12/70N	3O	00	00	OG	300.000	5000.000	1	
0.51996828E+01	0.24335678E-02-0.10192340E-05	0.19062350E-09-0.13212412E-13						2	
0.47963131E+05-0.35547759E+01	0.30624389E+01	0.73590658E-02-0.38229374E-05						3	
-0.71824202E-09	0.91110236E-12	0.48614547E+05	0.77570129E+01					4	
O	J 6/62O	1O	100	000	000	OG	300.000	5000.000	1
0.25420596E 01-0.27550619E-04-0.31028033E-08	0.45510674E-11-0.43680515E-15							2	
0.29230803E 05	0.49203080E 01	0.29464287E 01-0.16381665E-02	0.24210316E-05					3	
-0.16028432E-08	0.38906964E-12	0.29147644E 05	0.29639949E 01					4	
O+	L12/66O	1E	-100	000	OG	300.000	5000.000	1	
0.25060486E 01-0.14464249E-04	0.12446049E-07-0.46858472E-11	0.65548873E-15						2	
0.18794700E 06	0.43479741E 01	0.24984794E 01	0.11410972E-04-0.29761395E-07					3	
0.32246539E-10-0.12375517E-13	0.18794908E 06	0.43864355E 01						4	
O-	J 6/65O	1E	100	000	OG	300.000	5000.000	1	
0.25437173E 01-0.53258700E-04	0.25119617E-07-0.51851466E-11	0.39011542E-15						2	
0.11480516E 05	0.45202538E 01	0.28115796E 01	0.11905697E-02 0.18710553E-05					3	
-0.13479178E-08	0.36663554E-12	0.11428431E 05	0.32402855E 01					4	

<sup>H</sup>  
 OH J12/700 1H 10 00 OG 300.000 5000.000  
 0.29131230E+01 0.95418248E-03-0.19084325E-06 0.12730795E-10 0.24803941E-15  
 0.39647060E+04 0.54288735E+01 0.383655518E+01-0.10702014E-02 0.94849757E-06  
 0.20843575E-09-0.23384265E-12 0.36715807E+04 0.49805456E+00  
 OH+ J12/700 1H 1E -10 OG 300.000 5000.000  
 0.27381495E+01 0.14613173E-02-0.46950536E-06 0.73663560E-10-0.41410922E-14  
 0.15761683E+06 0.61343811E+01 0.35365969E+01-0.47029254E-04-0.62344259E-06  
 0.17601461E-08-0.82678699E-12 0.15736677E+06 0.18477172E+01  
 OH- J12/700 1H 1E 10 OG 300.000 5000.000  
 0.28881148E+01 0.96560229E-03-0.19659254E-06 0.14053802E-10 0.12080617E-15  
 -0.18086455E+05 0.41896259E+01 0.34621427E+01 0.40525802E-03-0.13516992E-05  
 0.17899459E-08-0.63434810E-12-0.18312355E+05 0.92893220E+00  
 O2 J 9/650 20 00 00 OG 300.000 5000.000  
 0.36219535E 01 0.73618264E-03-0.19652228E-06 0.36201558E-10-0.28945627E-14  
 -0.12019825E 04 0.36150960E 01 0.36255985E 01-0.18782184E-02 0.70554544E-05  
 -0.67635137E-08 0.21555993E-11-0.10475226E 04 0.43052778E 01  
 O2- J12/660 2E 100 000 OG 300.000 5000.000  
 0.38147234E 01 0.77444546E-03-0.30677649E-06 0.56618118E-10-0.38229492E-14  
 -0.69910087E 04 0.29587995E 01 0.31440525E 01 0.12127972E-02 0.23812161E-05  
 -0.40914092E-08 0.16885304E-11-0.67369752E 04 0.67688687E 01  
 O3 J 6/610 30 00 00 OG 300.000 5000.000  
 0.54665239E+01 0.17326031E-02-0.72204889E-06 0.13721660E-09-0.96233828E-14  
 0.15214096E+05-0.34712616E+01 0.24660617E+01 0.91703209E-02-0.49698480E-05  
 -0.20634230E-08 0.20015595E-11 0.16059556E+05 0.12172130E+02  
 C12H24 KEROSENE DATA FROM LIEW'S SNECKS (HT 4/6 1991)  
 1.72800000E+01 7.71300000E-02 6.68200000E-11-1.52900000E-14 1.15200000E-18  
 -4.12200000E+04 0.00000000E+00 1.72800000E+01 7.71300000E-02 8.05000000E-10  
 -9.19100000E-13 3.70800000E-16-4.12200000E+04 0.00000000E+00  
 END

B:4. The structure of LENNARD\_JONES.DAT

This file contains Lennard-Jones Potential Parameters

Source: <.....>

SPECIE	COLLISION COEFF	$\epsilon_{jj}/k_{LJ}$
N2	3.798	71.4
H	2.247	99.8
OH	3.110	93.8
O	3.068	102.2
HO2	4.200	289.0
CH3	3.822	136.5
CH2O	3.500	100.0
CHO	3.500	100.0
CH2	3.000	100.0
CH	3.000	100.0
CO	2.968	91.7
CO2	3.941	195.2
H2O	2.641	809.0
O2	3.467	106.7
CH4	3.758	148.6
H2	2.827	59.7
END		



## Appendix C

The example of VAX/VMS-command procedure for running SNECKS

```
$!A COMMAND FILE FOR RUNNING SNECKS WITH READCHKIN SUBROUTINE
$!HEIMO TUOVINEN 1991-06-24 Cranfield Institute of Technology/SME
$ SET DEF [JASMIN.ME008.TEMP]
$ FORTRAN READCHKIN
$ FORTRAN SNECKS_CH4
$ LINK SNECKS_CH4,READCHKIN
$ ASSIGN CH4VTR-60.RES FOR006
$ ASSIGN CH4VT-60.PLT FOR007
$ SHOW STATUS
$ RUN SNECKS_CH4
$ SHOW STATUS
$ RENAME SNECKSPLT.DAT CH4VTR-60.PLT
$ DELETE SNECKS_CH4.OBJ;*
$ DELETE READCHKIN.OBJ;*
$ DELETE SNECKS_CH4.EXE;*
$ DELETE SNECKS_CH4.LIS;*
$ DELETE READCHKIN.LIS;*
$ DELETE *.MAP;*
$ DEASSIGN FOR006
```



Appendix D: Output file from SNECKS, SNE\_OUT.DAT

\*\*\*\*\* RESULTS FROM READCHKIN RUN \*\*\*\*\*

CHEMICAL REACTION SCHEME HAS BEEN READ

THE MODEL CONTAINS:

4 ELEMENTS  
 11 SPECIES  
 13 REACTION STEPS  
 1 IRREVERSIBLE REACTIONS  
 12 REVERSIBLE REACTIONS

ELEMENTS:

SYMBOL	ATOMIC WEIGHT	NAME
====	=====	====
O	15.999400	OXYGEN
C	12.011000	CARBON
H	1.008000	HYDROGEN
N	14.006700	NITROGEN

SPECIES:

SYMBOL	MOLECULAR WEIGHT
====	=====
N2	28.0134
H	1.0080
OH	17.0074
O	15.9994
HO2	33.0068
CO	28.0104
CO2	44.0098
H2O	18.0154
O2	31.9988
CH4	16.0430
H2	2.0160

NUMBER OF ELEMENTS IN SPECIES

	O	C	H	N
N2	0	0	0	2
H	0	0	1	0
OH	1	0	1	0
O	1	0	0	0
HO2	2	0	1	0
CO	1	1	0	0
CO2	2	1	0	0
H2O	1	0	2	0
O2	2	0	0	0
CH4	0	1	4	0
H2	0	0	2	0

REACTIONS:

RSE REACTION	FORWARD REACTION	REVE
NO. REACTION 1/cm3] Temp.exp. Eact [Cal]	A[mol/cm3] Temp.exp. Eact [Cal]	A[mo
====	=====	====
1 O + H2O = OH + OH 5.5E+08 0.00 0.0	17.6E+09 -0.02 16747.3	1

2	H	+ H	=	H2		10.0E+11	-1.00	0.0
1.5E+03	-0.82	103328.0						
3	O	+ O	=	O2		60.0E+01	0.00	0.0
8.3E+09	-1.00	119837.0						
4	H	+ OH	=	H2O		20.0E+16	-2.00	0.0
2.0E+12	0.00	105217.0						
5	H	+ O2	=	OH	+ O	20.0E+10	0.00	16665.8
6.5E+08	0.27	0.0						
6	O	+ H2	=	OH	+ H	60.0E+09	0.00	10008.6
9.4E+09	-0.03	8059.0						
7	O2	+ H	=	HO2		15.0E+08	0.00	994.5
1.0E+11	0.00	46039.0						
8	H	+ HO2	=	OH	+ OH	15.9E+10	0.00	1080.0
2.6E+09	0.00	39873.0						
9	CO	+ OH	=	CO2	+ H	15.0E+07	0.00	1000.5
5.0E+09	0.00	23519.0						
10	H2	+ OH	=	H2O	+ H	15.0E+09	0.00	5004.3
5.5E+09	-0.01	19802.0						
11	CO	+ O	=	CO2		60.0E+06	0.00	0.0
3.1E+09	-0.58	125843.0						
12	H	+ O	=	OH		30.0E+07	0.00	0.0
9.6E+09	0.21	101379.0						
13	2CH4	+ O2	-	2CO	+ 4H2	17.5E+06	1.00	24265.7

REACTION : 1 \*\*\* REVERSIBLE REACTION \*\*\*\*

LEFT HAND SIDE:

SPEC. INDEX	STM.CONST.	SPECIE
4	1	O
8	1	H2O

RIGHT HAND SIDE:

SPEC. INDEX	STM.CONST.	SPECIE
3	1	OH
3	1	OH

REACTION : 2 \*\*\* REVERSIBLE REACTION \*\*\*\*

LEFT HAND SIDE:

SPEC. INDEX	STM.CONST.	SPECIE
2	1	H
2	1	H

RIGHT HAND SIDE:

SPEC. INDEX	STM.CONST.	SPECIE
11	1	H2

REACTION : 3 \*\*\* REVERSIBLE REACTION \*\*\*\*

LEFT HAND SIDE:

SPEC. INDEX	STM.CONST.	SPECIE
4	1	O
4	1	O

RIGHT HAND SIDE:

SPEC. INDEX	STM.CONST.	SPECIE
9	1	O2

REACTION : 4 \*\*\* REVERSIBLE REACTION \*\*\*\*

LEFT HAND SIDE:

SPEC. INDEX	STM.CONST.	SPECIE
2	1	H
3	1	OH

RIGHT HAND SIDE:

SPEC. INDEX	STM.CONST.	SPECIE
8	1	H2O

REACTION : 5 \*\*\* REVERSIBLE REACTION \*\*\*\*

LEFT HAND SIDE:

SPEC. INDEX	STM.CONST.	SPECIE
2	1	H
9	1	O2

RIGHT HAND SIDE:

SPEC. INDEX STM.CONST. SPECIE  
3 1 OH  
4 1 O

REACTION : 6 \*\*\* REVERSIBLE REACTION \*\*\*\*

LEFT HAND SIDE:

SPEC. INDEX STM.CONST. SPECIE  
4 1 O  
11 1 H2

RIGHT HAND SIDE:

SPEC. INDEX STM.CONST. SPECIE  
3 1 OH  
2 1 H

REACTION : 7 \*\*\* REVERSIBLE REACTION \*\*\*\*

LEFT HAND SIDE:

SPEC. INDEX STM.CONST. SPECIE  
9 1 O2  
2 1 H

RIGHT HAND SIDE:

SPEC. INDEX STM.CONST. SPECIE  
5 1 HO2

REACTION : 8 \*\*\* REVERSIBLE REACTION \*\*\*\*

LEFT HAND SIDE:

SPEC. INDEX STM.CONST. SPECIE  
2 1 H  
5 1 HO2

RIGHT HAND SIDE:

SPEC. INDEX STM.CONST. SPECIE  
3 1 OH  
3 1 OH

REACTION : 9 \*\*\* REVERSIBLE REACTION \*\*\*\*

LEFT HAND SIDE:

SPEC. INDEX STM.CONST. SPECIE  
6 1 CO  
3 1 OH

RIGHT HAND SIDE:

SPEC. INDEX STM.CONST. SPECIE  
7 1 CO2  
2 1 H

REACTION : 10 \*\*\* REVERSIBLE REACTION \*\*\*\*

LEFT HAND SIDE:

SPEC. INDEX STM.CONST. SPECIE  
11 1 H2  
3 1 OH

RIGHT HAND SIDE:

SPEC. INDEX STM.CONST. SPECIE  
8 1 H2O  
2 1 H

REACTION : 11 \*\*\* REVERSIBLE REACTION \*\*\*\*

LEFT HAND SIDE:

SPEC. INDEX STM.CONST. SPECIE  
6 1 CO  
4 1 O

RIGHT HAND SIDE:

SPEC. INDEX STM.CONST. SPECIE  
7 1 CO2

REACTION : 12 \*\*\* REVERSIBLE REACTION \*\*\*\*

LEFT HAND SIDE:

SPEC. INDEX STM.CONST. SPECIE

2 1 H  
 4 1 O  
 RIGHT HAND SIDE:  
 SPEC. INDEX STM.CONST. SPECIE  
 3 1 OH

REACTION : 13 \*\*\* IRREVERSIBLE REACTION \*\*\*\*  
 LEFT HAND SIDE:  
 SPEC. INDEX STM.CONST. SPECIE  
 10 2 CH4  
 9 1 O2  
 RIGHT HAND SIDE:  
 SPEC. INDEX STM.CONST. SPECIE  
 6 2 CO  
 11 4 H2

THERMODYNAMIC DATA HAS BEEN READ

N2 2.896319 1.5154866E-03 -5.7235275E-07 9.9807392E-11 -6.5223557E-15  
 -905.8618 6.161515  
 3.674826 -1.2081499E-03 2.3240102E-06 -6.3217559E-10 -2.2577253E-13  
 -1061.159 2.358042

H 2.500000 0.0000000E+00 0.0000000E+00 0.0000000E+00 0.0000000E+00  
 25471.63 -0.4601176  
 2.500000 0.0000000E+00 0.0000000E+00 0.0000000E+00 0.0000000E+00  
 25471.63 -0.4601176

OH 2.913123 9.5418247E-04 -1.9084325E-07 1.2730795E-11 2.4803941E-16  
 3964.706 5.428874  
 3.836552 -1.0702014E-03 9.4849759E-07 2.0843575E-10 -2.3384265E-13  
 3671.581 0.4980546

O 2.542060 -2.7550619E-05 -3.1028033E-09 4.5510674E-12 -4.3680515E-16  
 29230.80 4.920308  
 2.946429 -1.6381665E-03 2.4210317E-06 -1.6028432E-09 3.8906964E-13  
 29147.64 2.963995

HO2 3.786628 2.7885404E-03 -1.0168708E-06 1.7183946E-10 -1.1021852E-14  
 1188.850 4.814761  
 3.509485 1.1499670E-03 5.8784258E-06 -7.7795521E-09 2.9607883E-12  
 1380.333 6.827632

CO 2.984070 1.4891390E-03 -5.7899683E-07 1.0364577E-10 -6.9353550E-15  
 -14245.23 6.347916  
 3.710093 -1.6190964E-03 3.6923593E-06 -2.0319675E-09 2.3953344E-13  
 -14356.31 2.955535

CO2 4.460804 3.0981719E-03 -1.2392571E-06 2.2741325E-10 -1.5525955E-14  
 -48961.44 -0.9863598  
 2.400780 8.7350961E-03 -6.6070879E-06 2.0021862E-09 6.3274039E-16  
 -48377.53 9.695146

H2O 2.716763 2.9451374E-03 -8.0224373E-07 1.0226682E-10 -4.8472147E-15  
 -29905.83 6.630567  
 4.070127 -1.1084499E-03 4.1521180E-06 -2.9637404E-09 8.0702101E-13  
 -30279.72 -0.3227005

O2 3.621953 7.3618261E-04 -1.9652228E-07 3.6201559E-11 -2.8945627E-15  
 -1201.983 3.615096  
 3.625598 -1.8782184E-03 7.0554543E-06 -6.7635137E-09 2.1555993E-12  
 -1047.523 4.305278

CH4 1.502707 1.0416798E-02 -3.9181523E-06 6.7777900E-10 -4.4283706E-14  
 -9978.708 10.70714  
 3.826193 -3.9794580E-03 2.4558340E-05 -2.2732927E-08 6.9626956E-12  
 -10144.95 0.8669007

H2 3.100190 5.1119464E-04 5.2644211E-08 -3.4909974E-11 3.6945345E-11  
 -877.3804 -1.962942

3.057445      2.6765200E-03 -5.8099163E-06  5.5210392E-09 -1.8122739E-12  
-988.9047    -2.299706

LENNARD-JONES PARAMETERS HAS BEEN READ

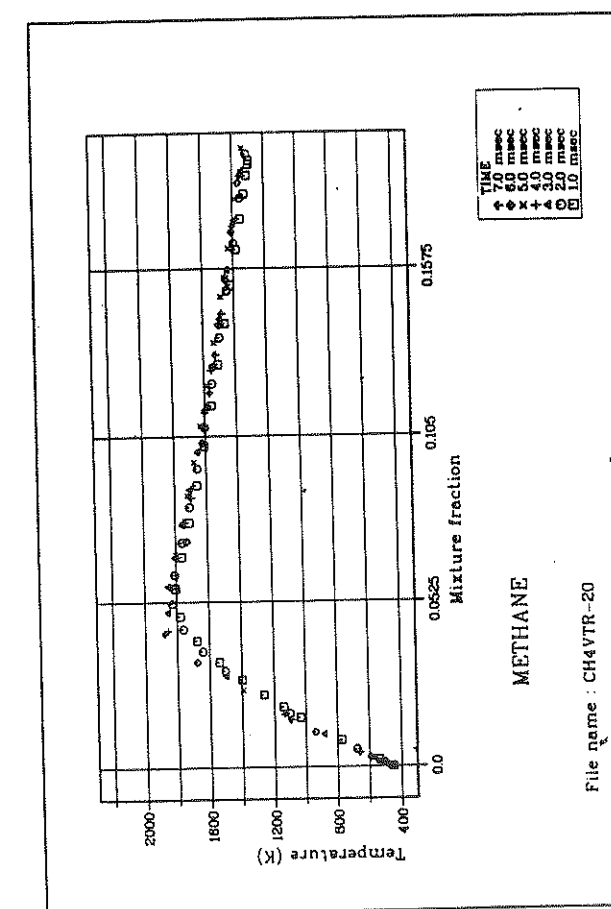
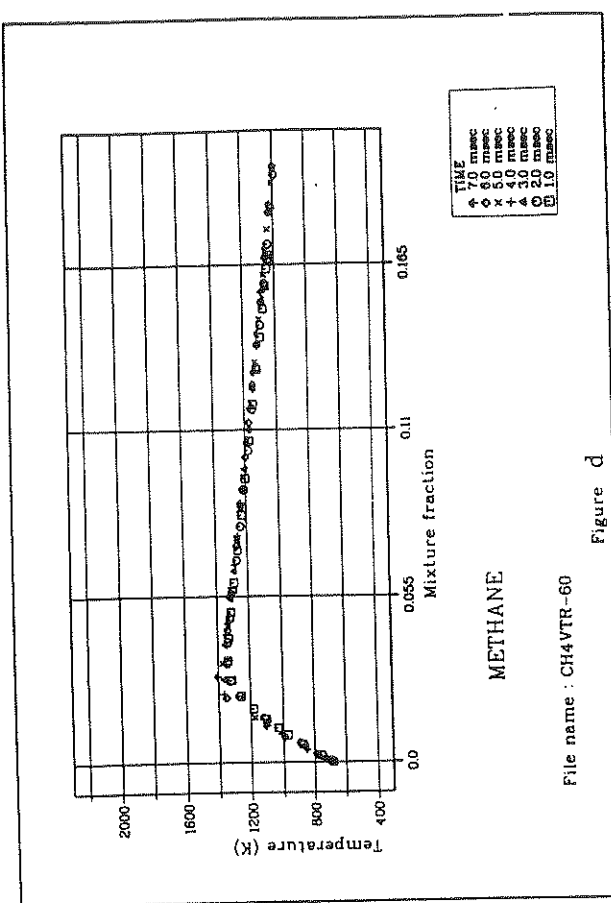
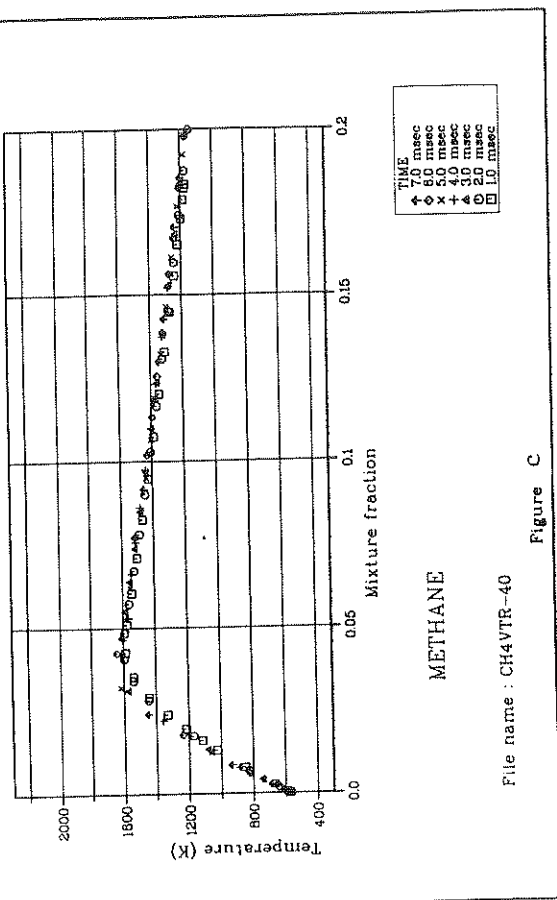
SPECIE	COLL COEFF	EPS/K
N2	3.798	71.4
H	2.247	99.8
OH	3.110	93.8
O	3.068	102.2
HO2	4.200	289.0
CO	2.968	91.7
CO2	3.941	195.2
H2O	2.641	809.0
O2	3.467	106.7
CH4	3.758	148.6
H2	2.827	59.7

NUMBER OF WARNINGS: 0



Appendix E

Figure E1



E1

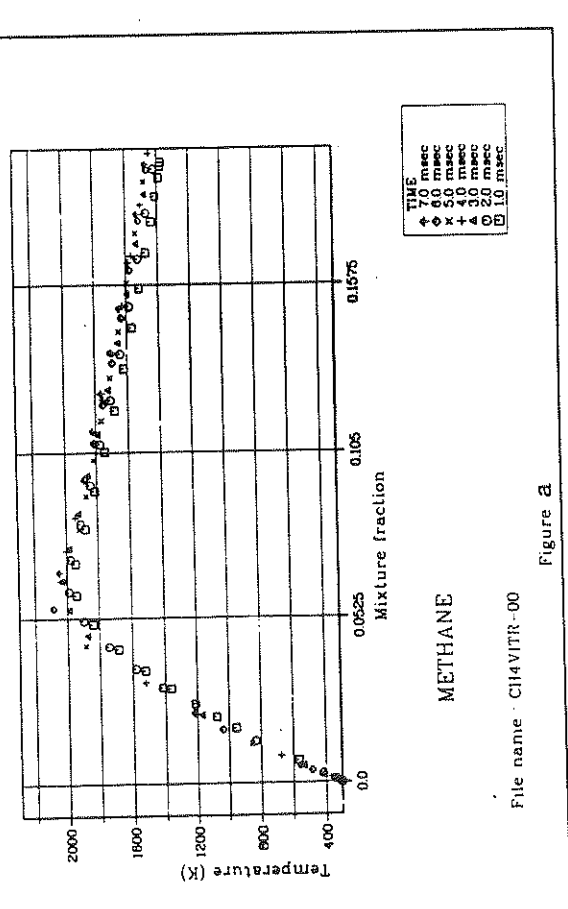


Figure E2

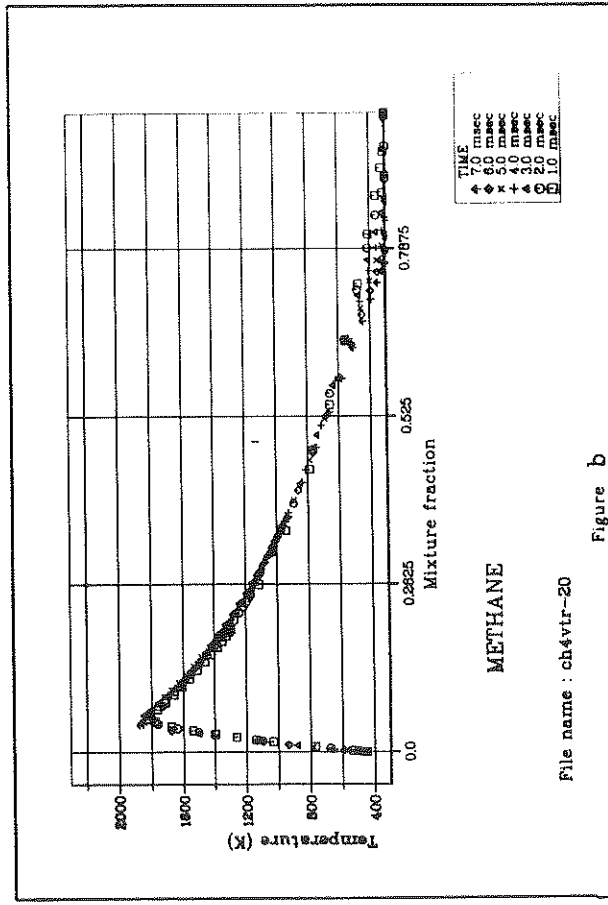
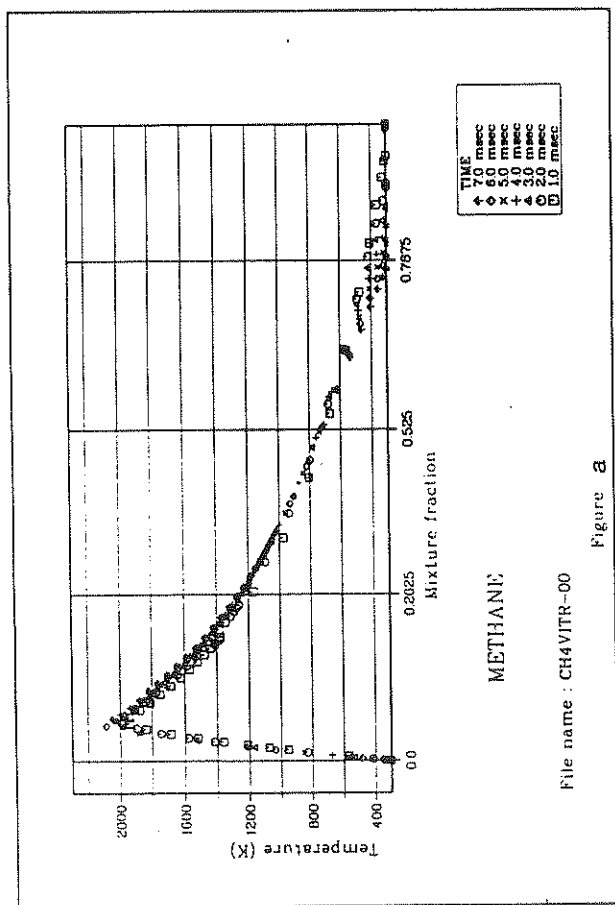
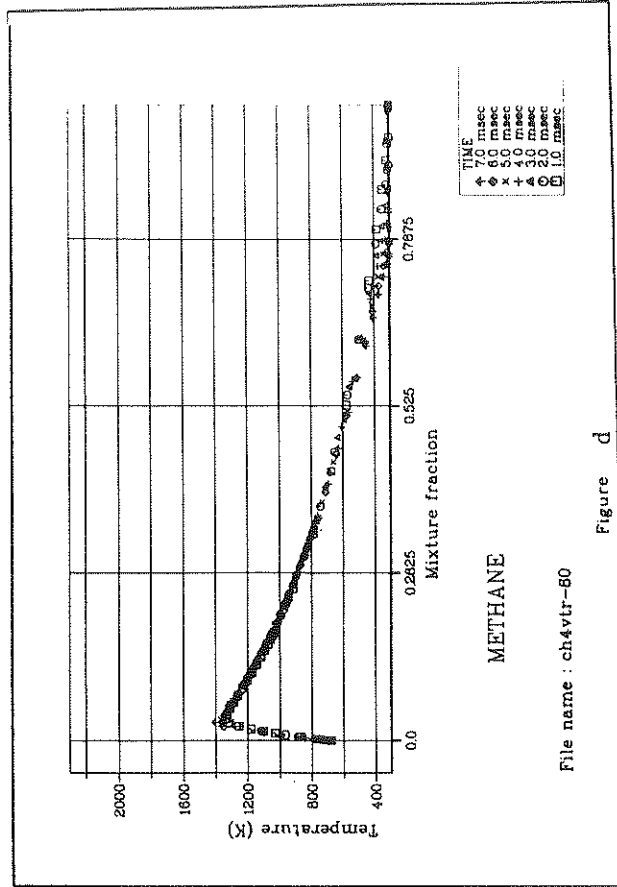
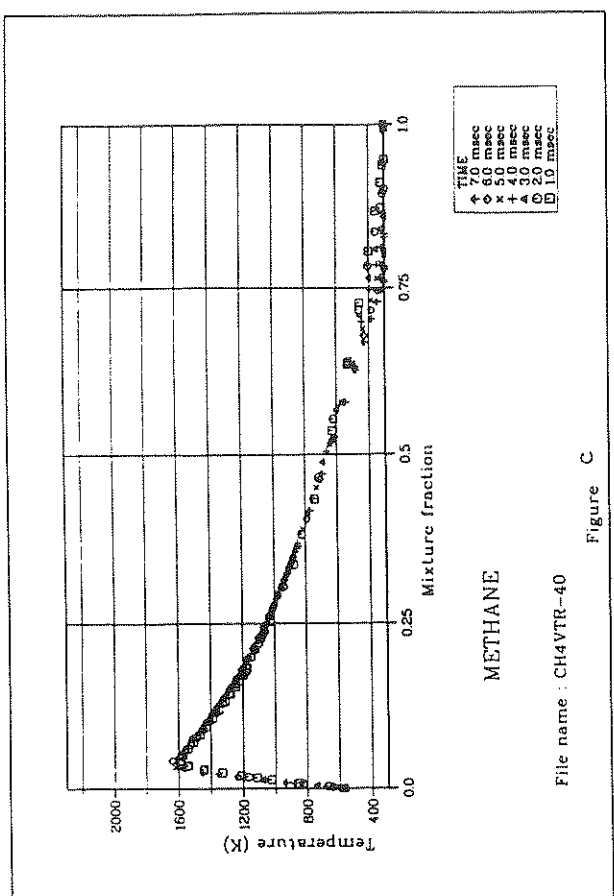


Figure E3

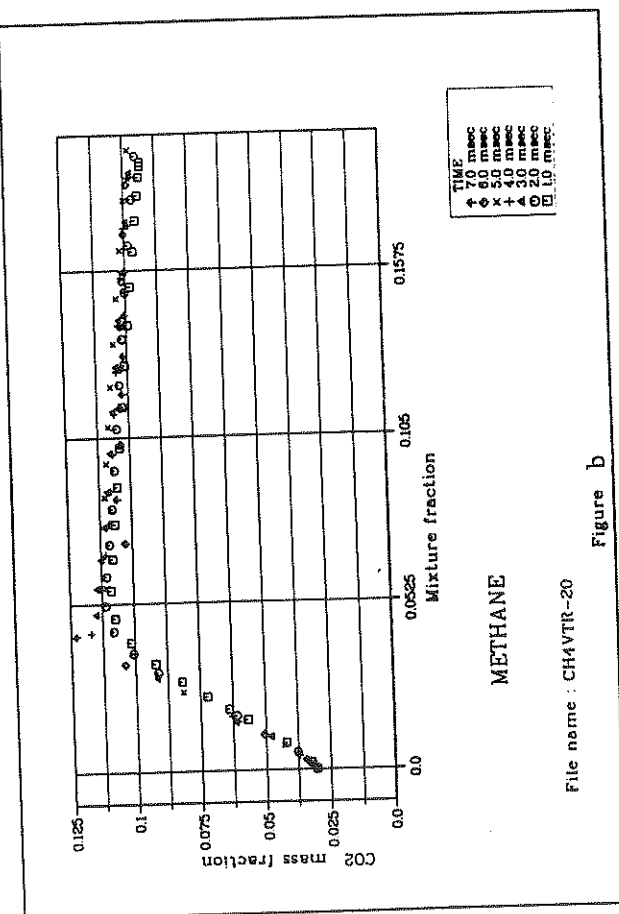
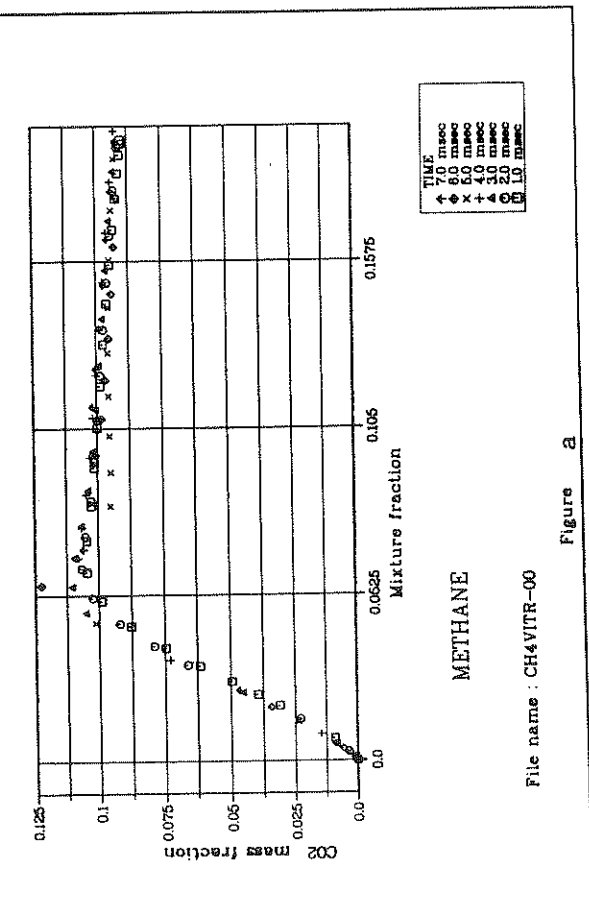
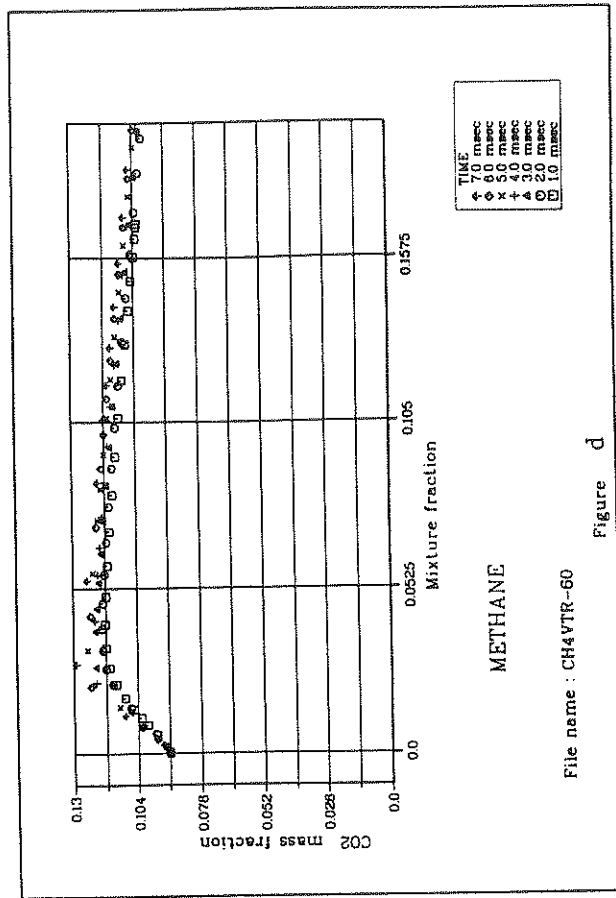
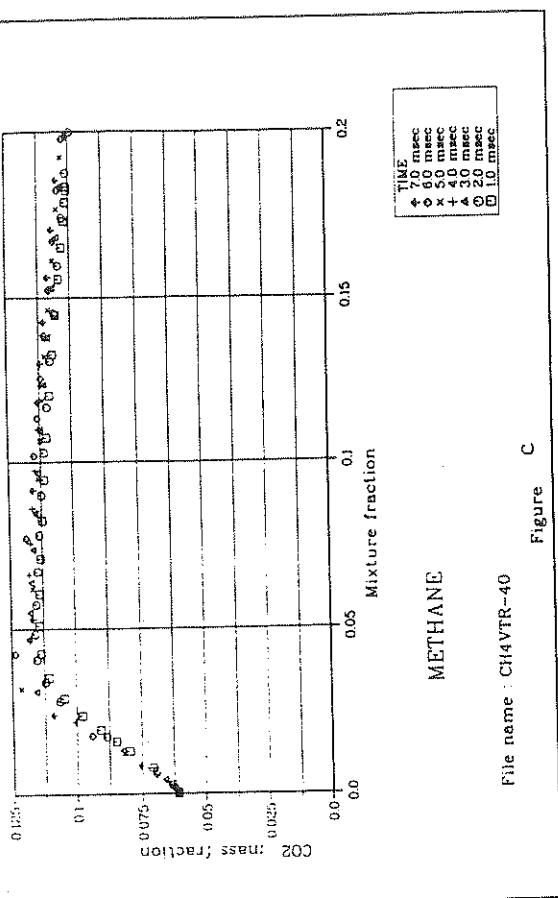


Figure E4

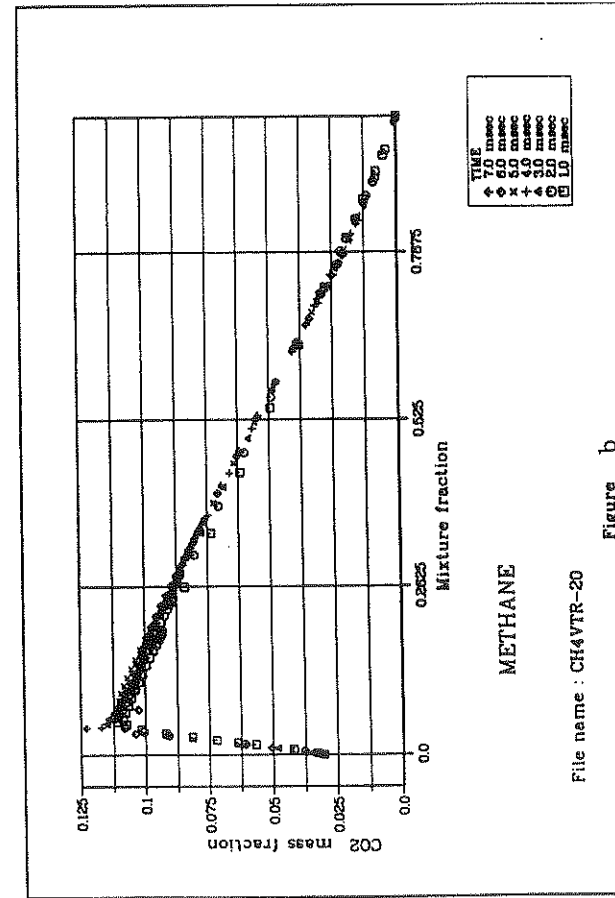
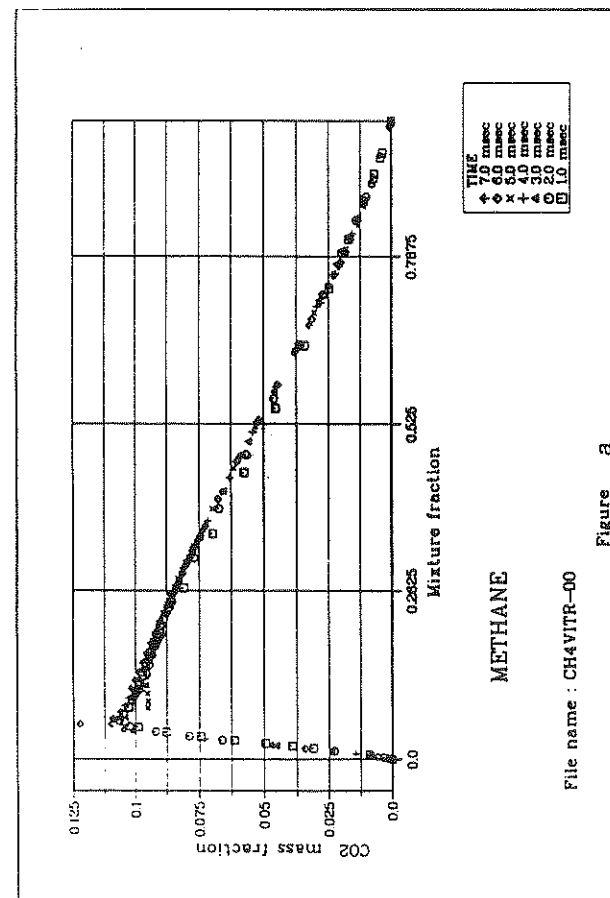
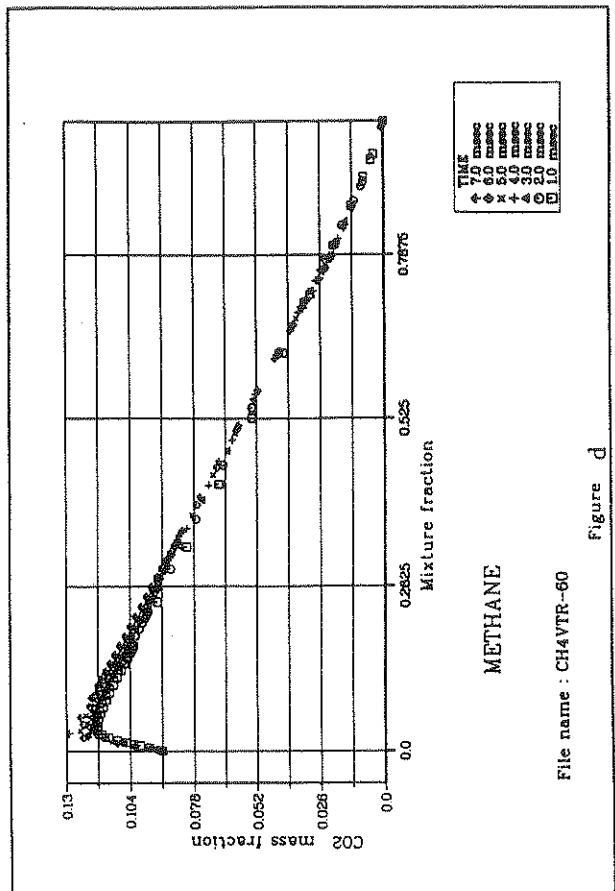
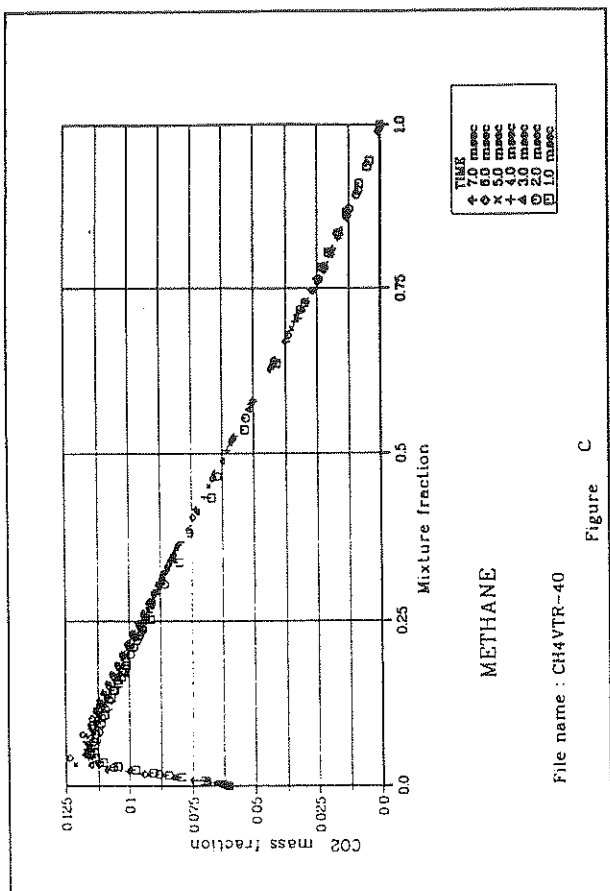


Figure E5

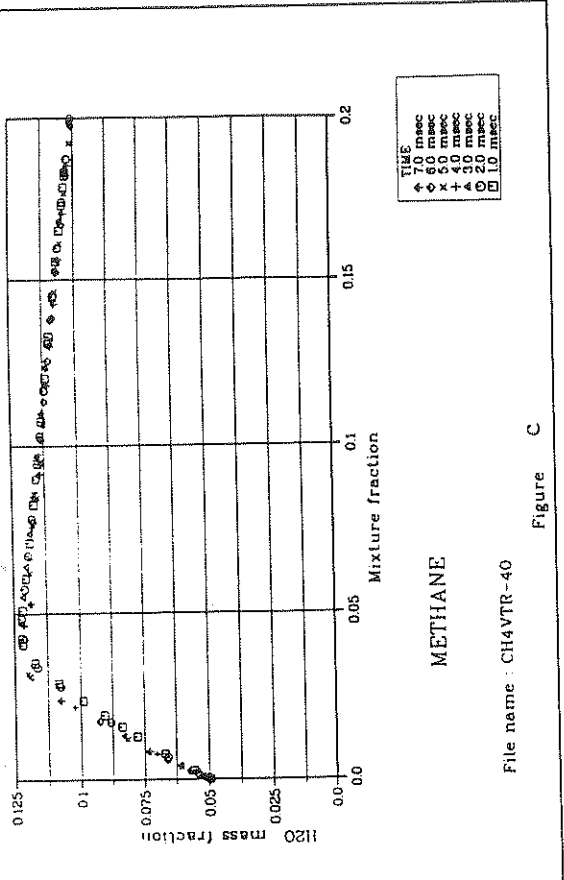
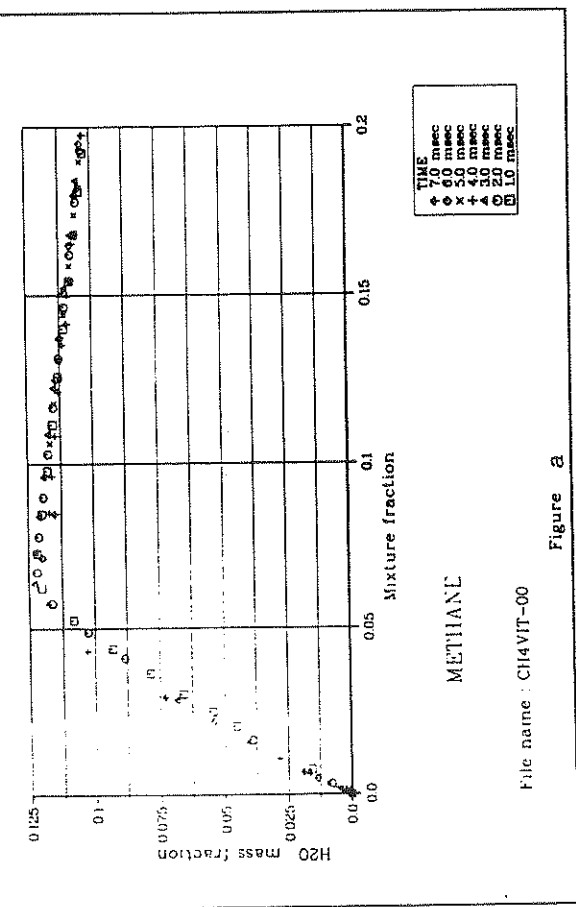
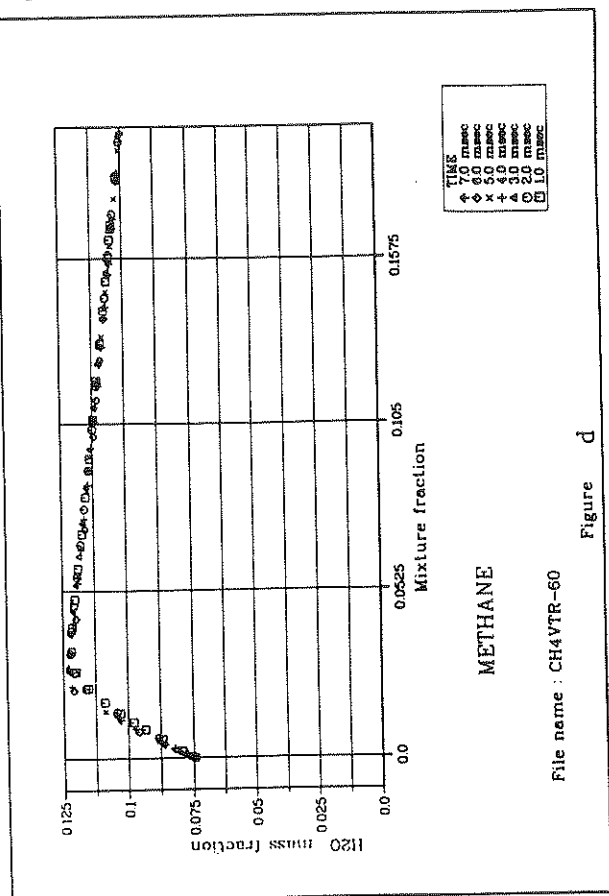


Figure c



E5

Figure E6

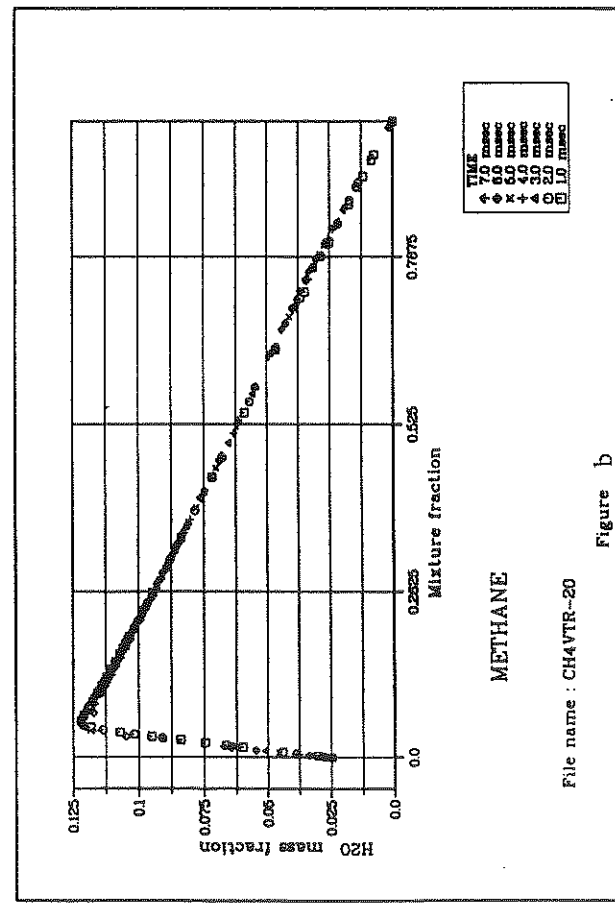
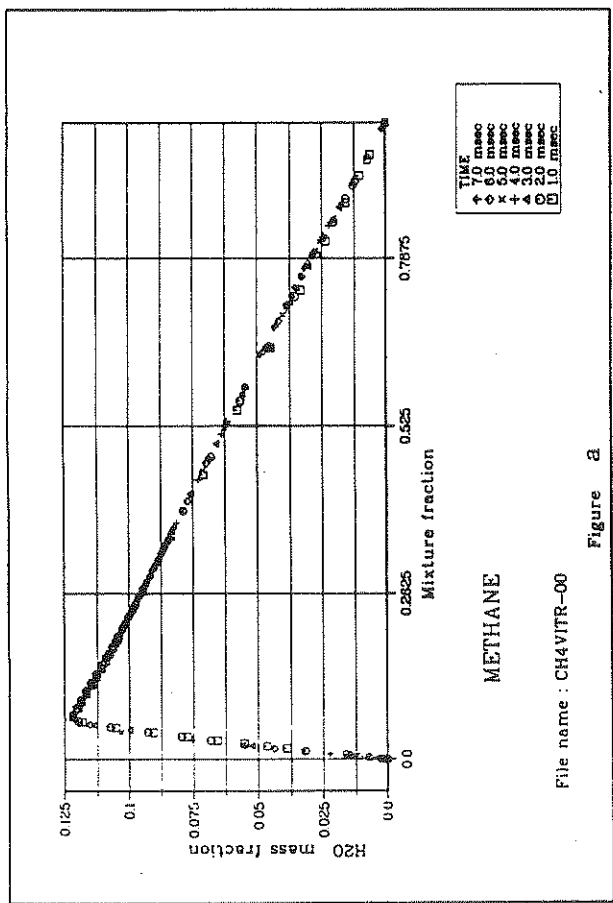
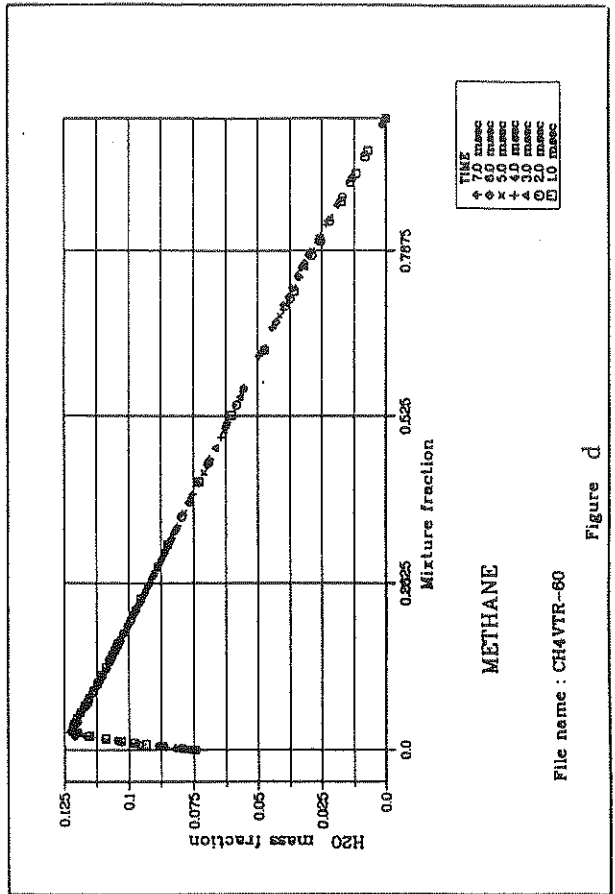
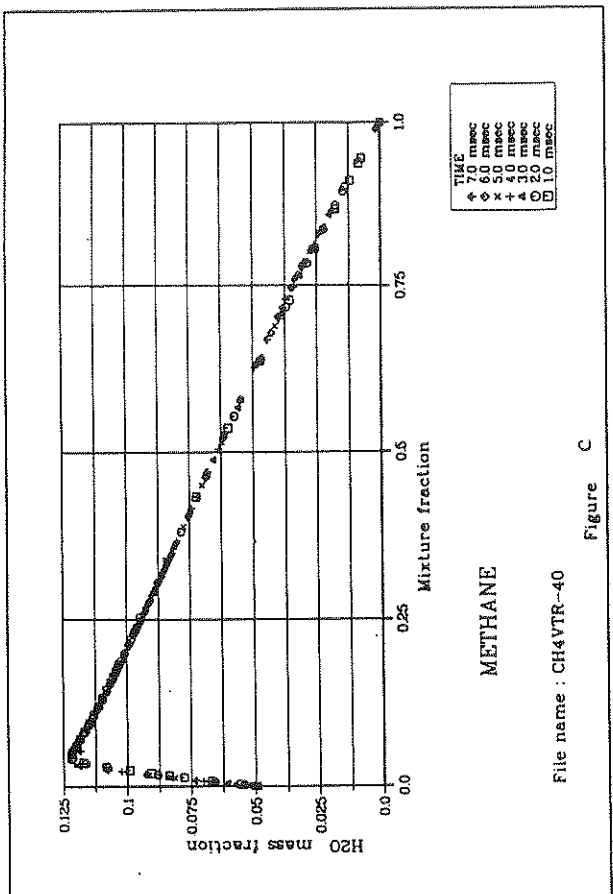


Figure E7

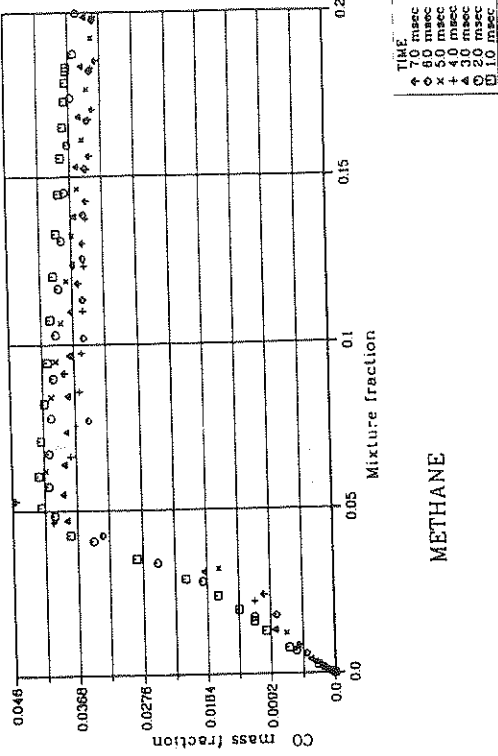


Figure C

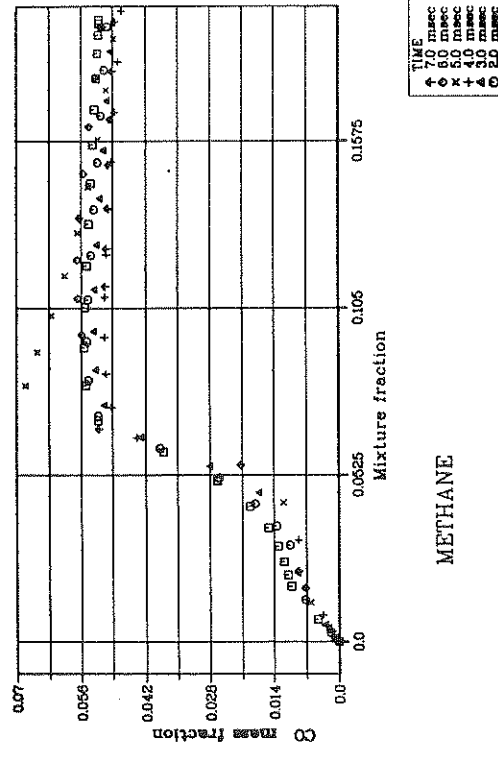


Figure b

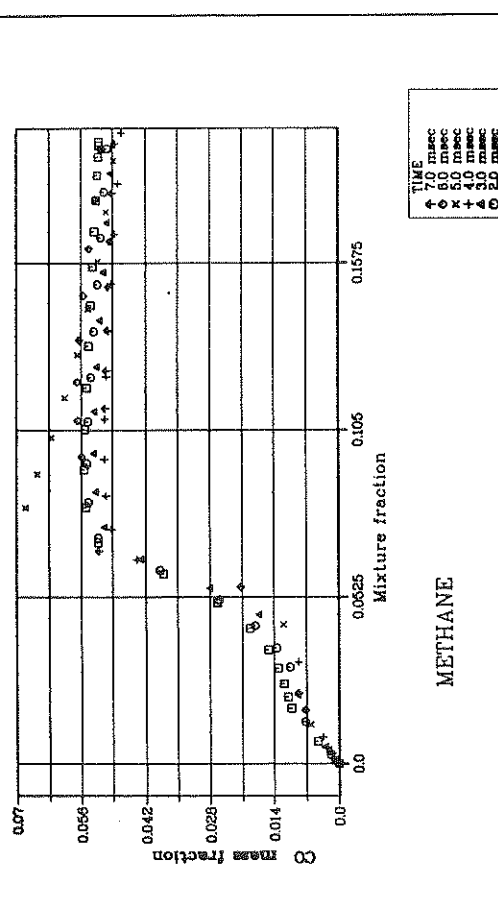


Figure d

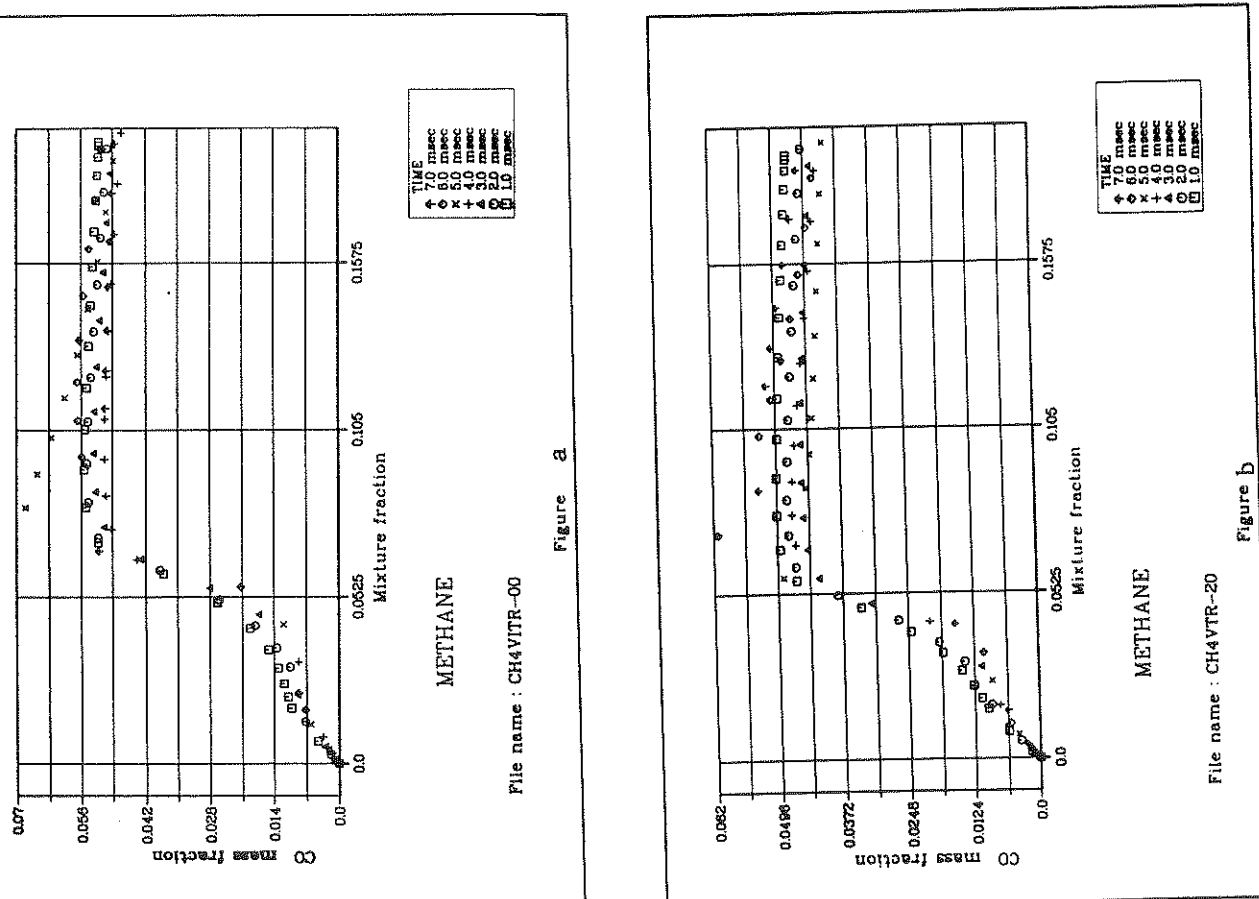


Figure E8

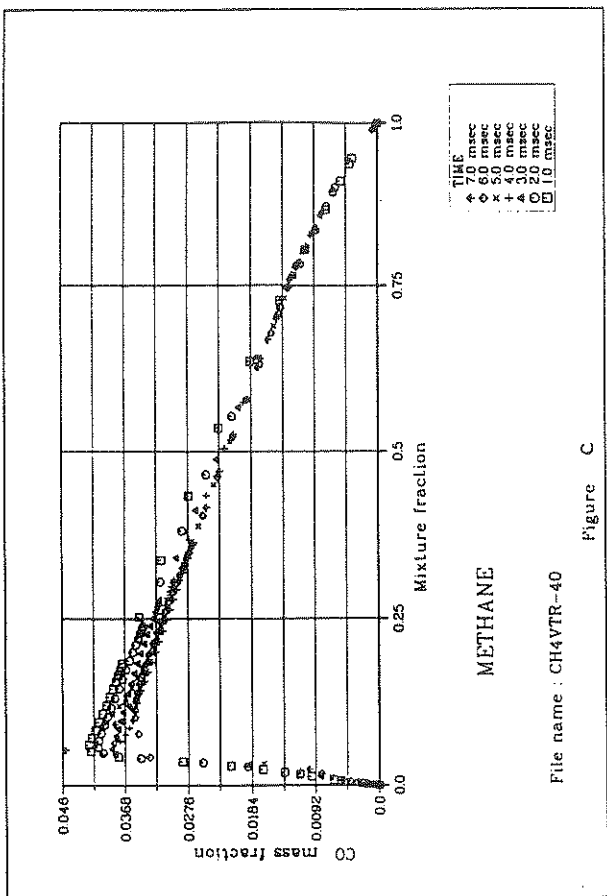


Figure C

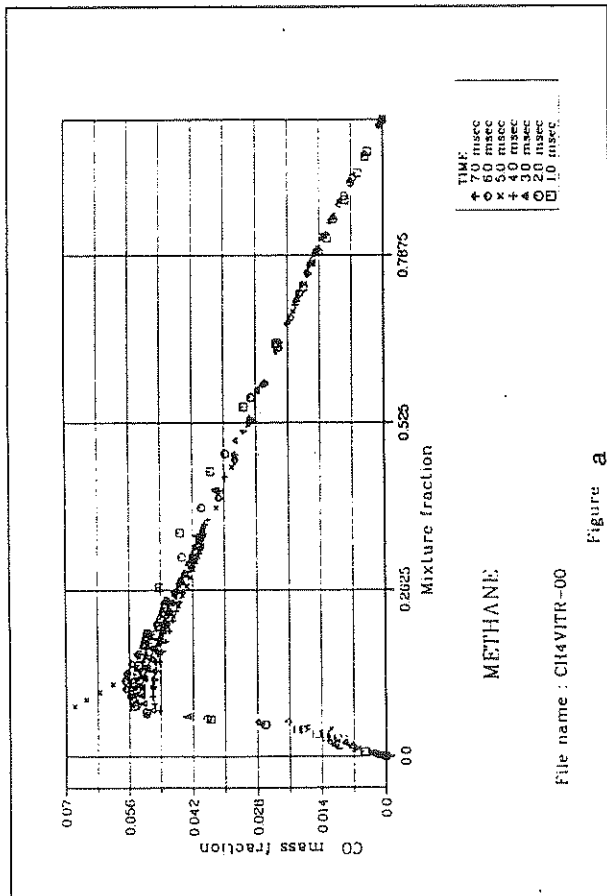


Figure a

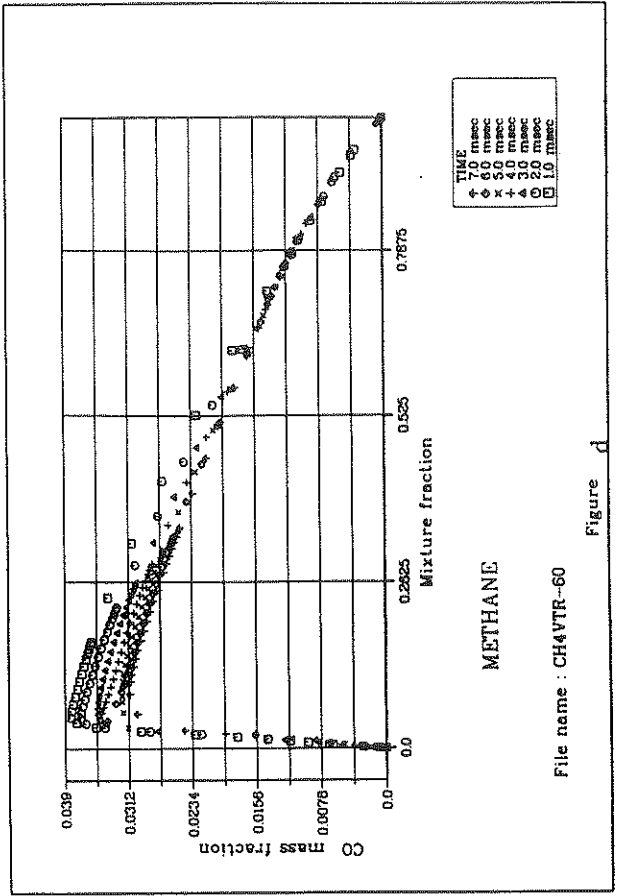


Figure C

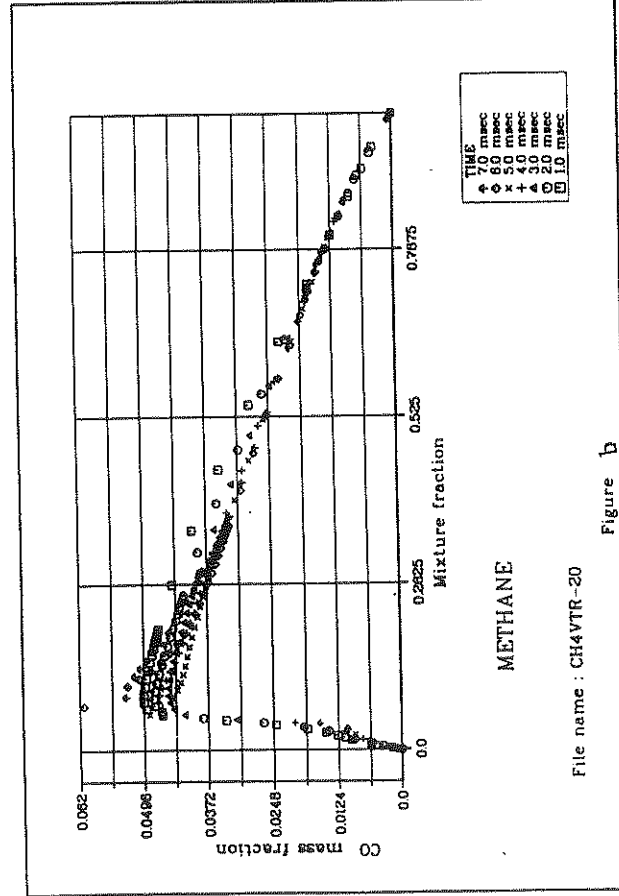
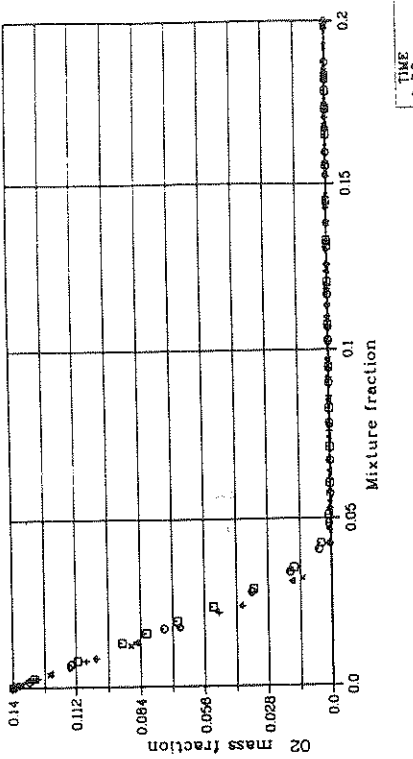


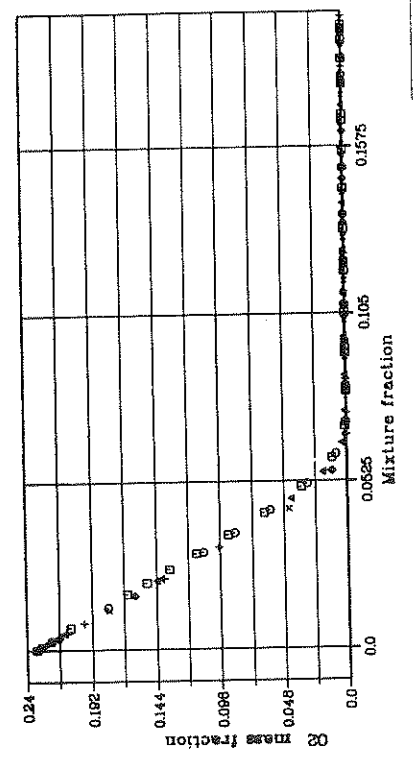
Figure d

Figure E9



File name : CH4VTR-0

Figure a



File name : CH4VTR-20

Figure b

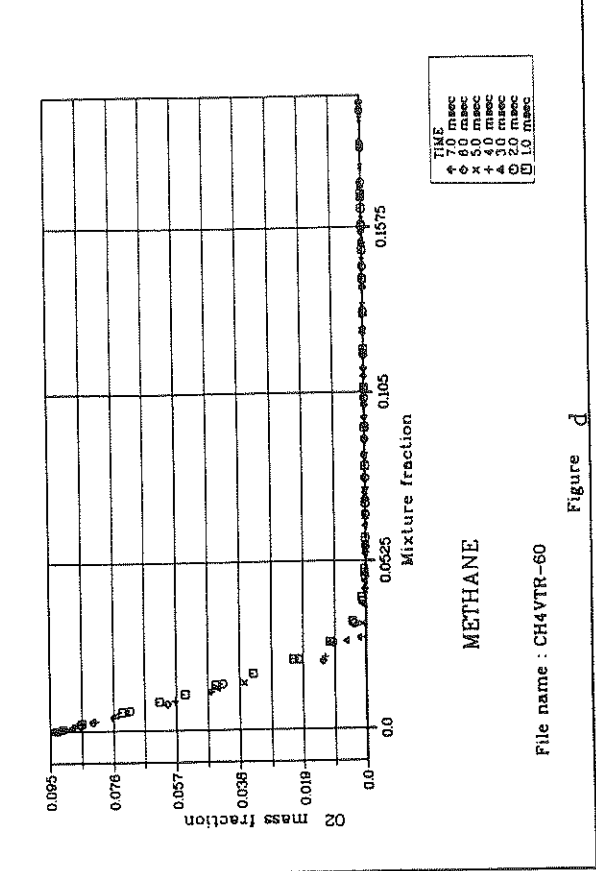


Figure c

File name : CH4VTR-60

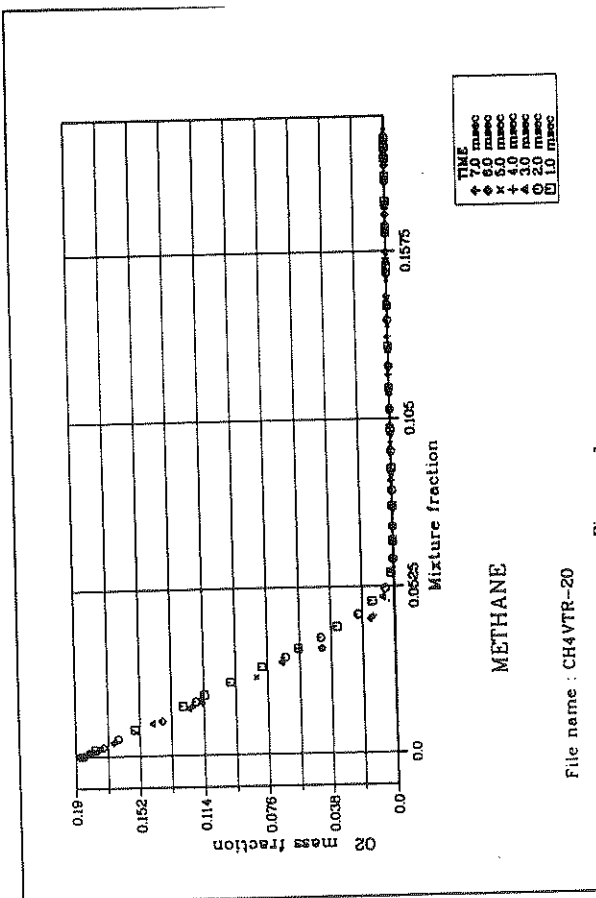


Figure d

File name : CH4VTR-70

Figure E10

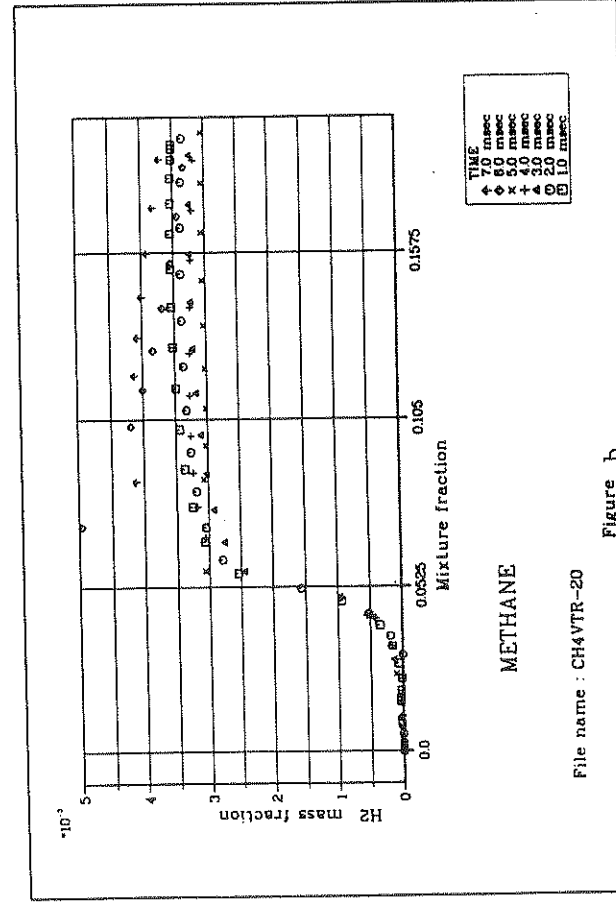
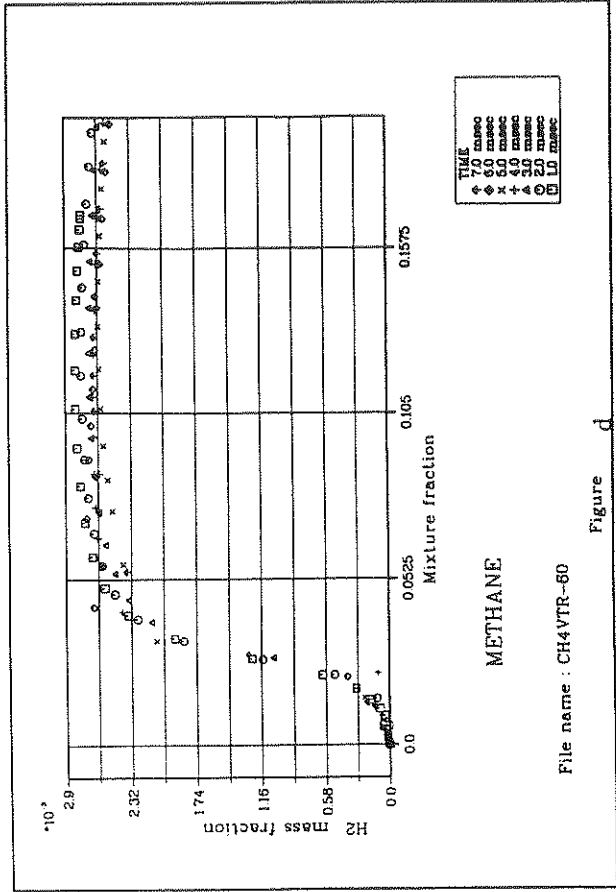
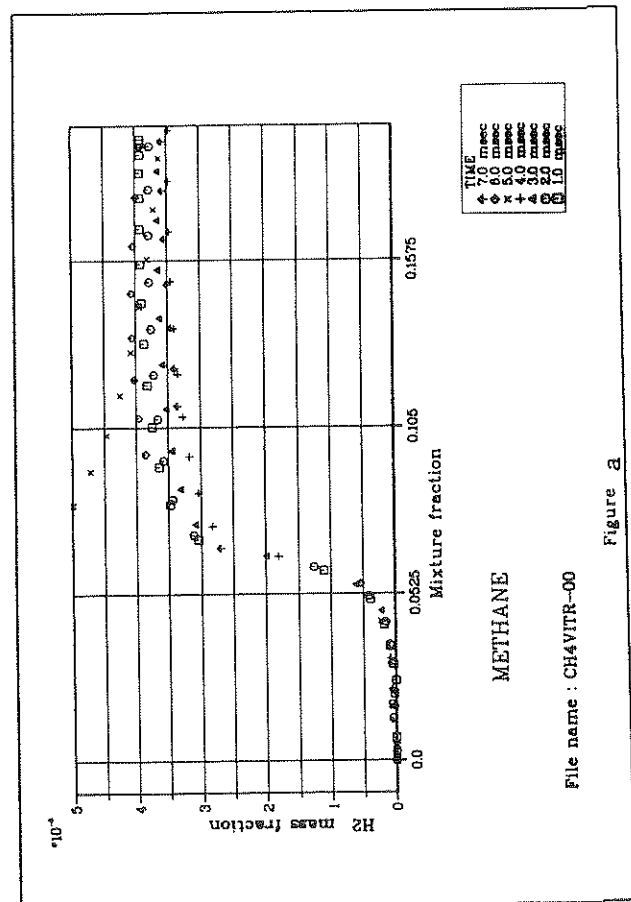
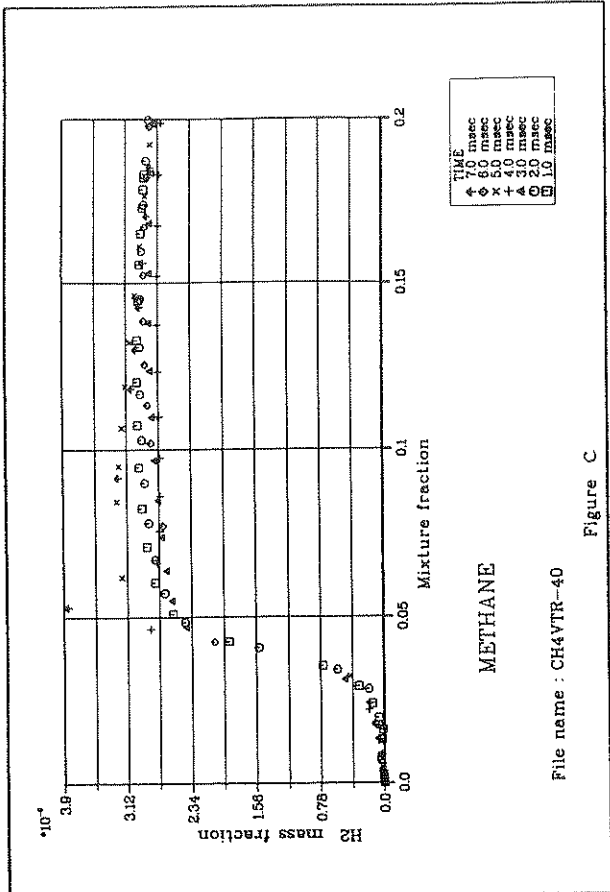
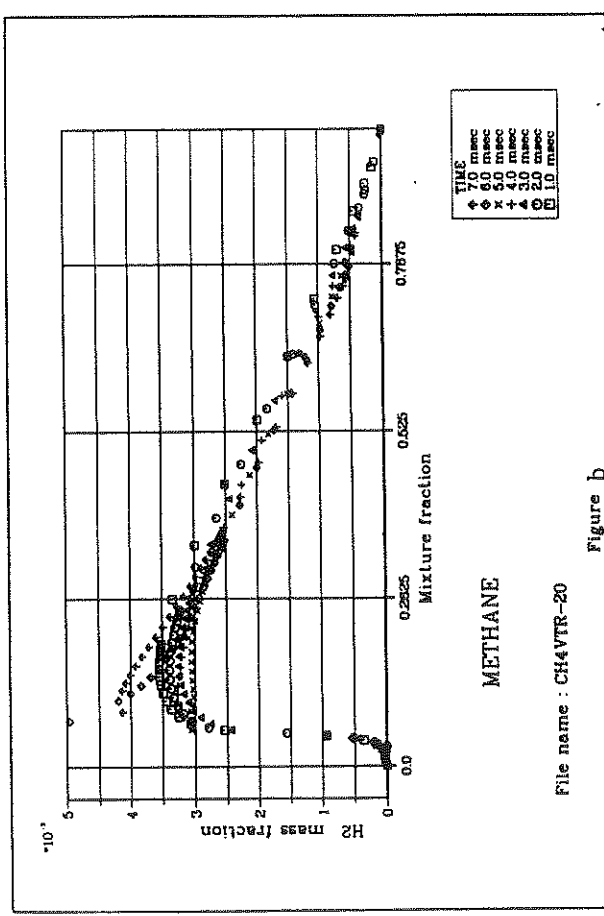
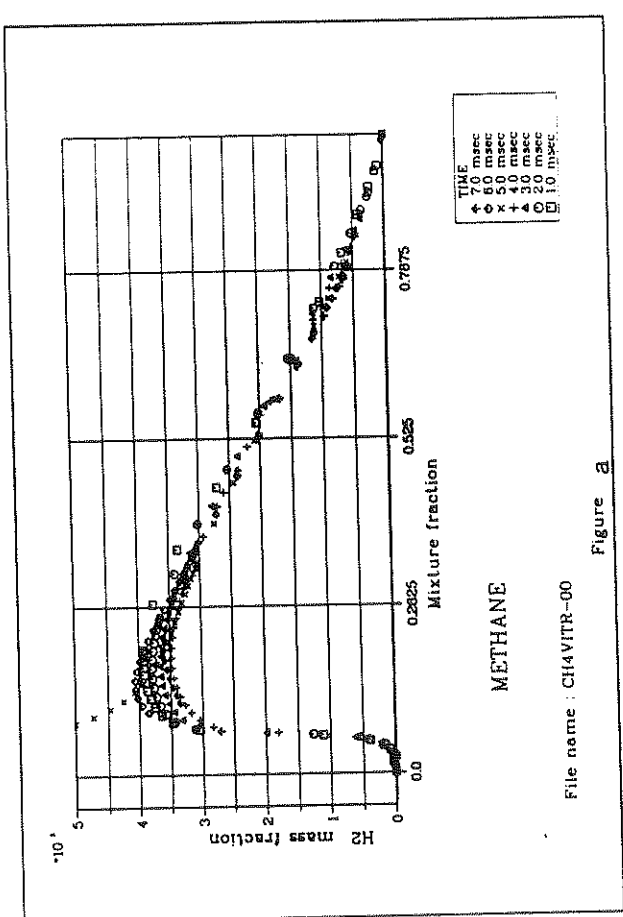
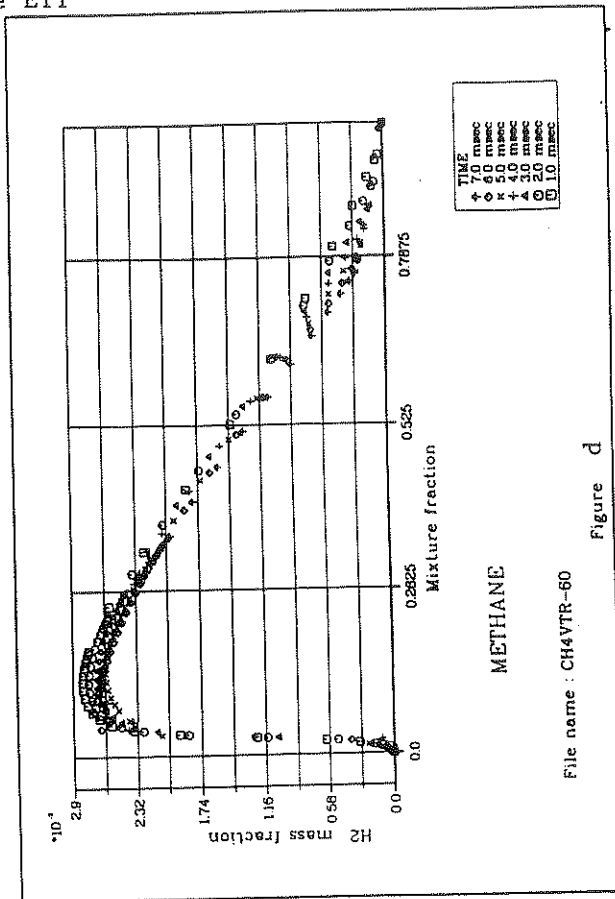
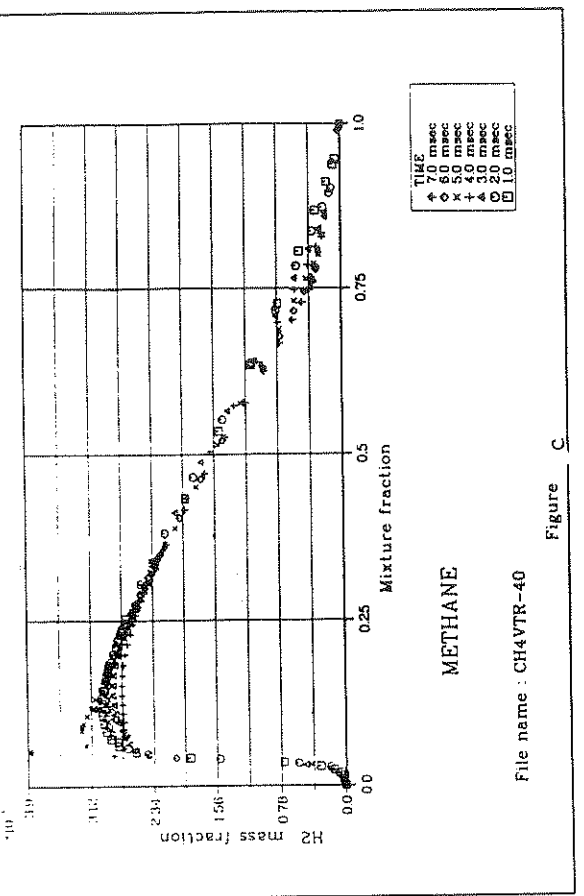


Figure E11



E11

Figure E12

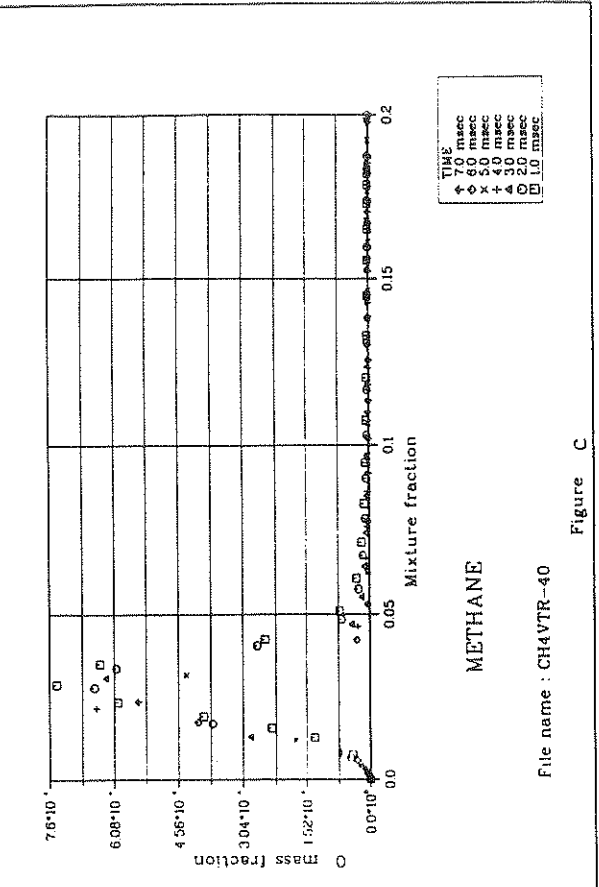


Figure a

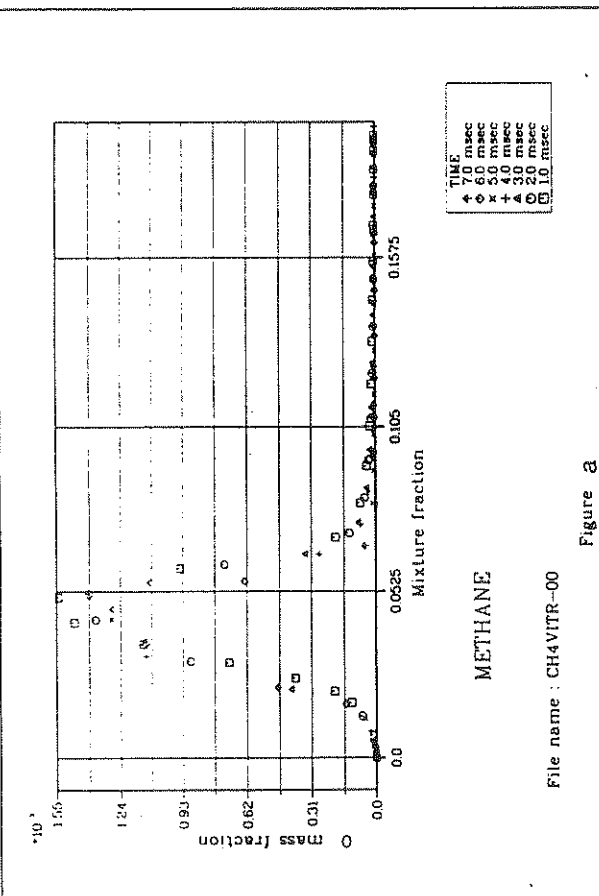


Figure b

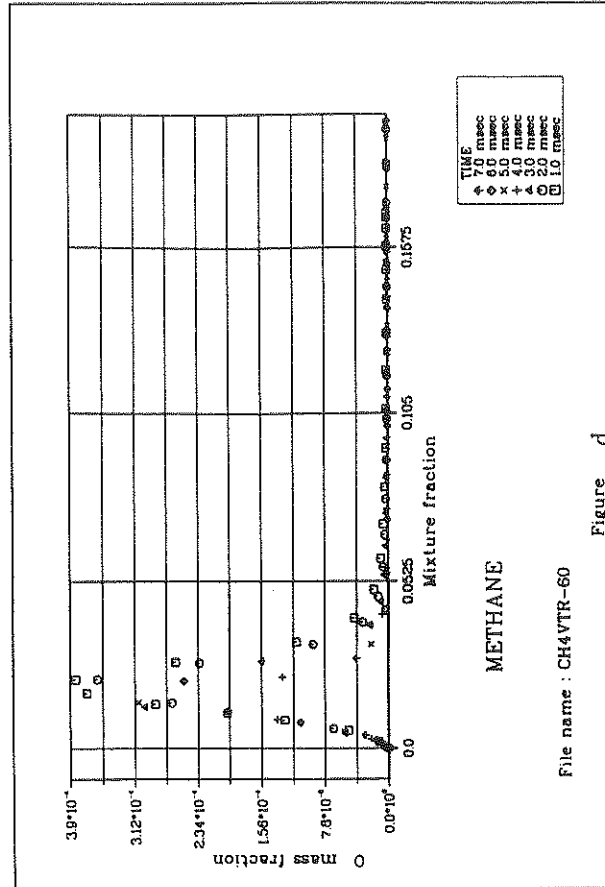


Figure c

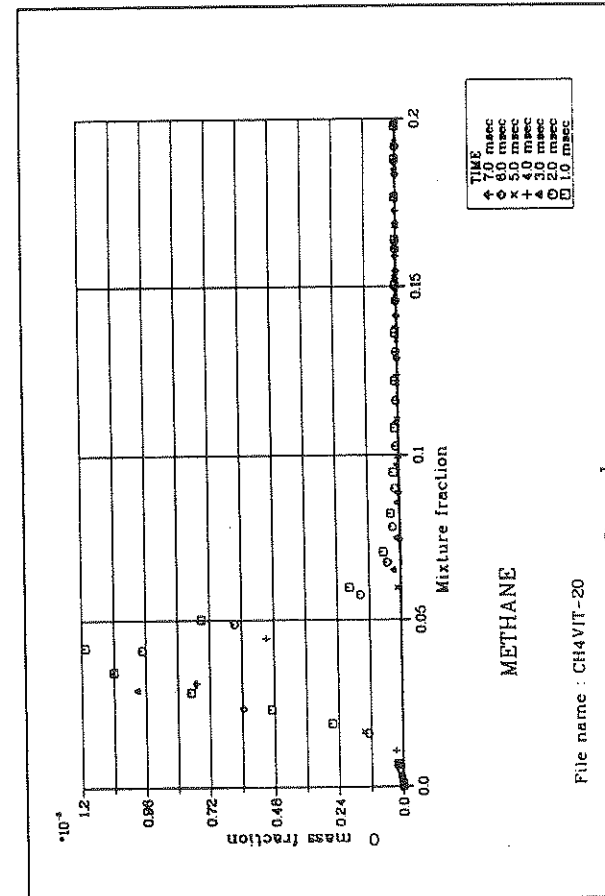


Figure d

Figure E13

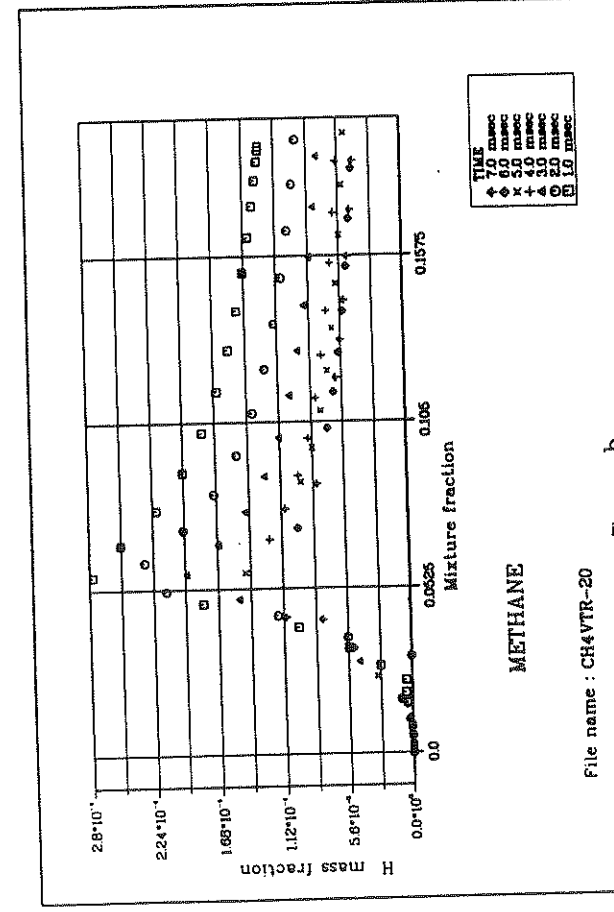
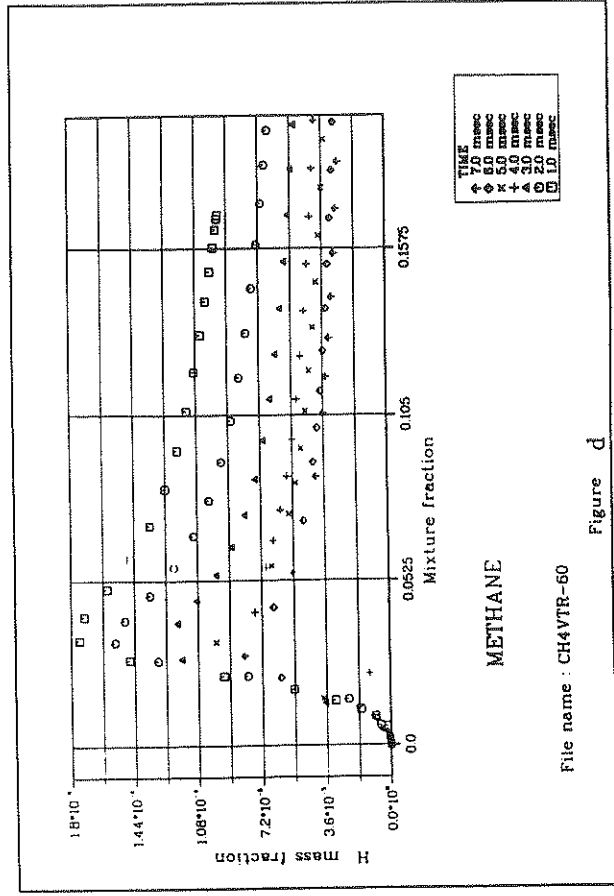
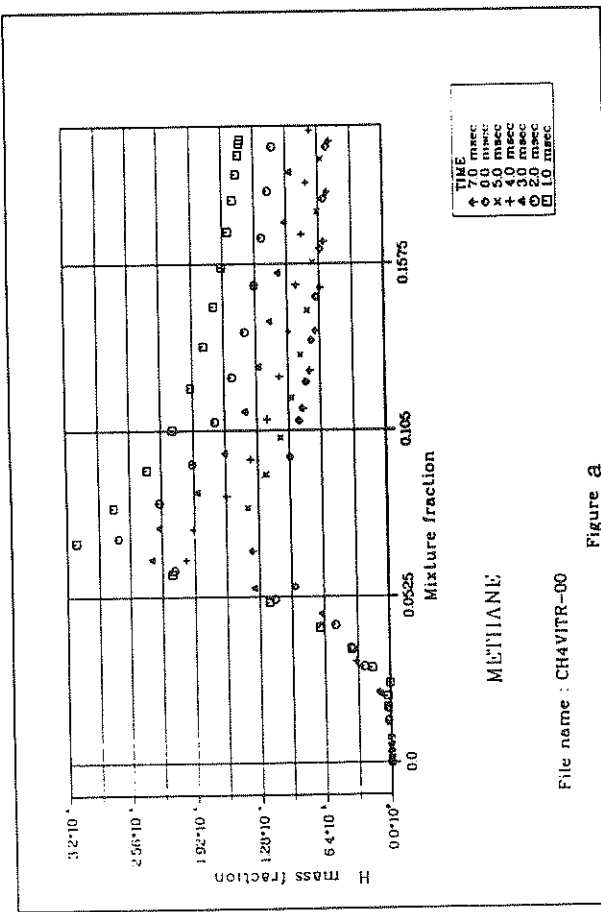
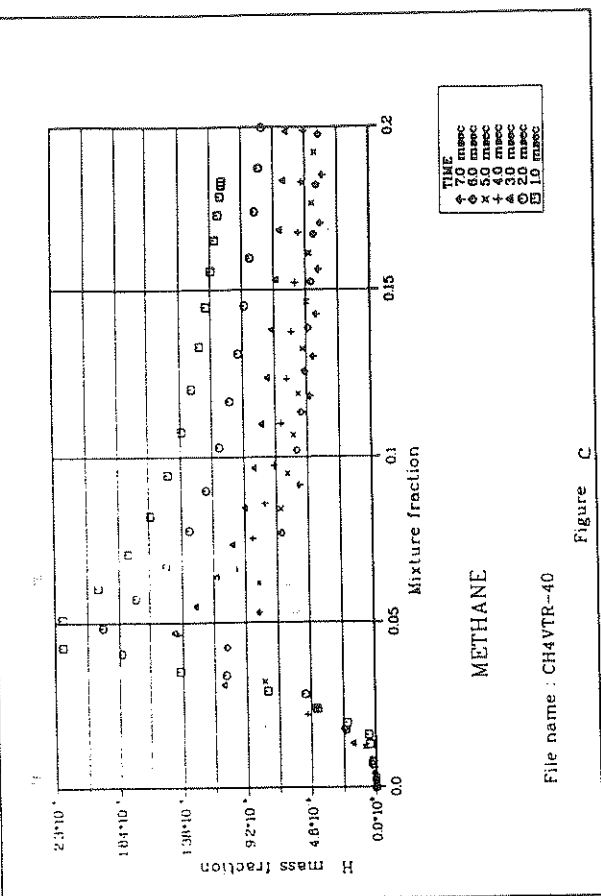


Figure E14

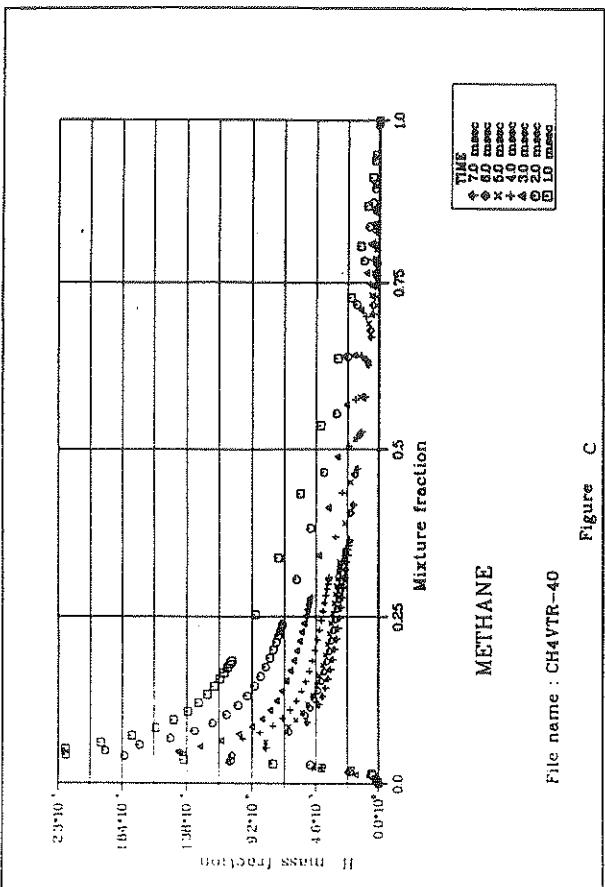


Figure C

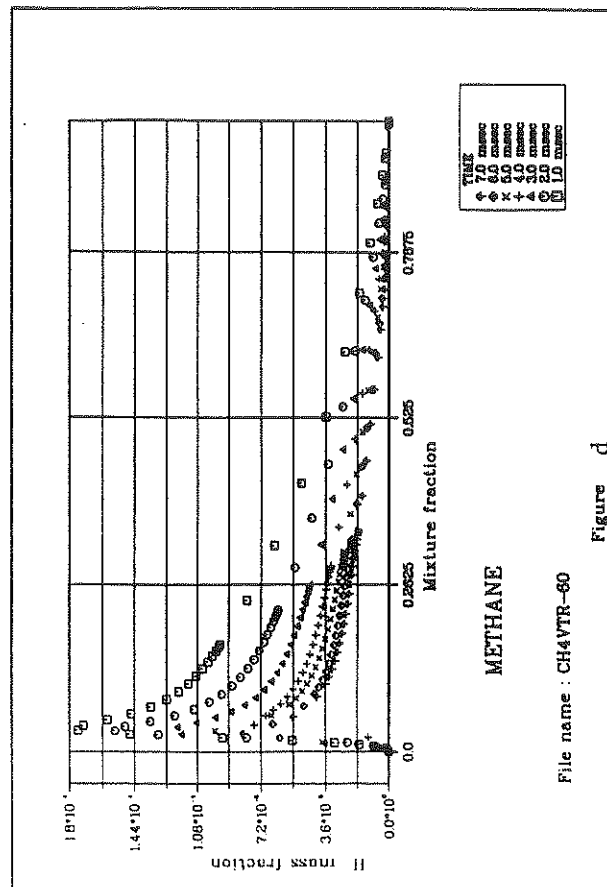


Figure d

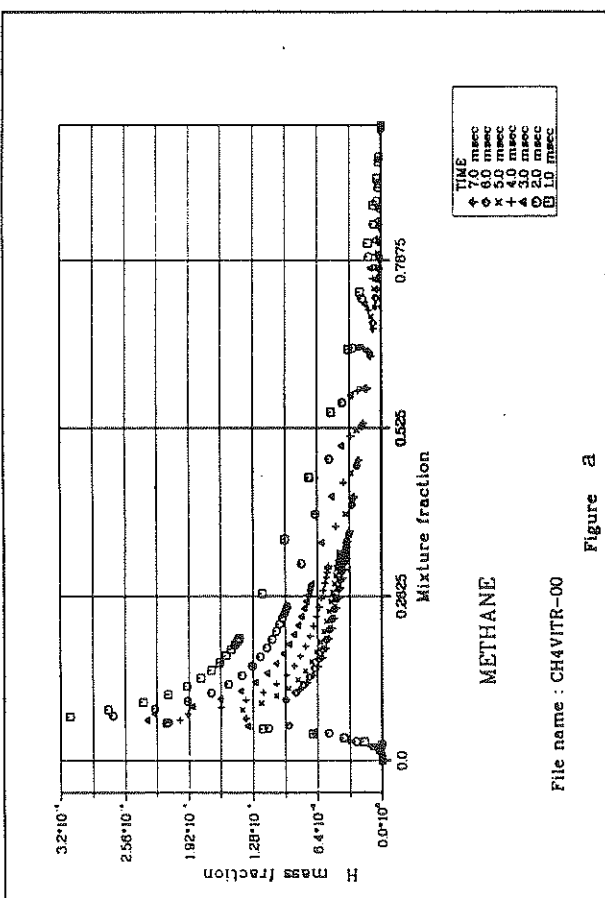


Figure b

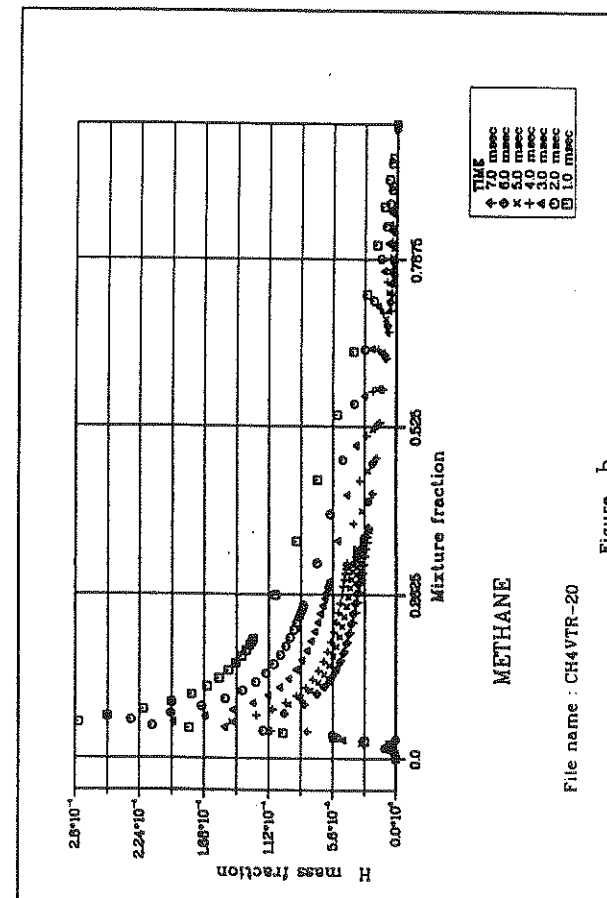


Figure d

Figure E15

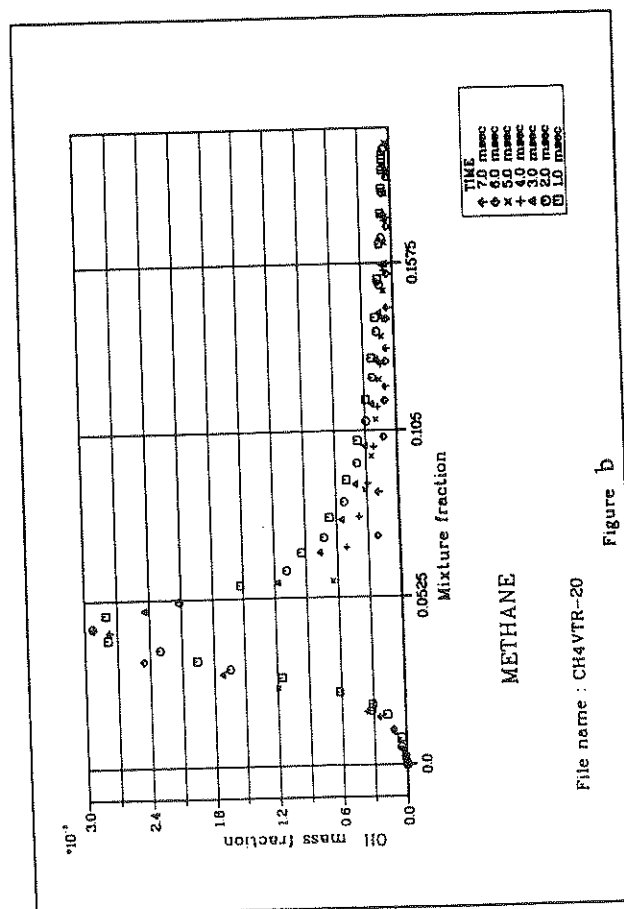
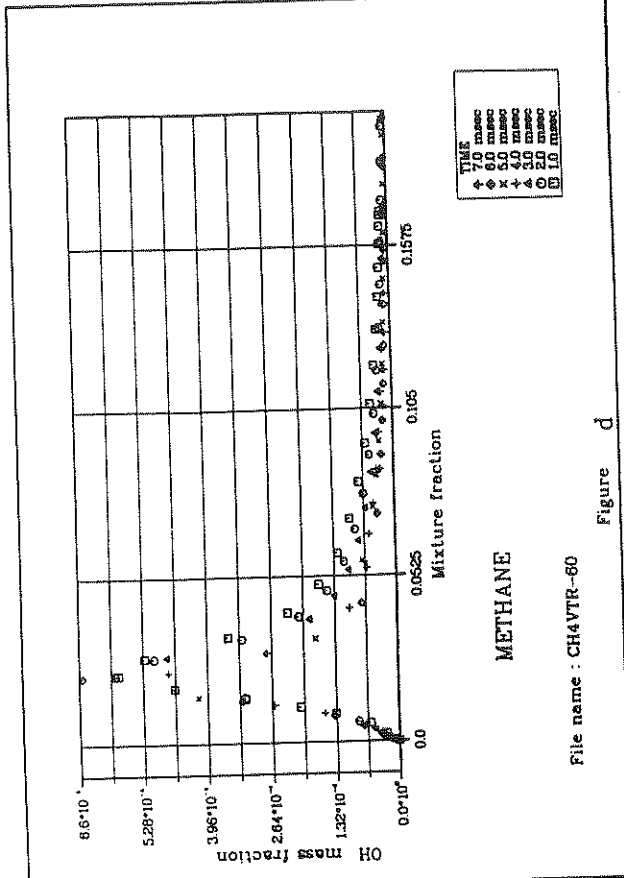
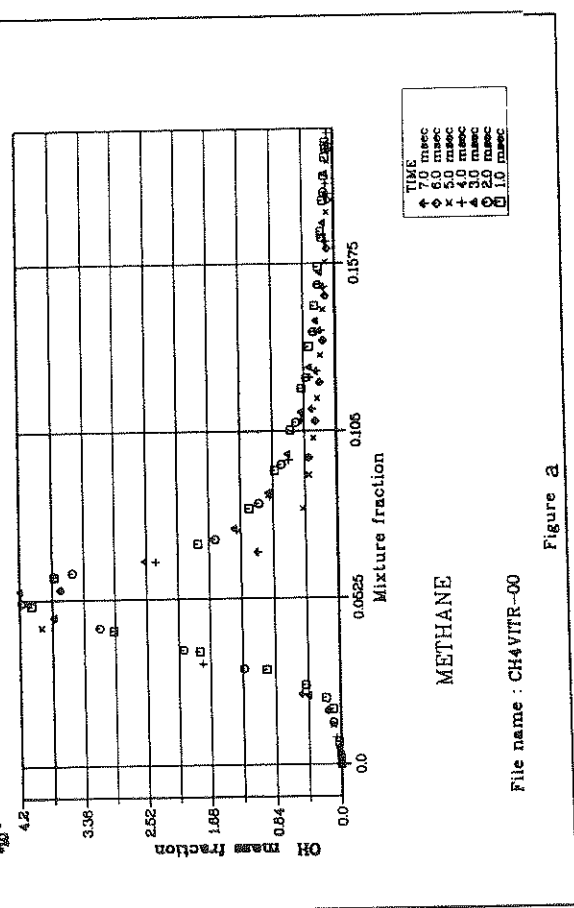
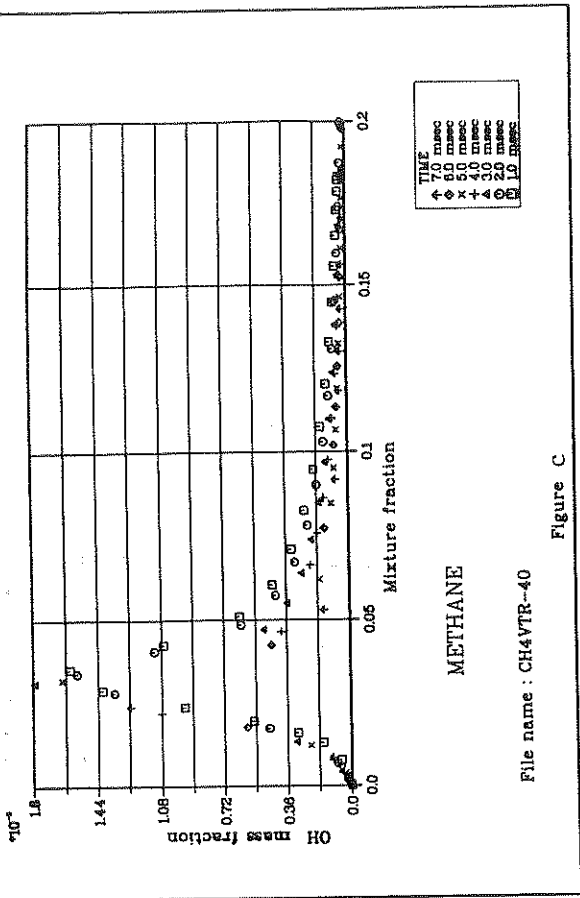


Figure E16

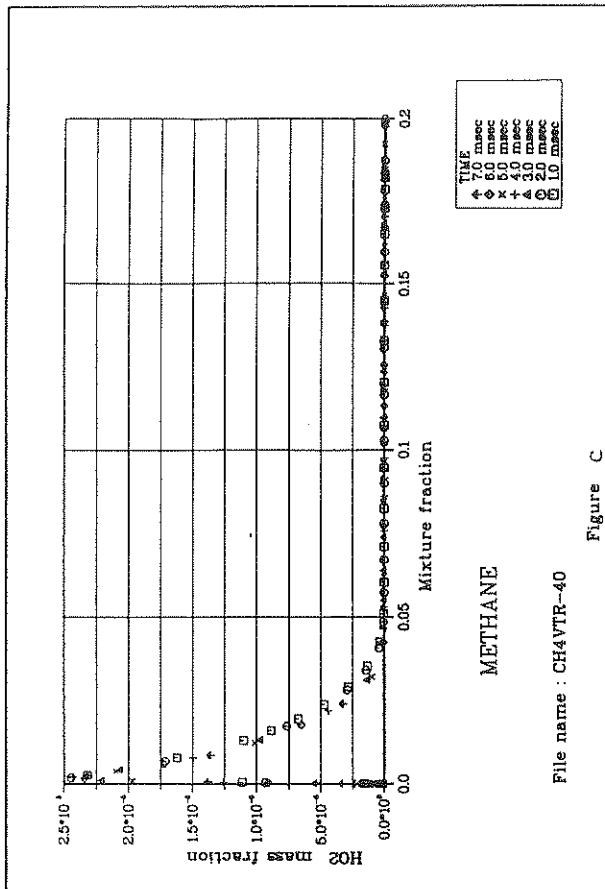


Figure a

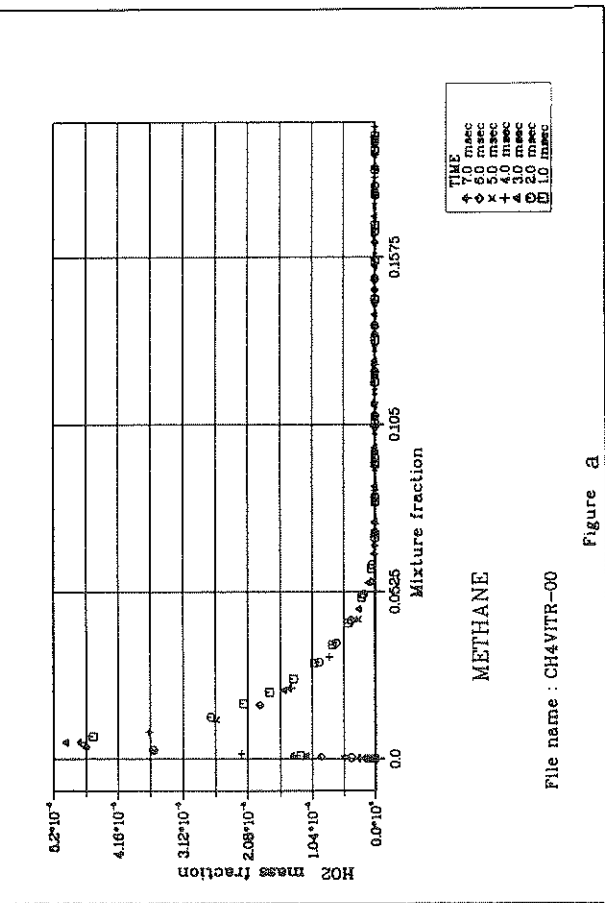


Figure b

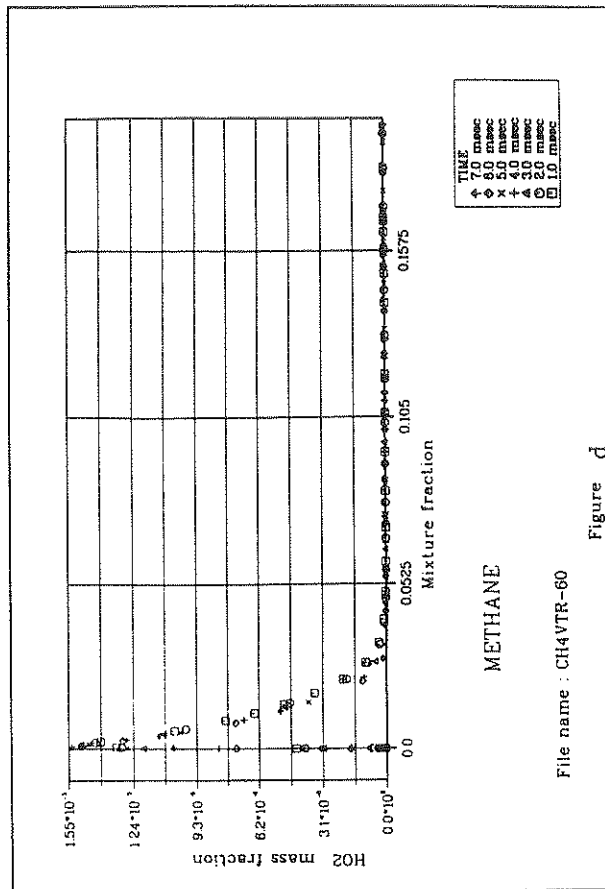


Figure c

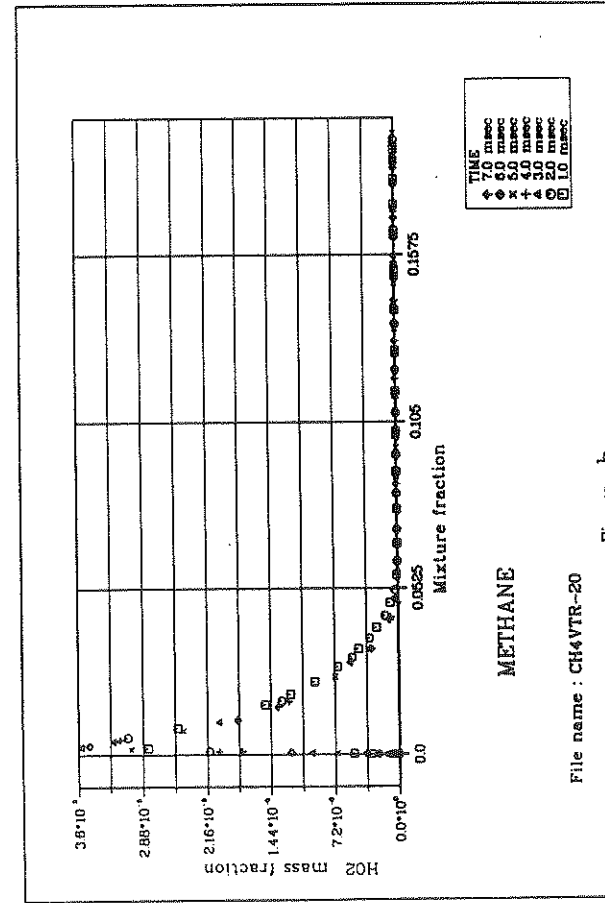


Figure d

Figure E17

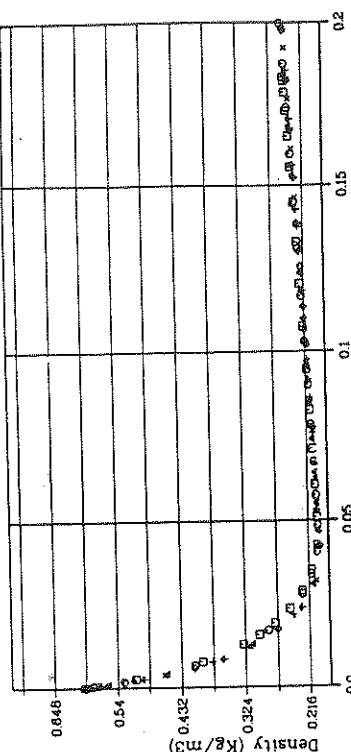
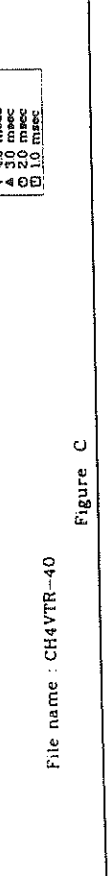


Figure a



E17

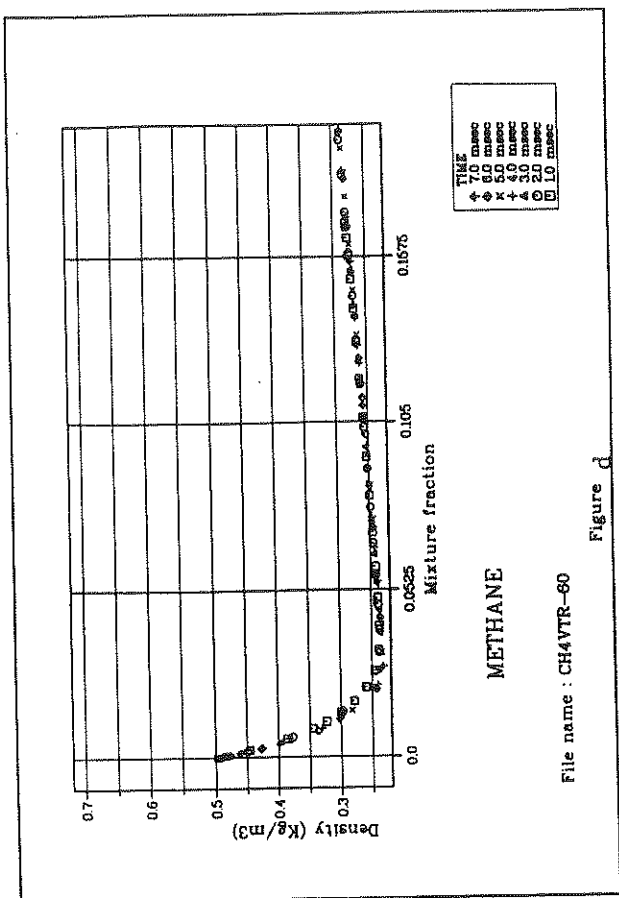


Figure c

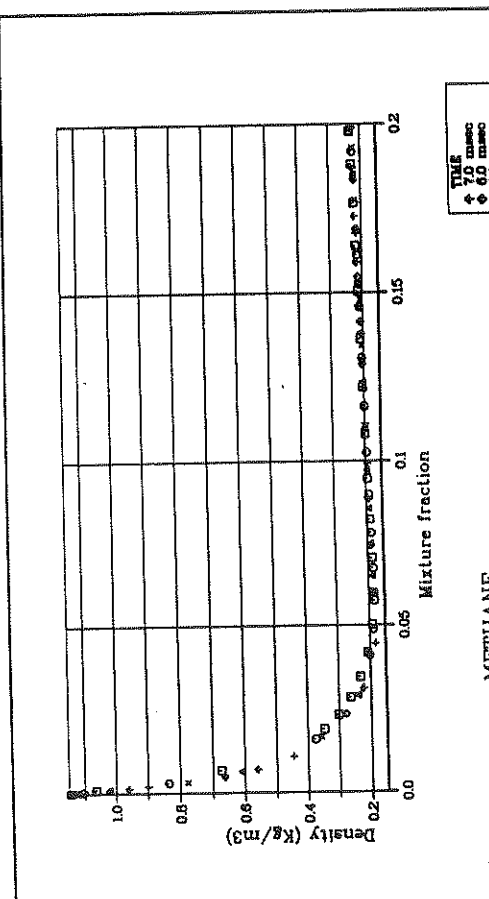


Figure d

Figure E18

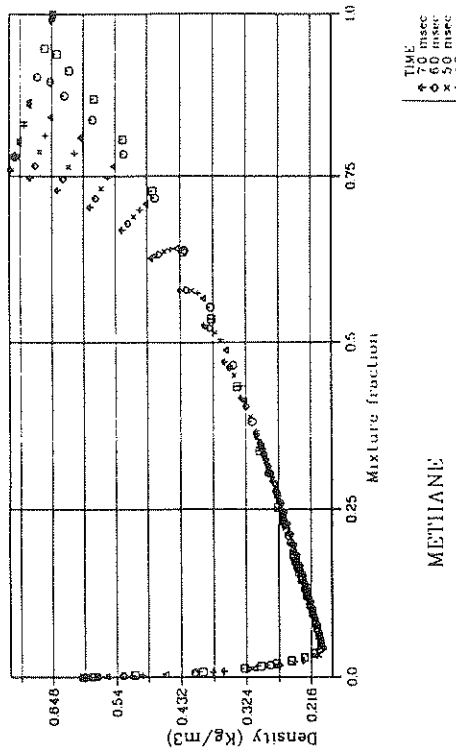


Figure C

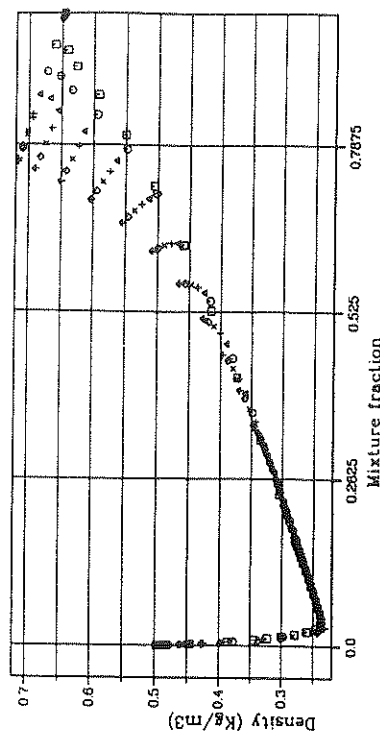


Figure d

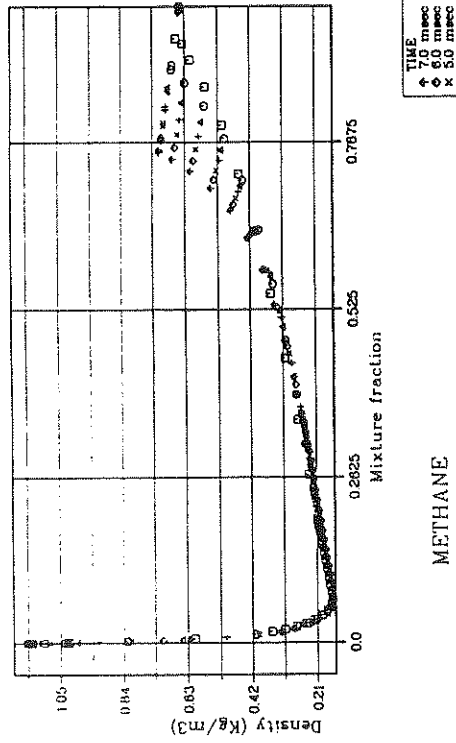


Figure a

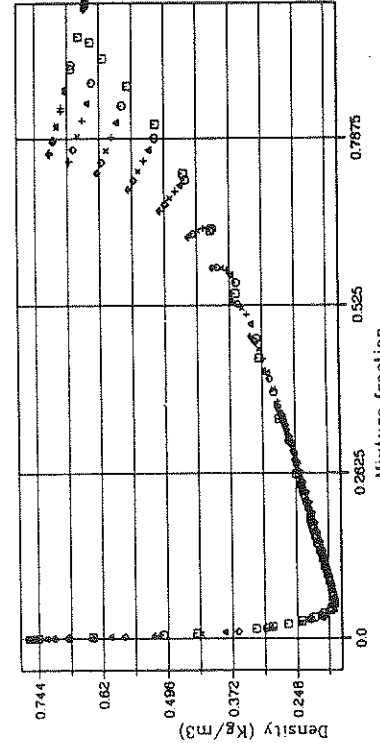
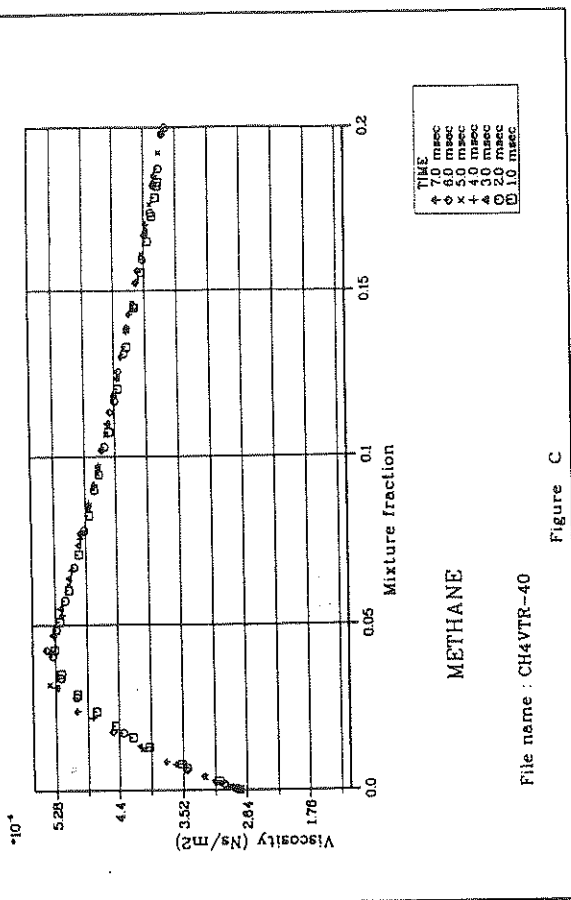


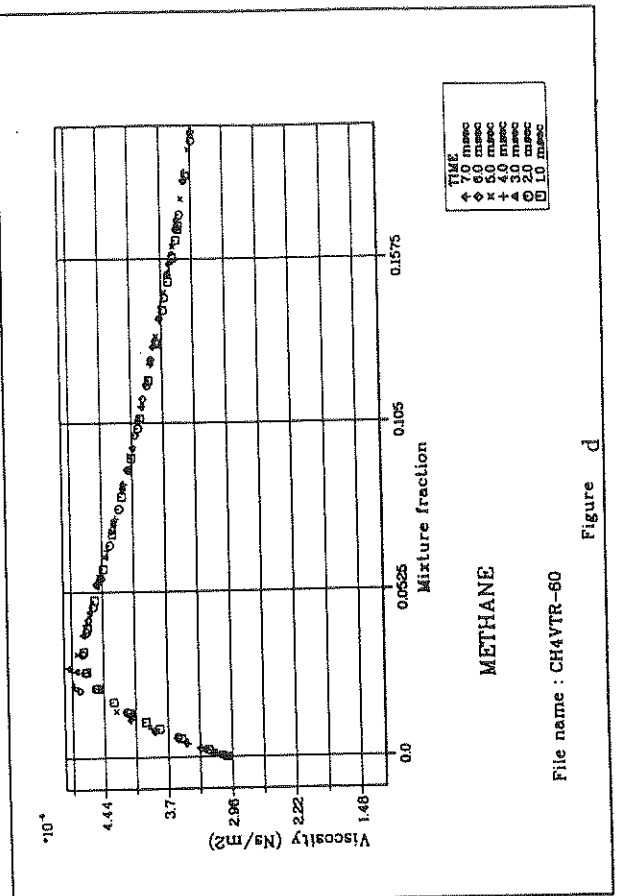
Figure b

Figure E19



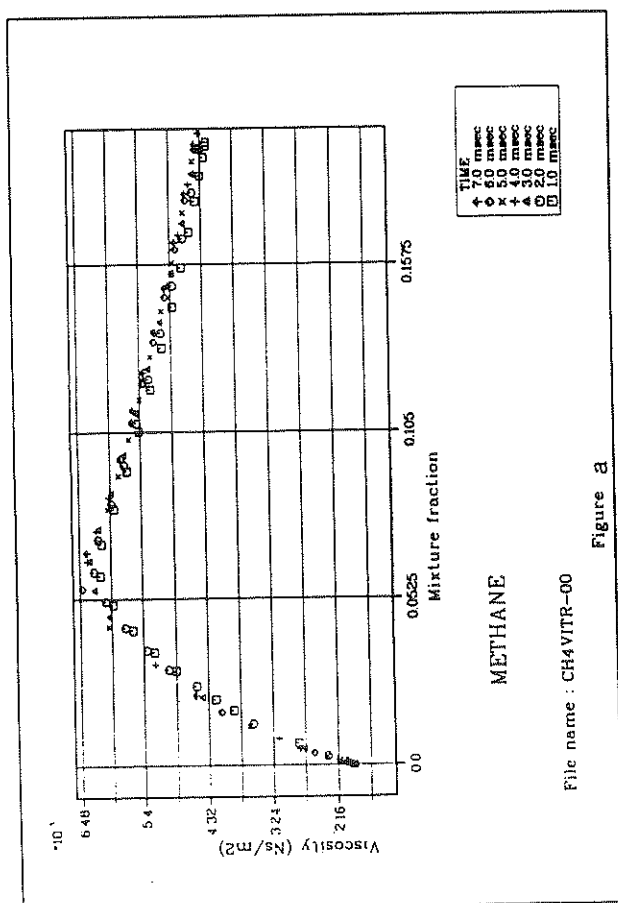
File name : CH4VTR-40

Figure C



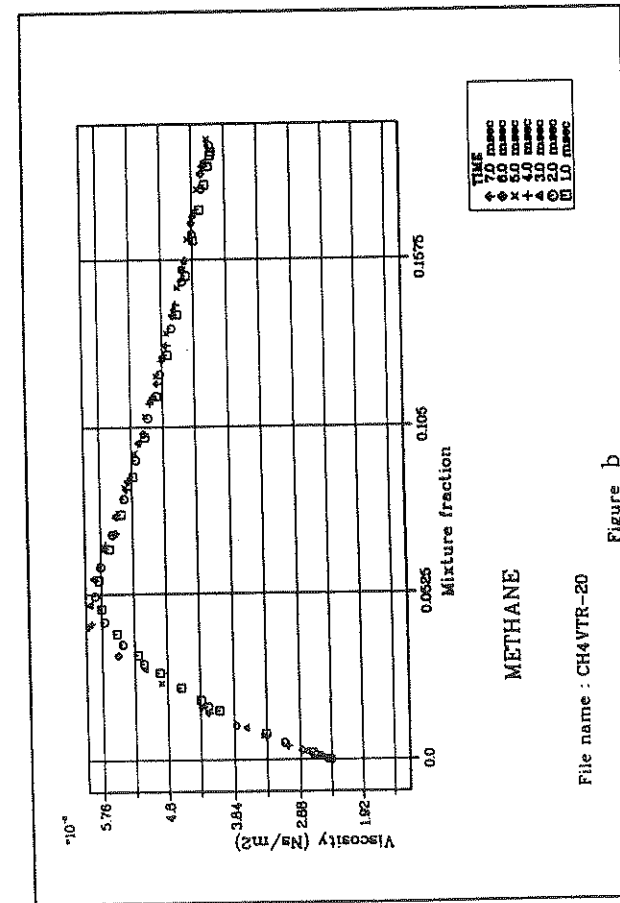
File name : CH4VTR-80

Figure d



File name : CH4VTR-20

Figure a



File name : CH4VTR-40

Figure b

Figure E20

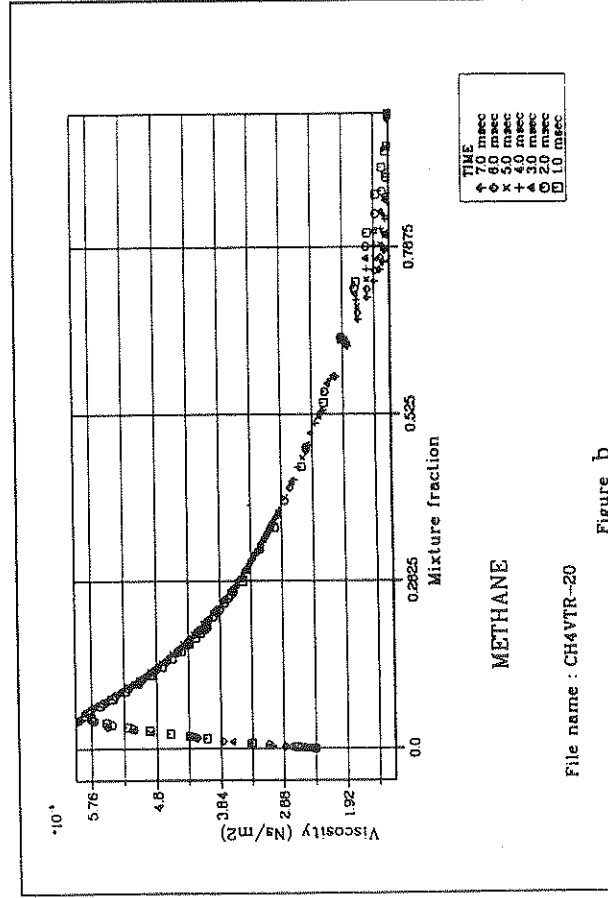
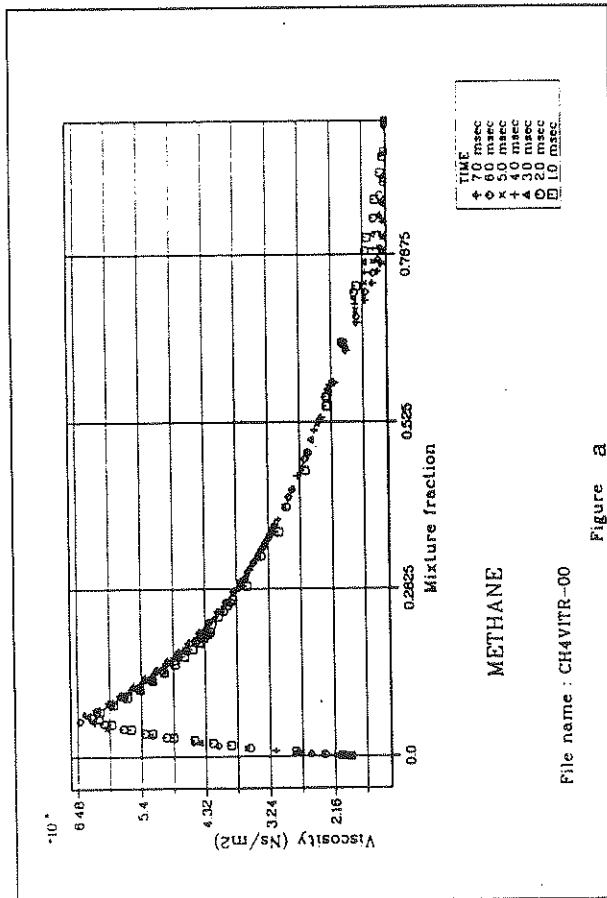
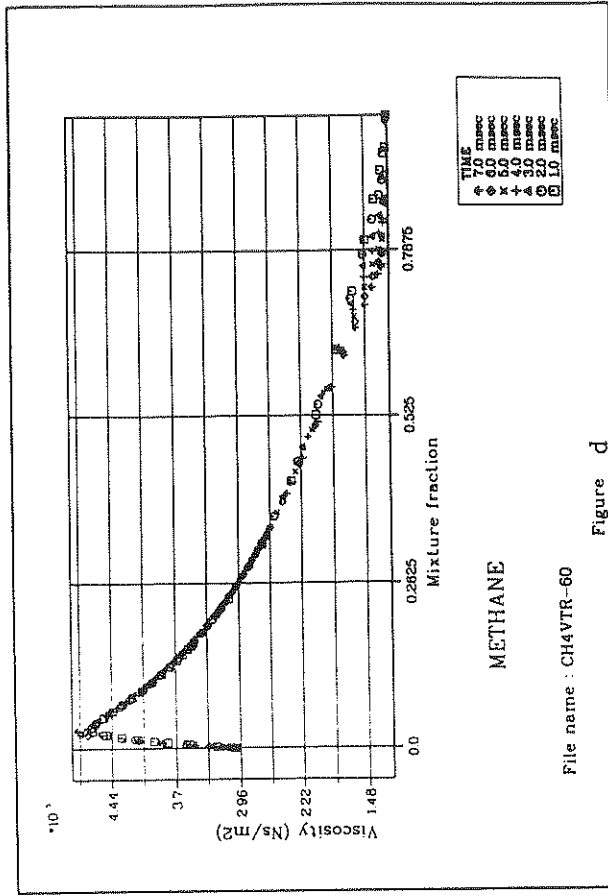
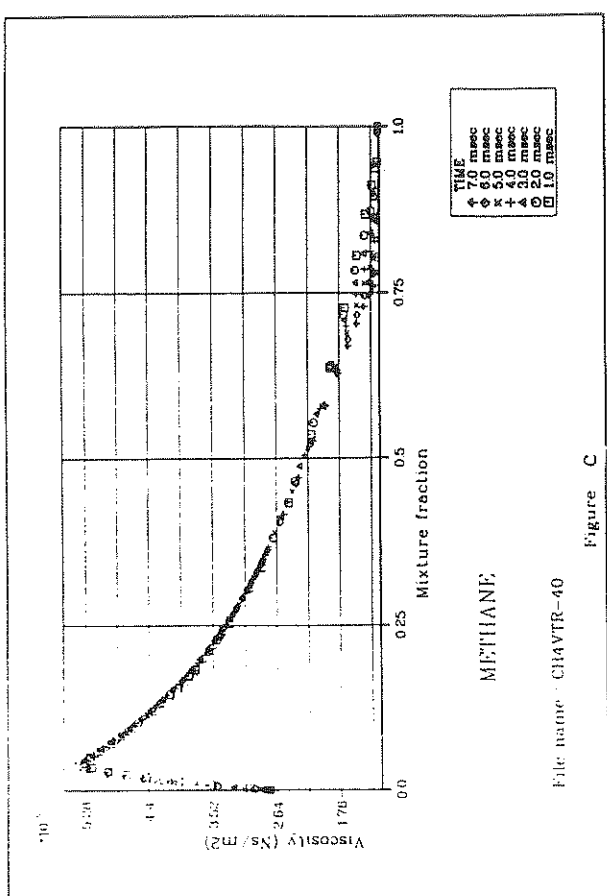
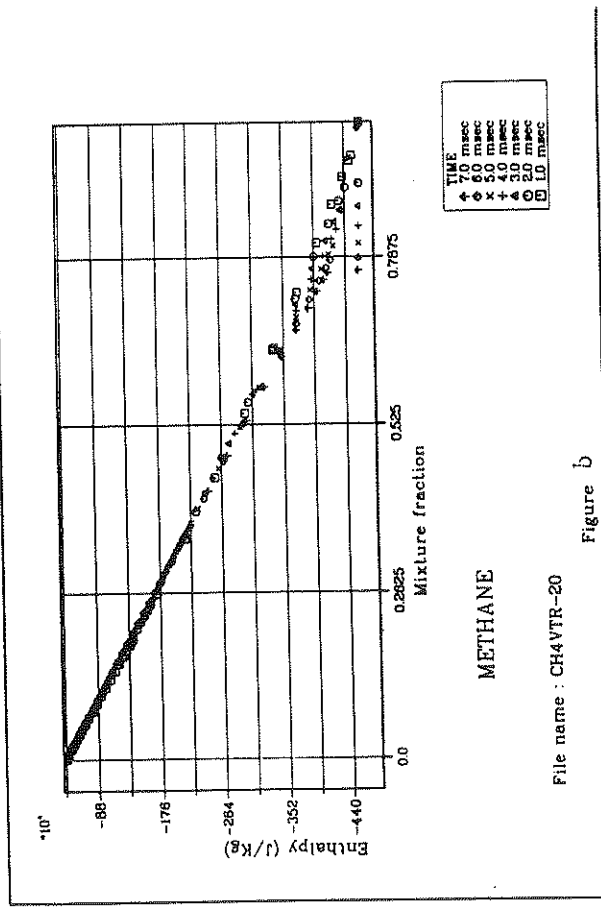
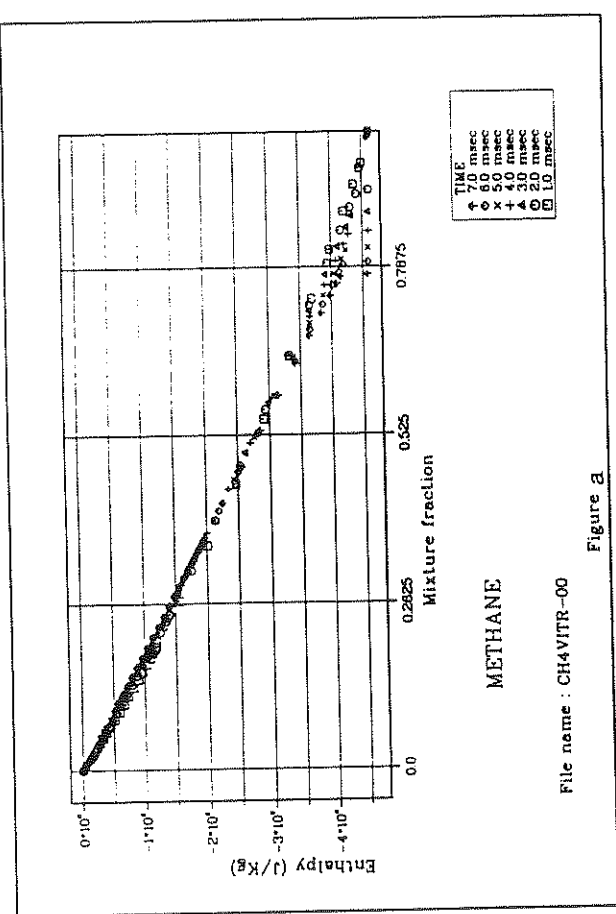
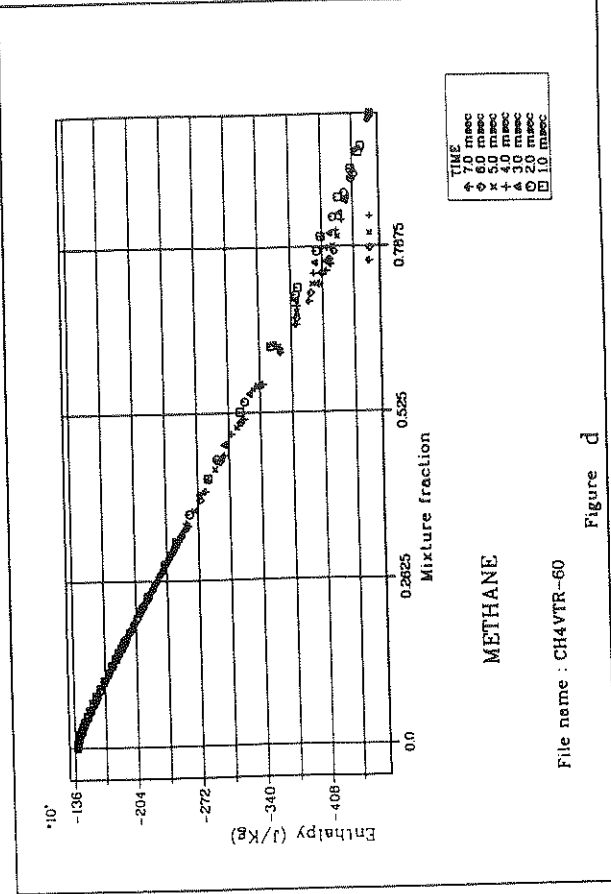
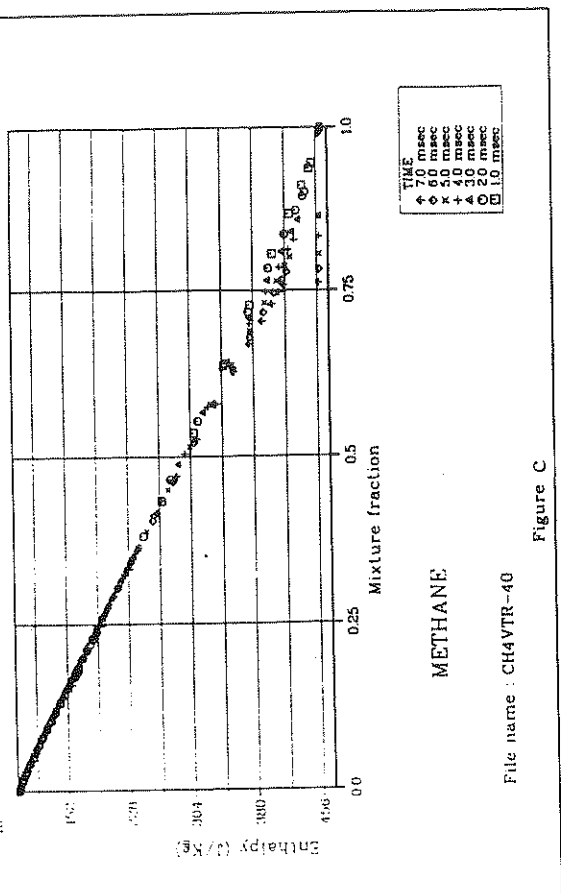


Figure E21



E21

Figure E22

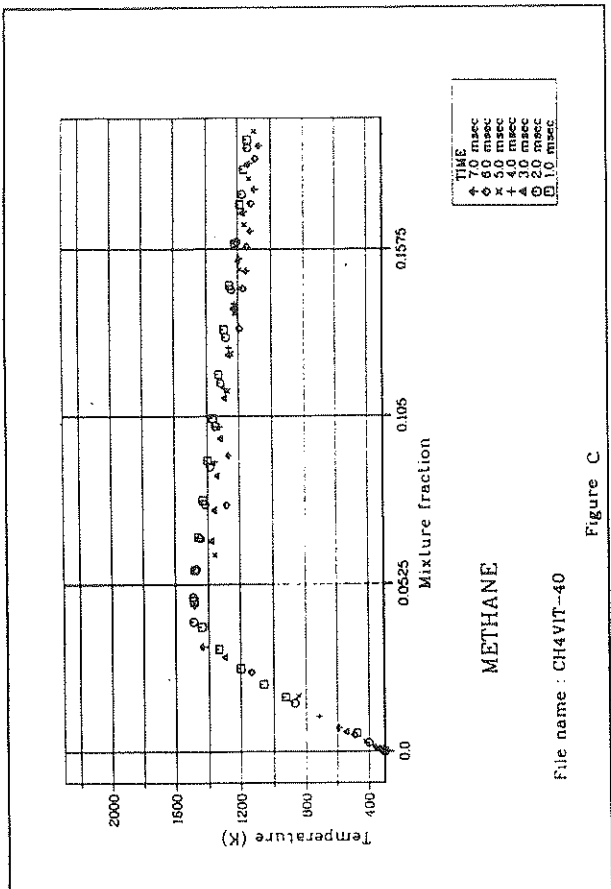


Figure C

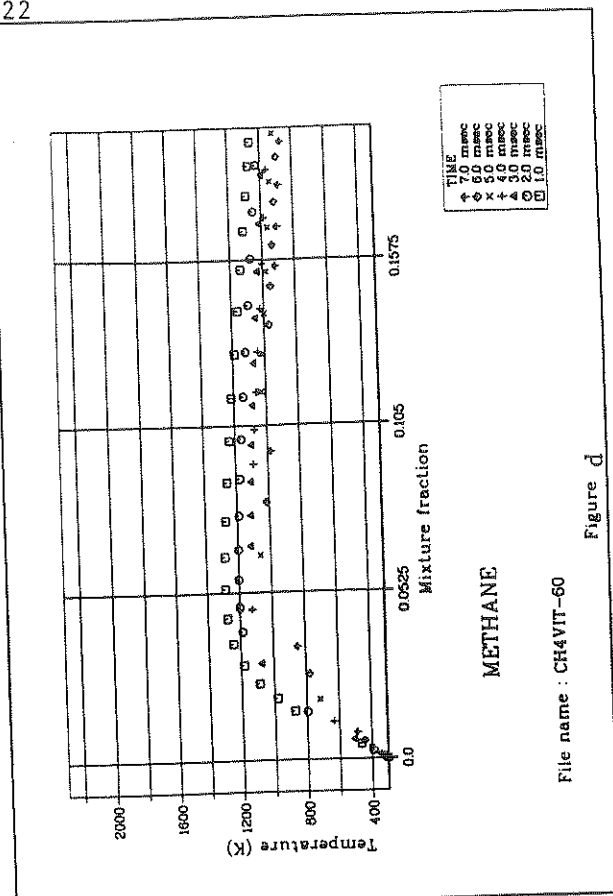


Figure d

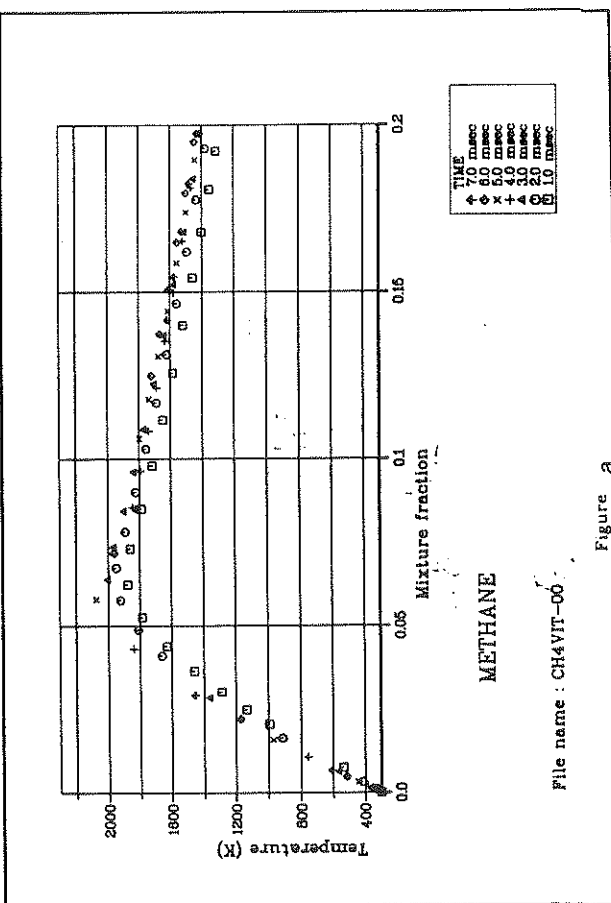


Figure a

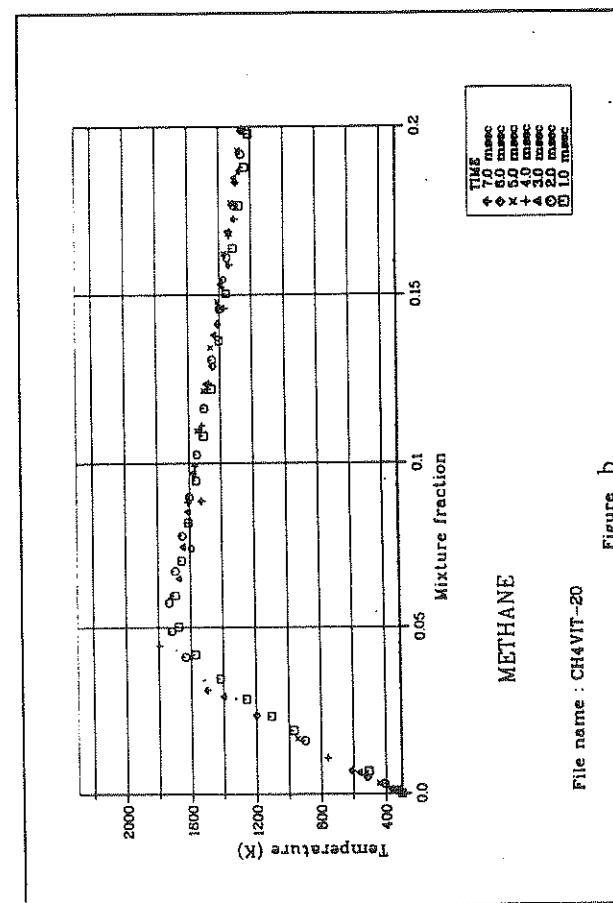


Figure b

Figure E23

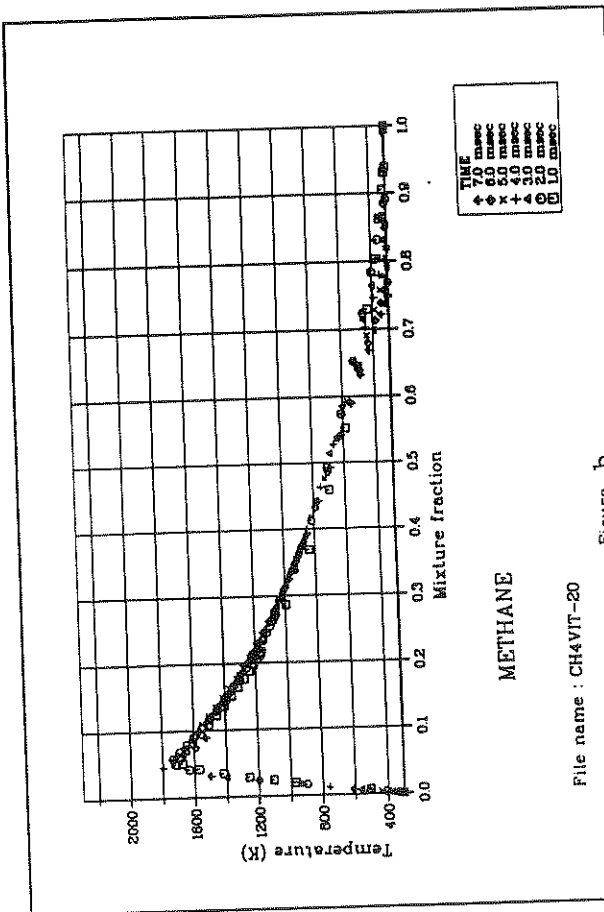
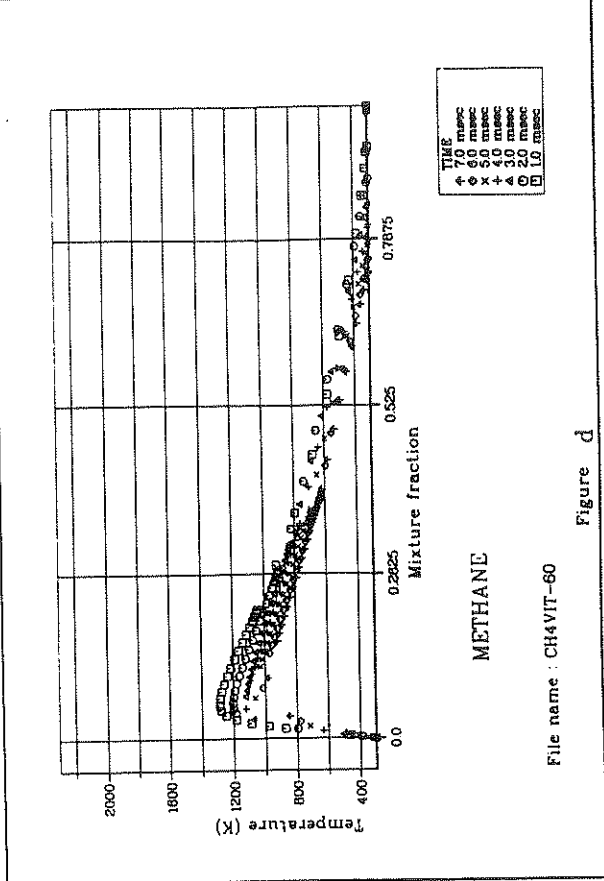
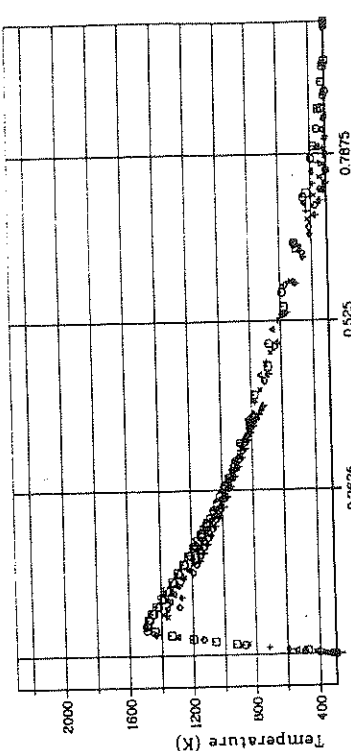


Figure E24

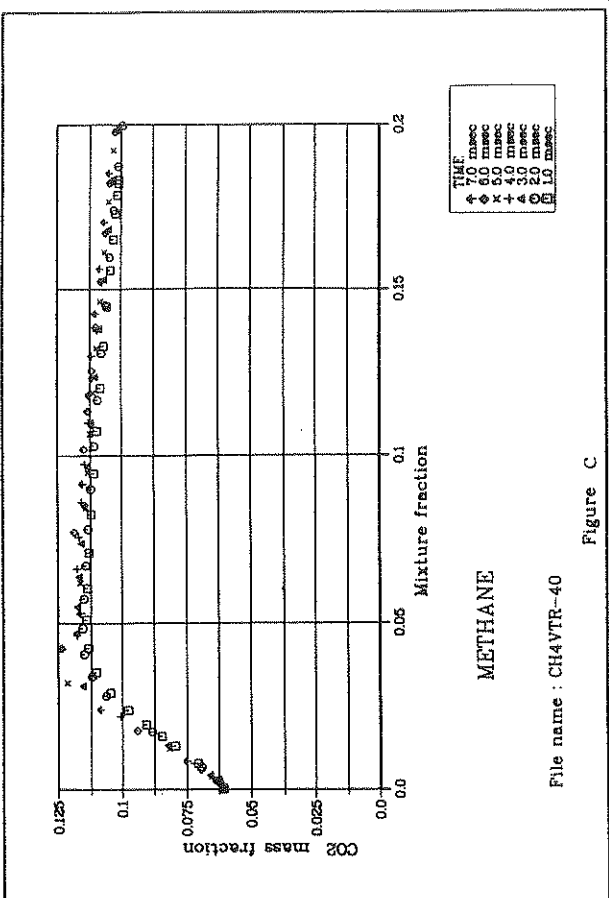


Figure C

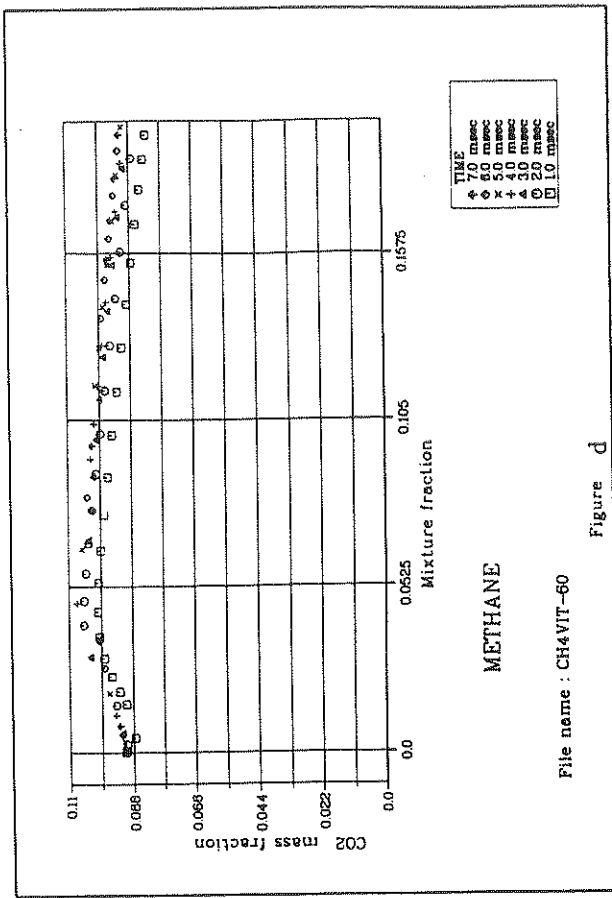


Figure d

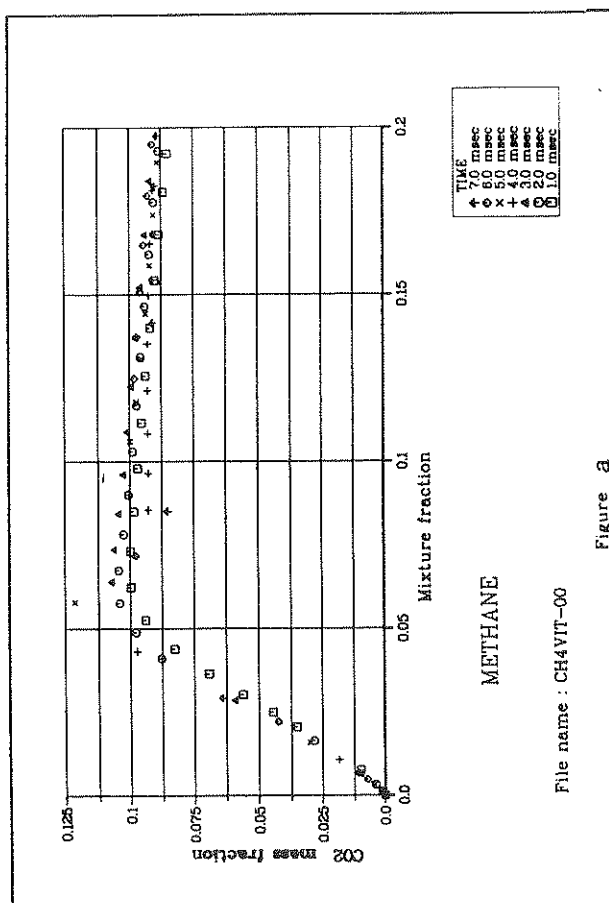


Figure a

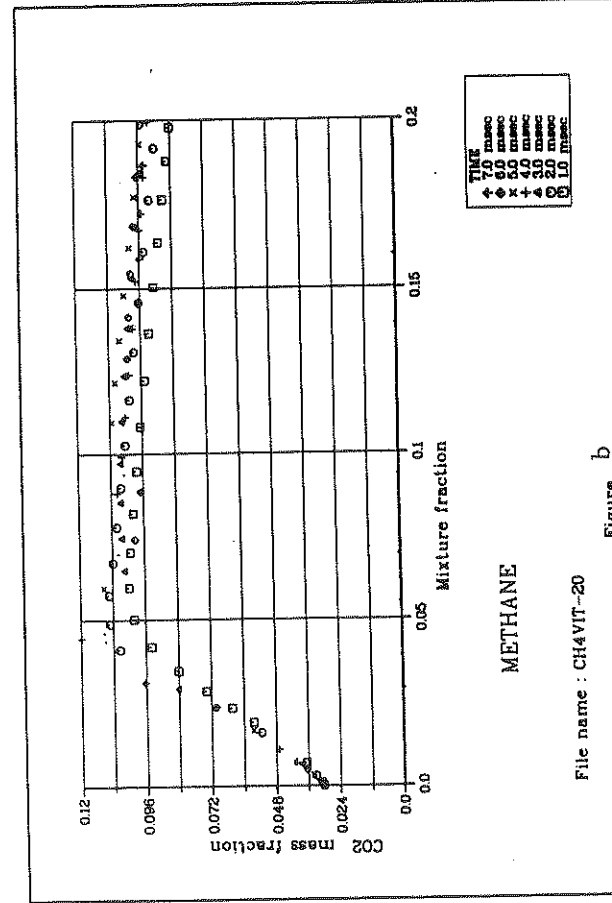


Figure b

Figure E25

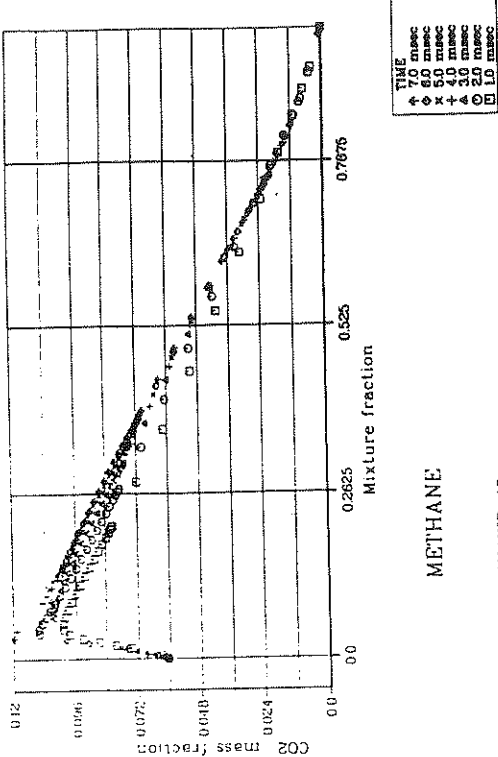


Figure c

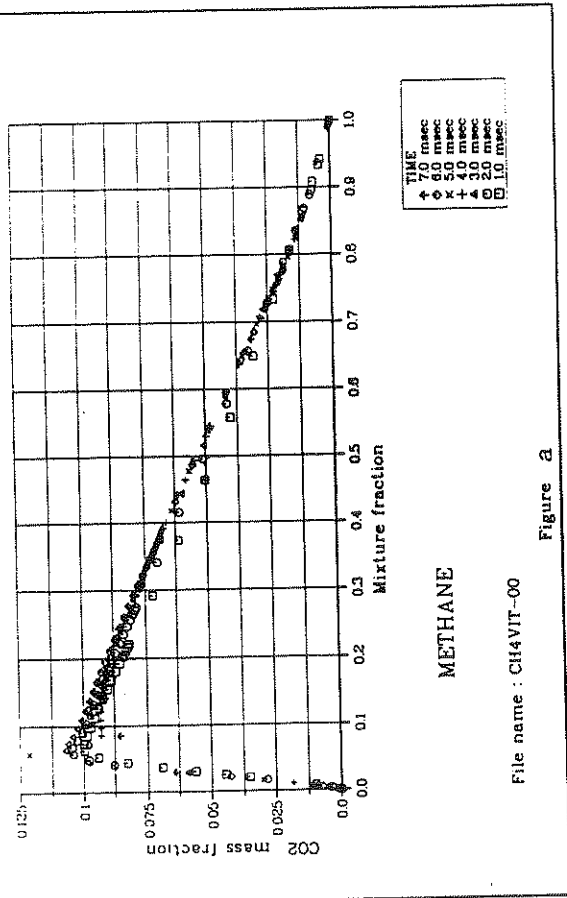
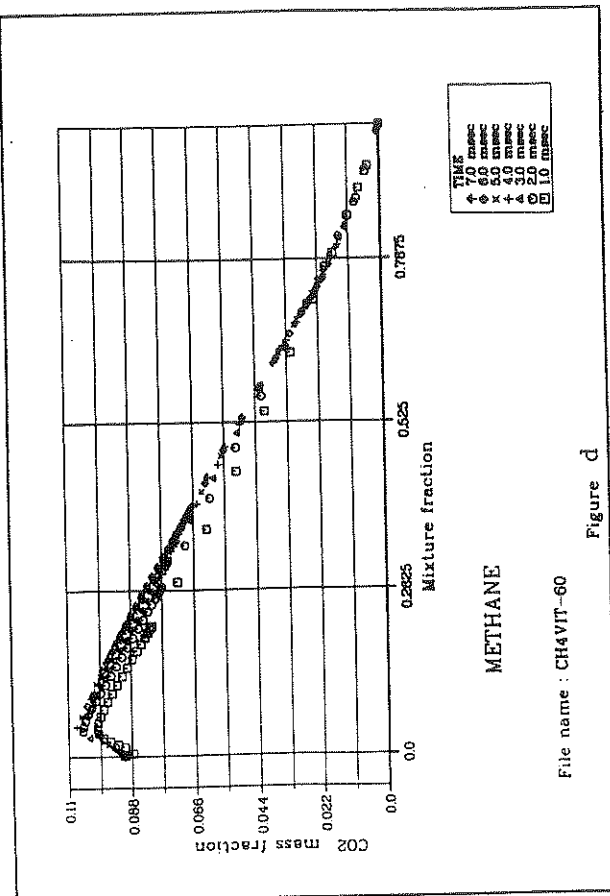


Figure E26

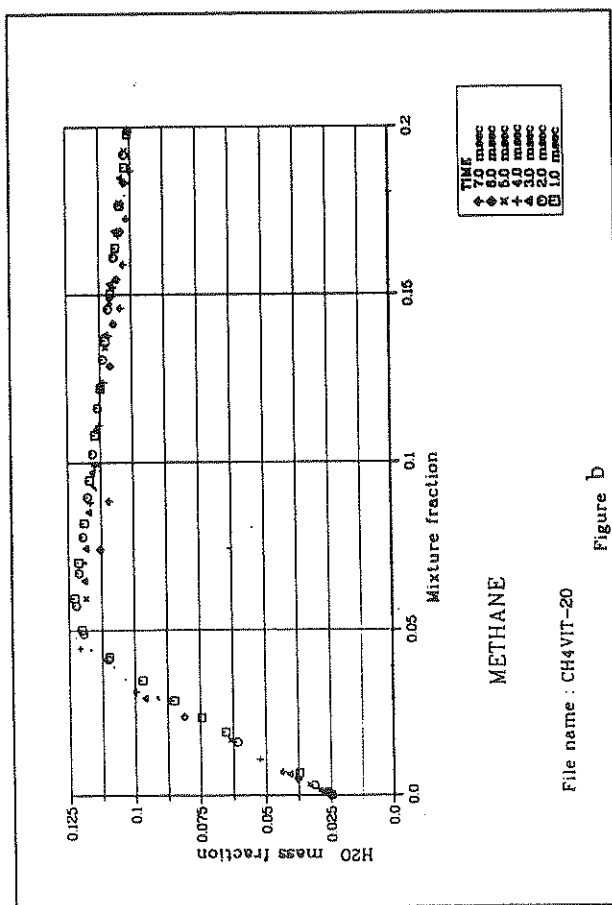
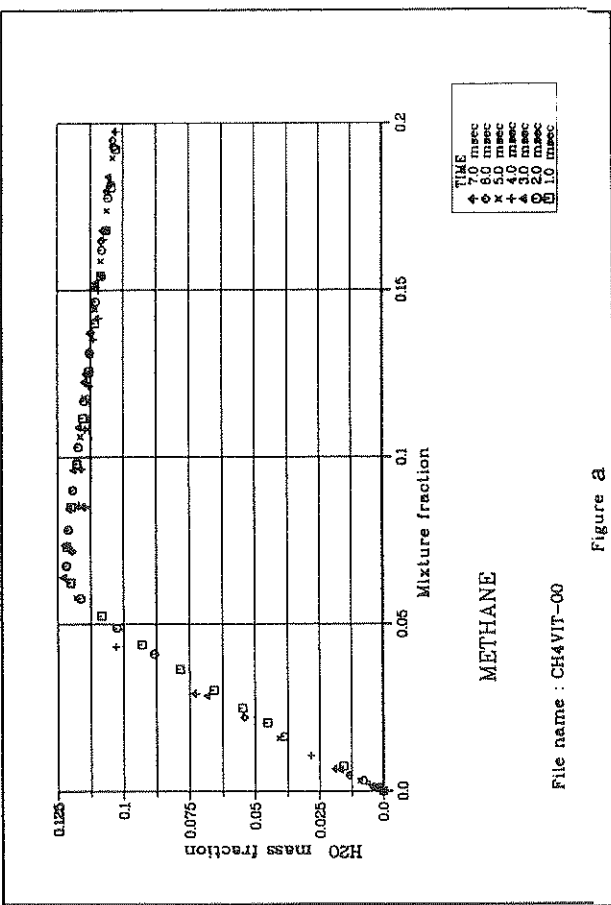
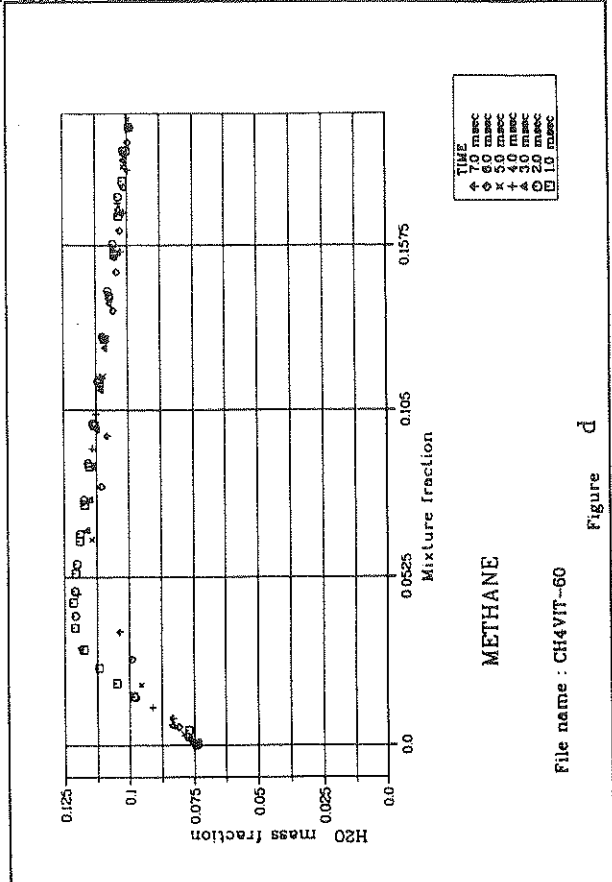
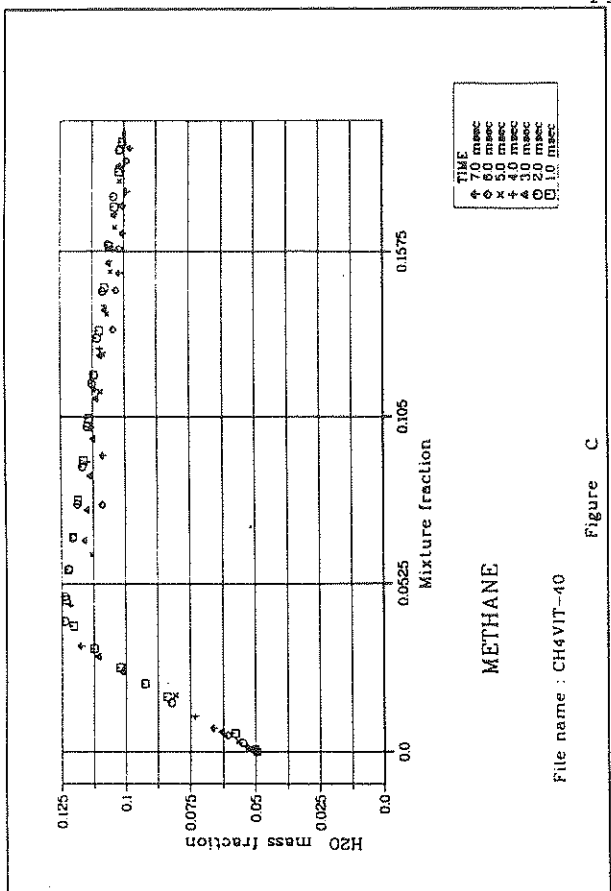


Figure E27

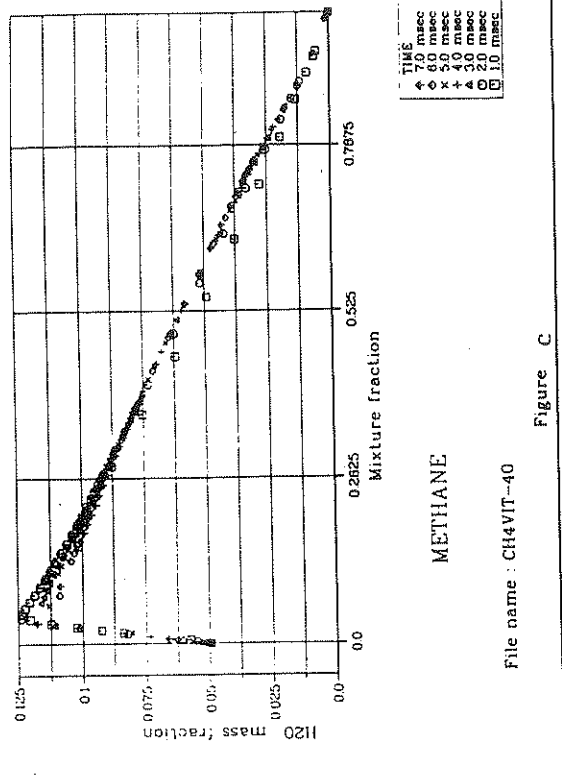


Figure C

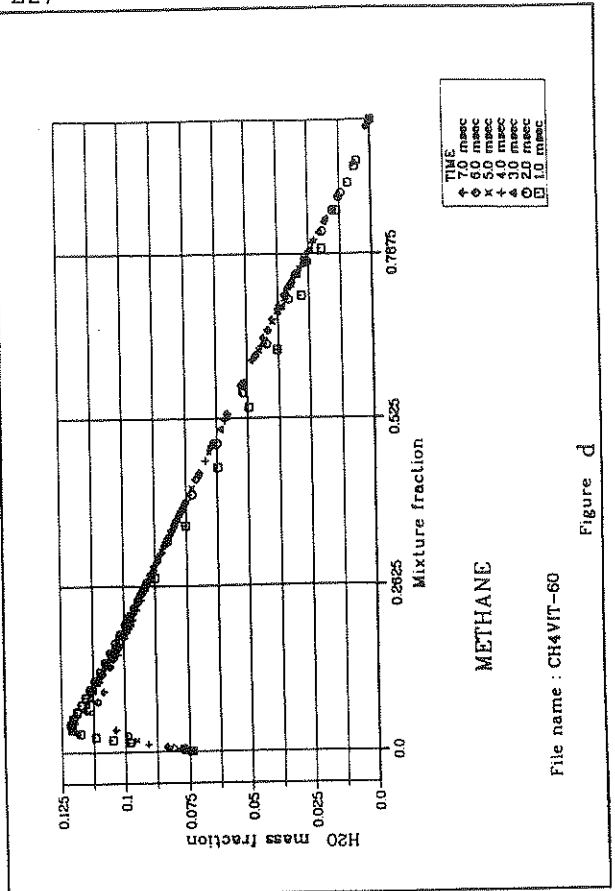


Figure d

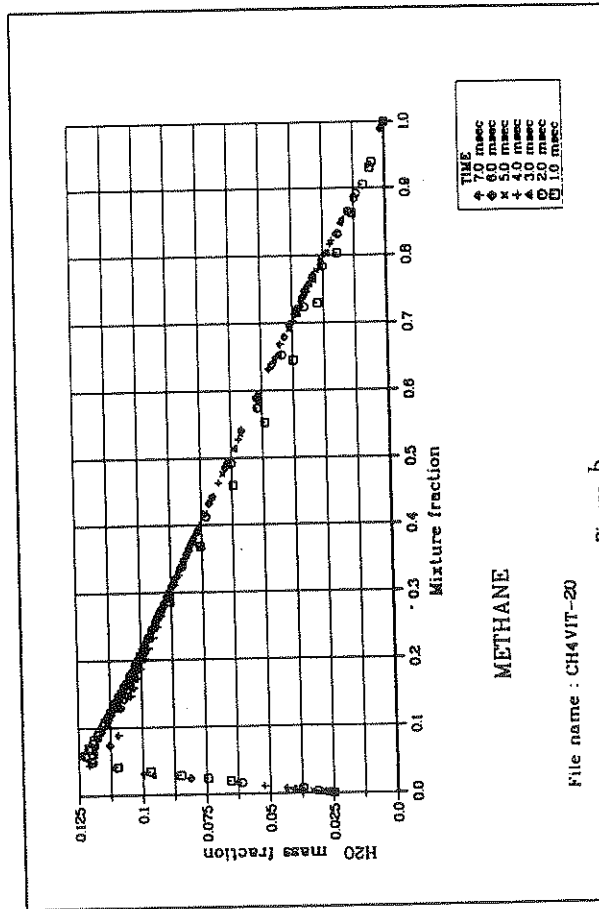


Figure b

Figure E28

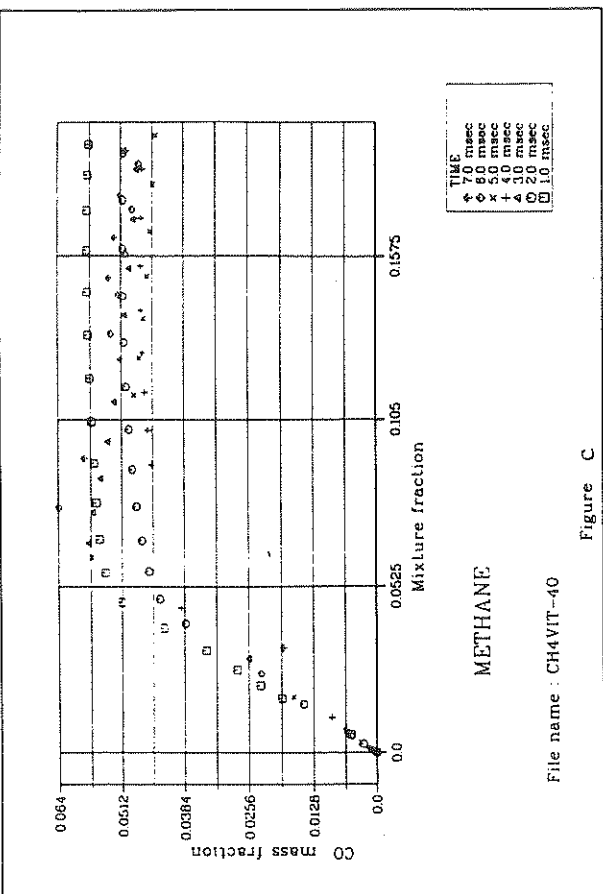


Figure C

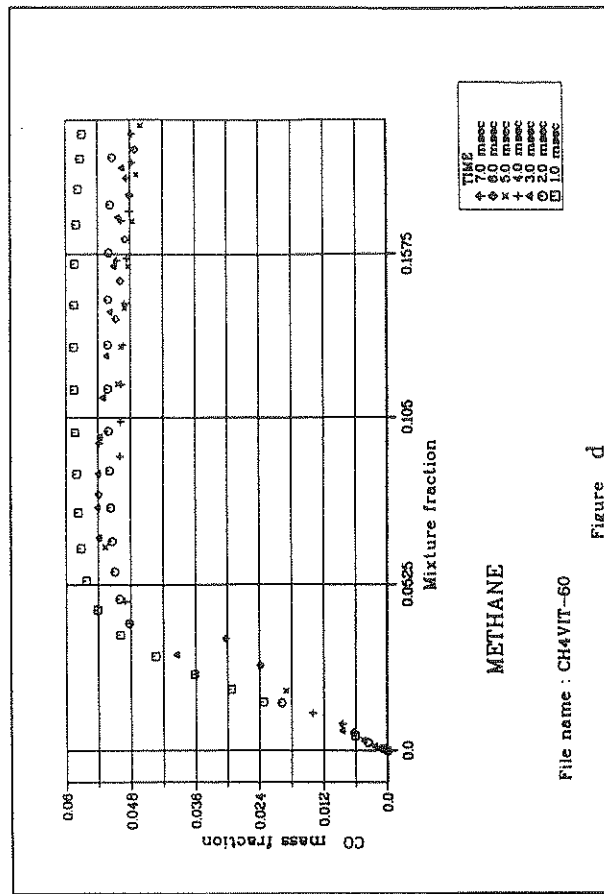


Figure d

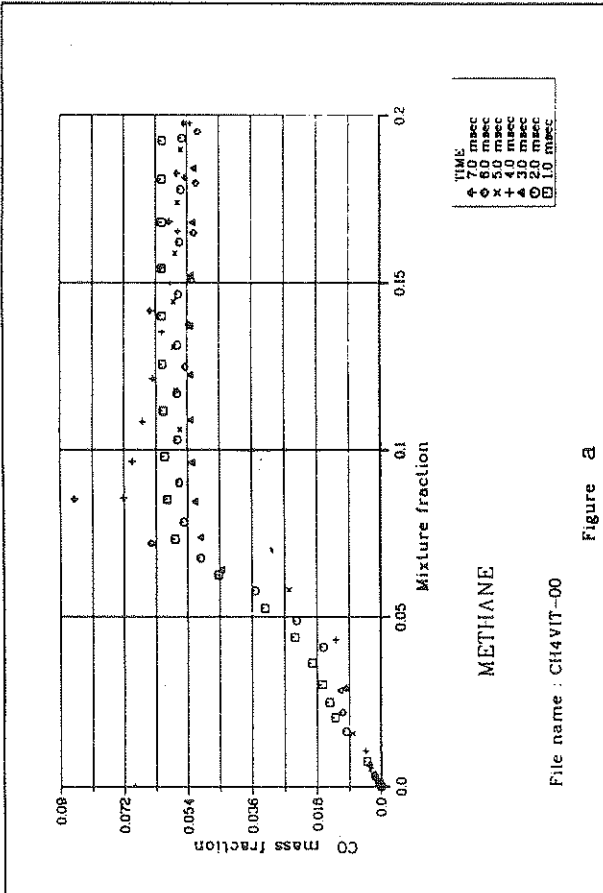


Figure a

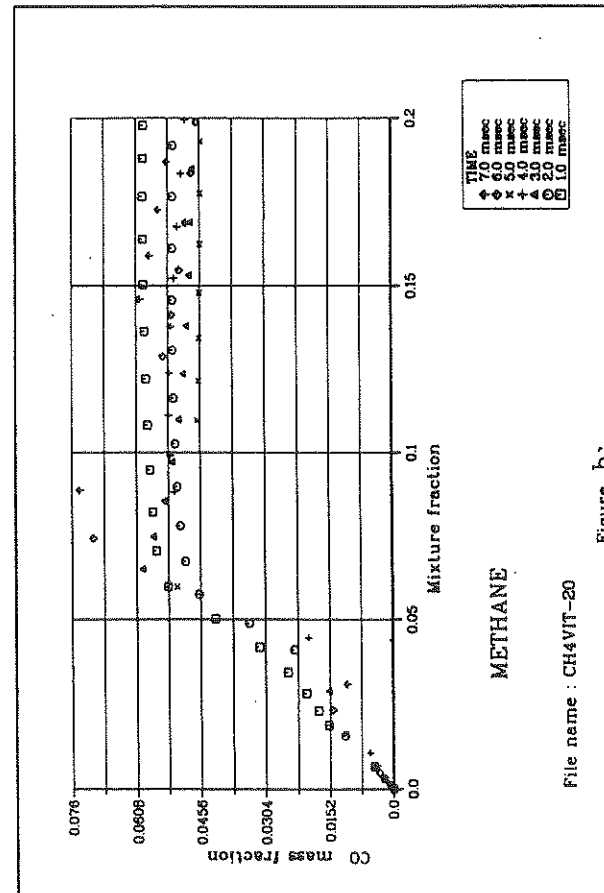
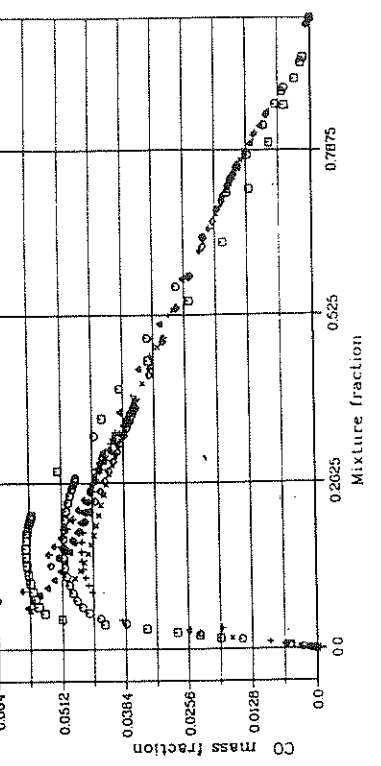


Figure b

Figure E29



File name : CH4 VIT-00

Figure a

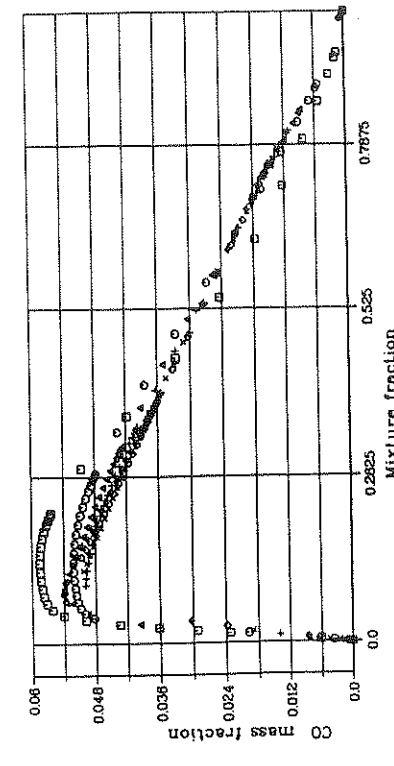
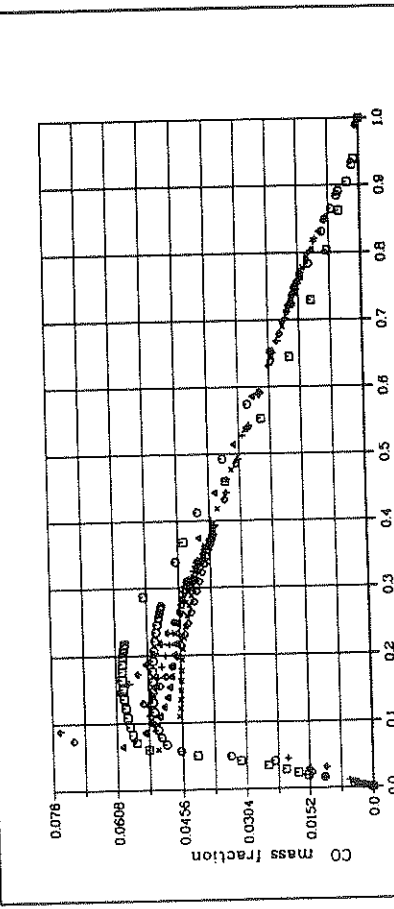


Figure C

File name : CH4 VIT-40

Figure d



File name : CH4 VIT-60

Figure b

Figure E30

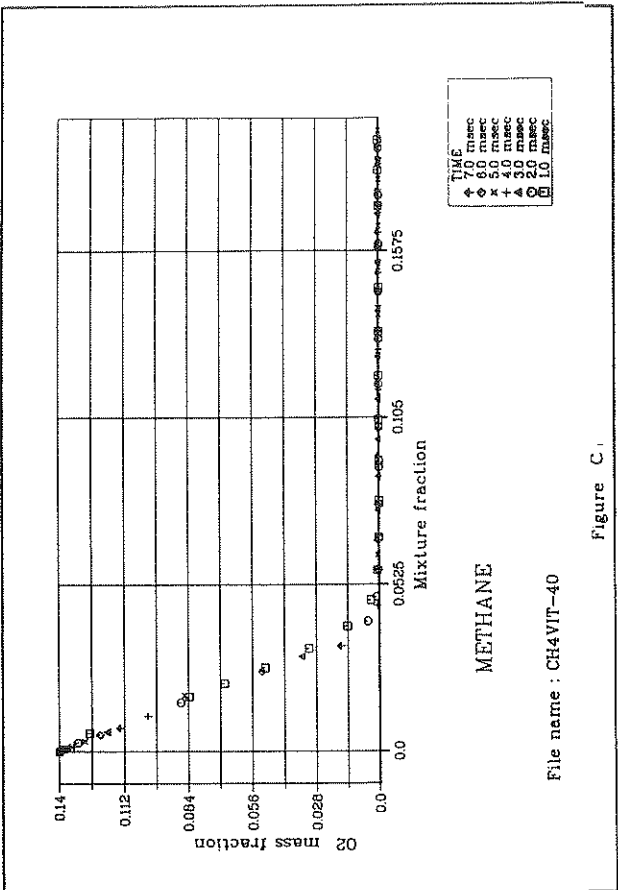


Figure C

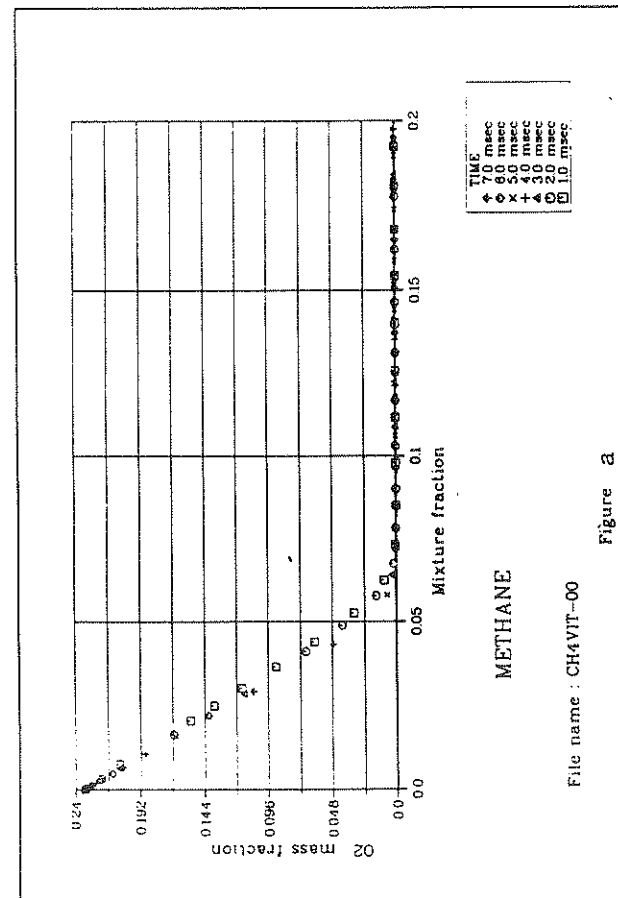
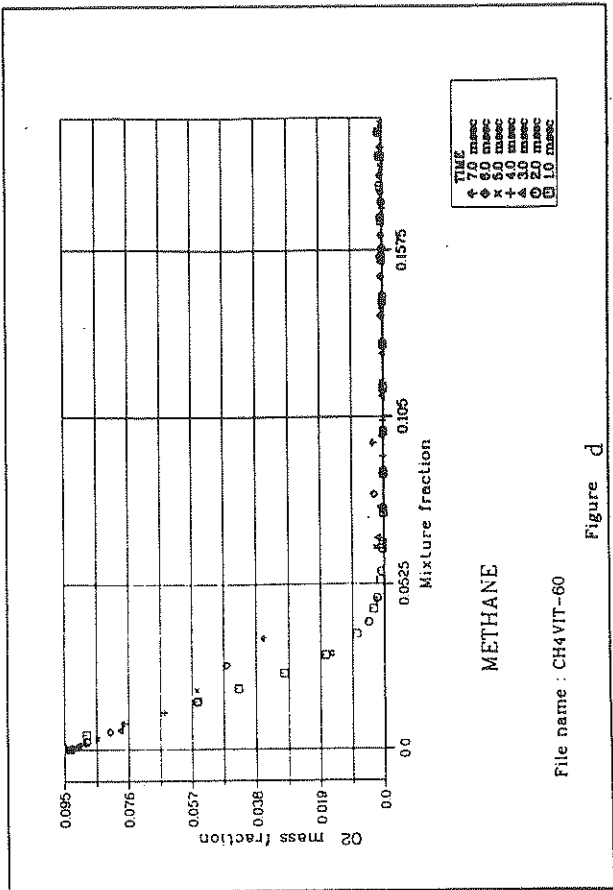


Figure E31

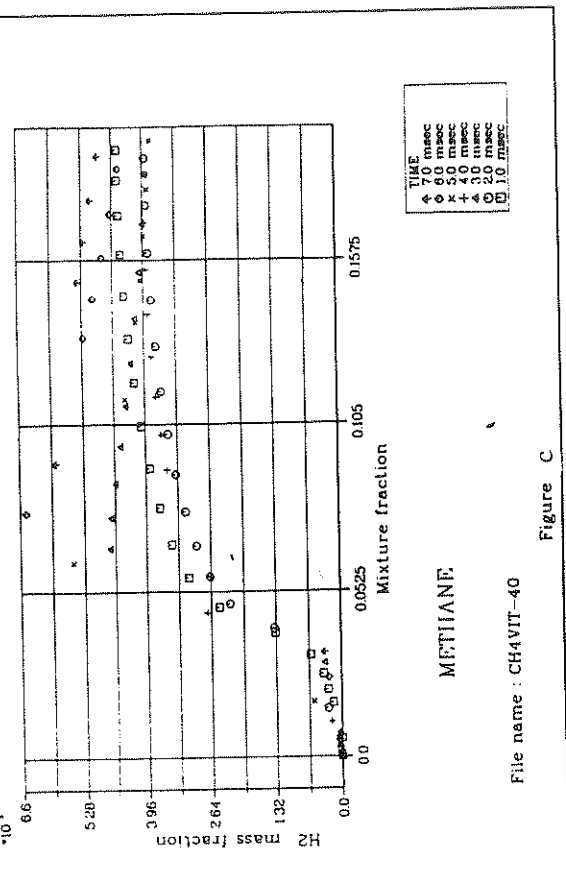


Figure C

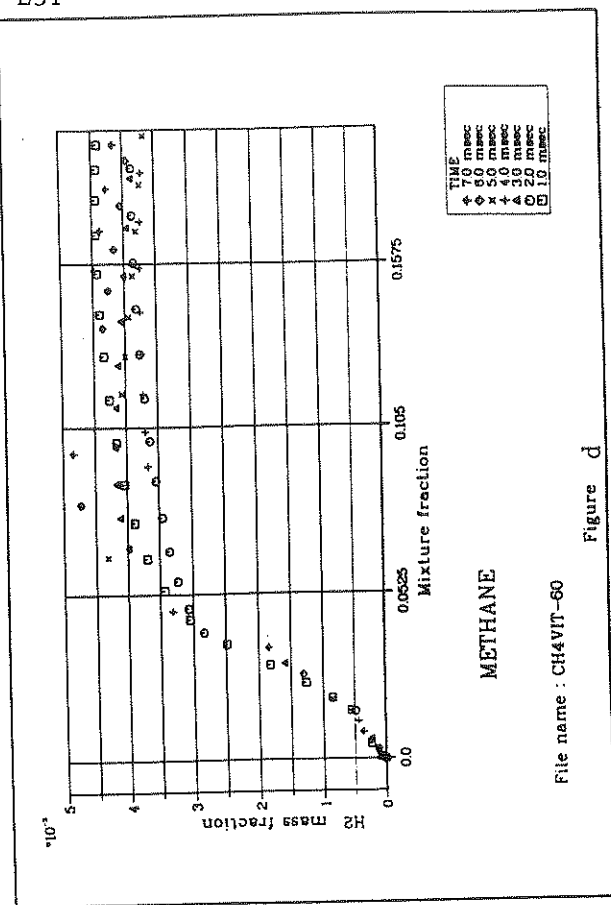


Figure d

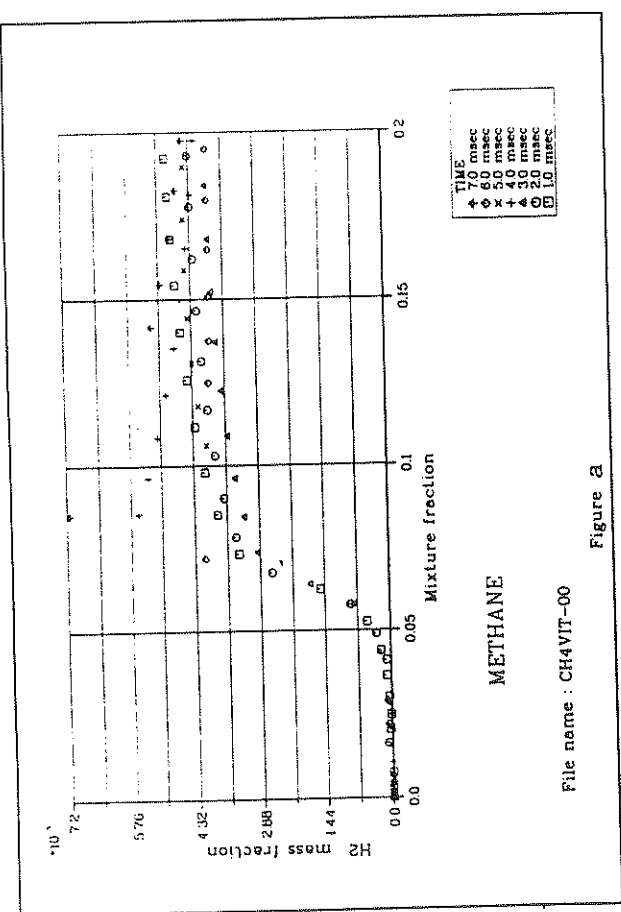


Figure b

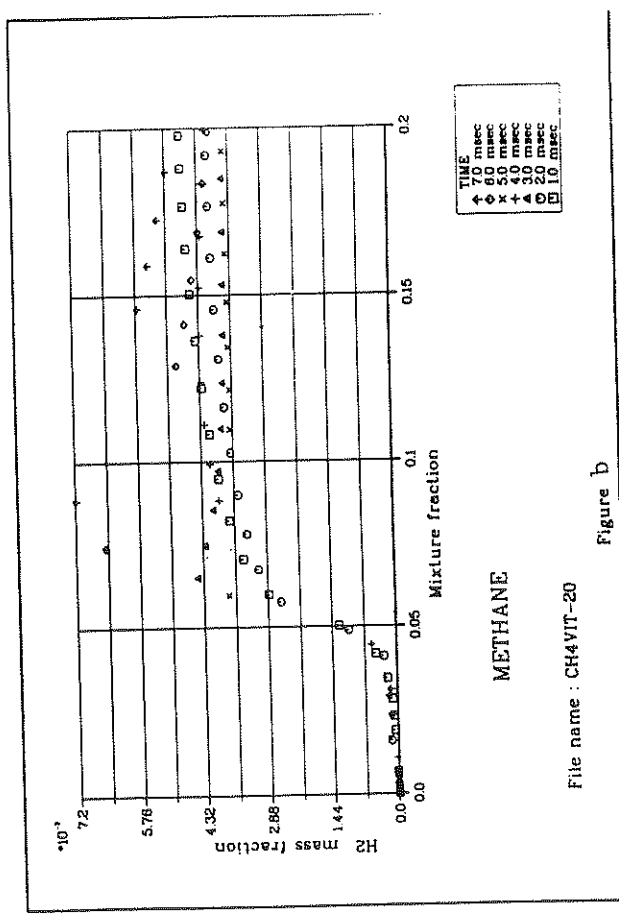


Figure a

Figure E32

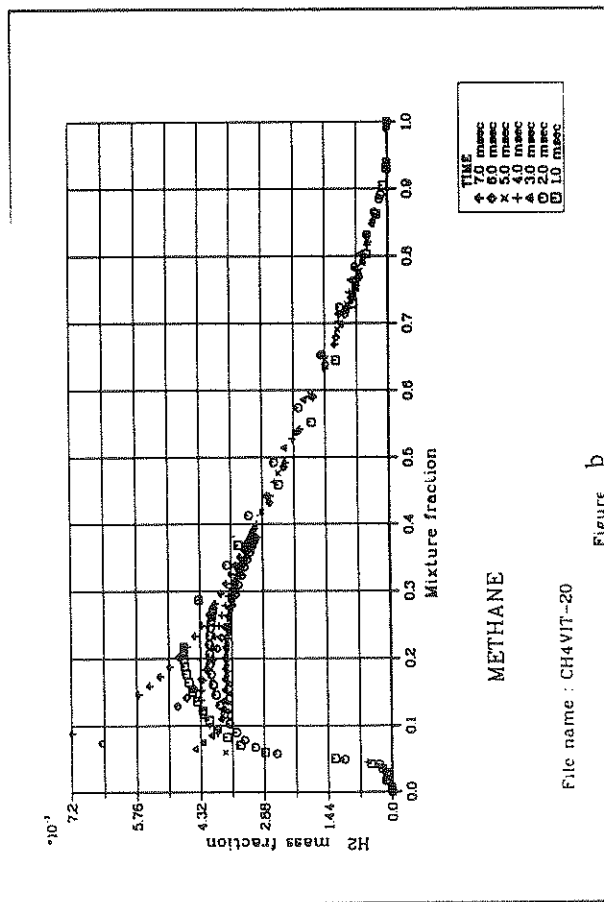
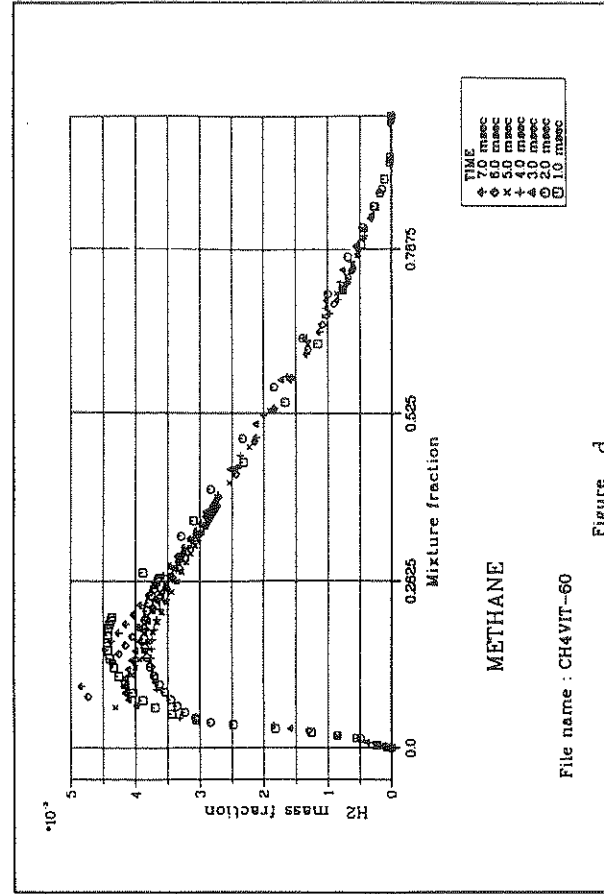
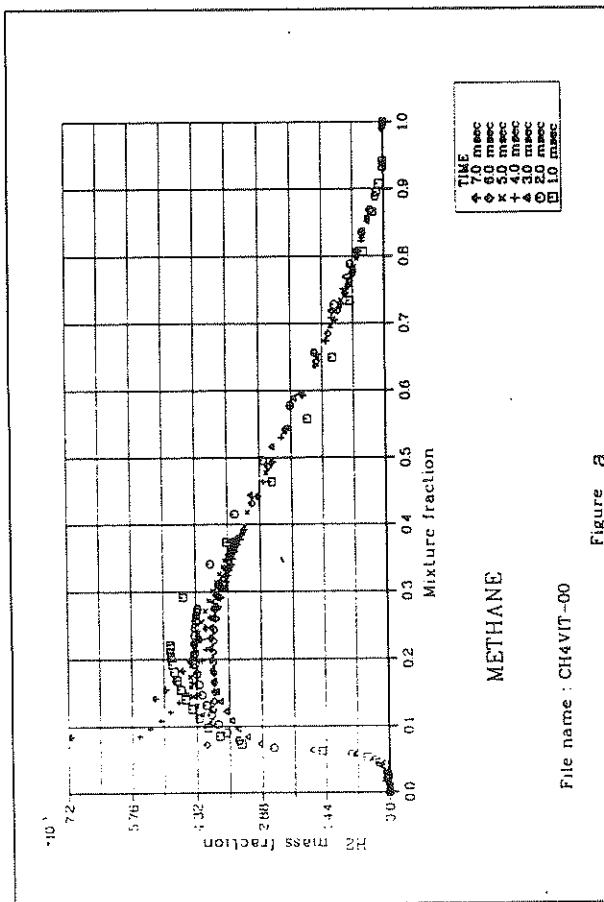
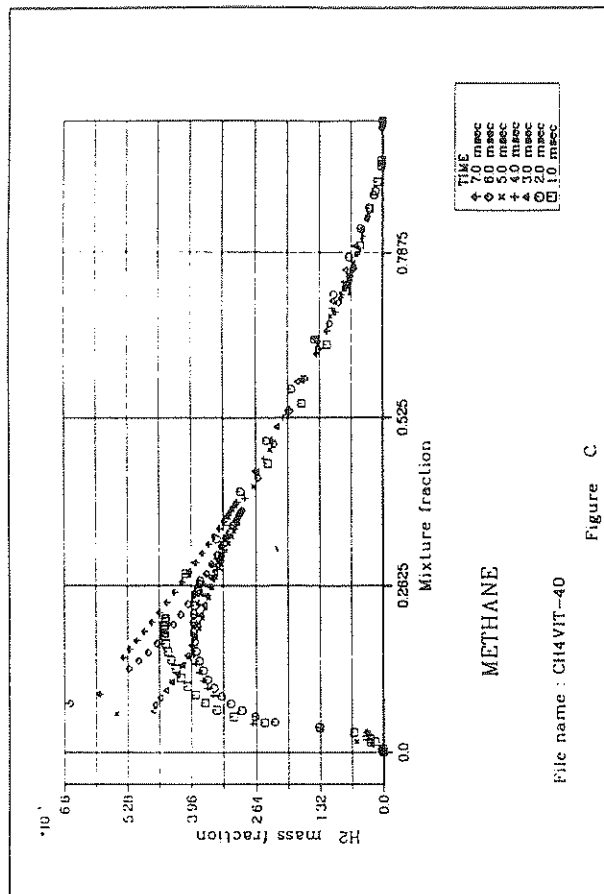


Figure E33

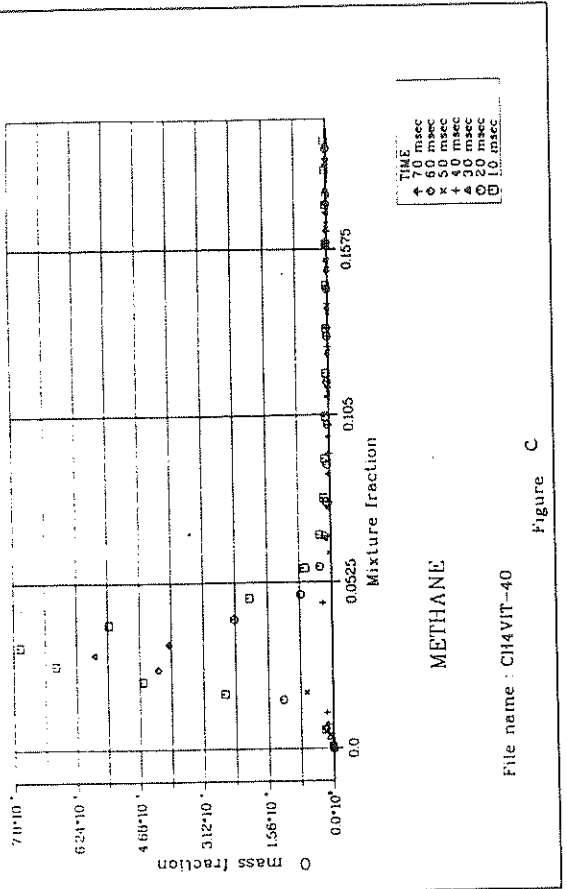
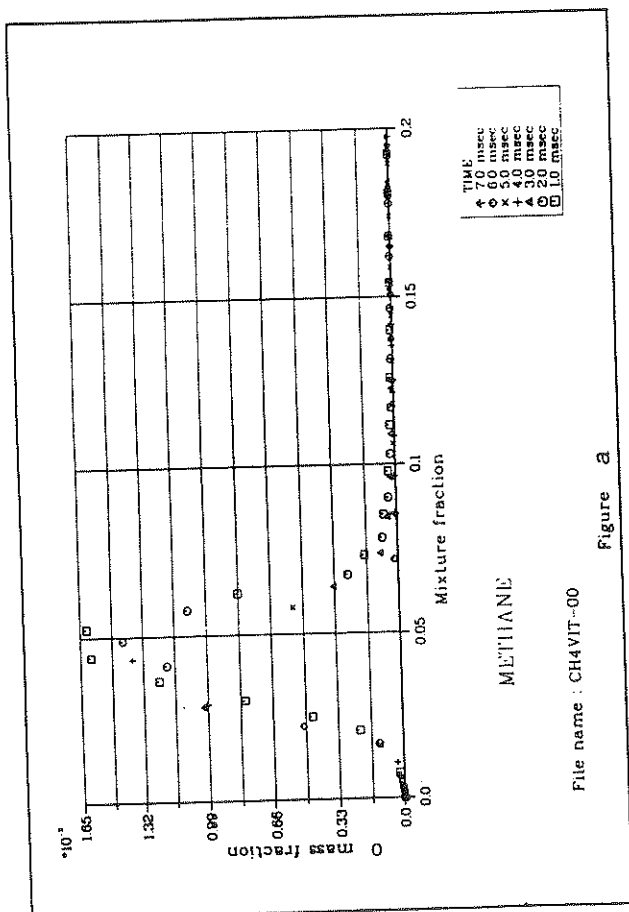


Figure c



E33

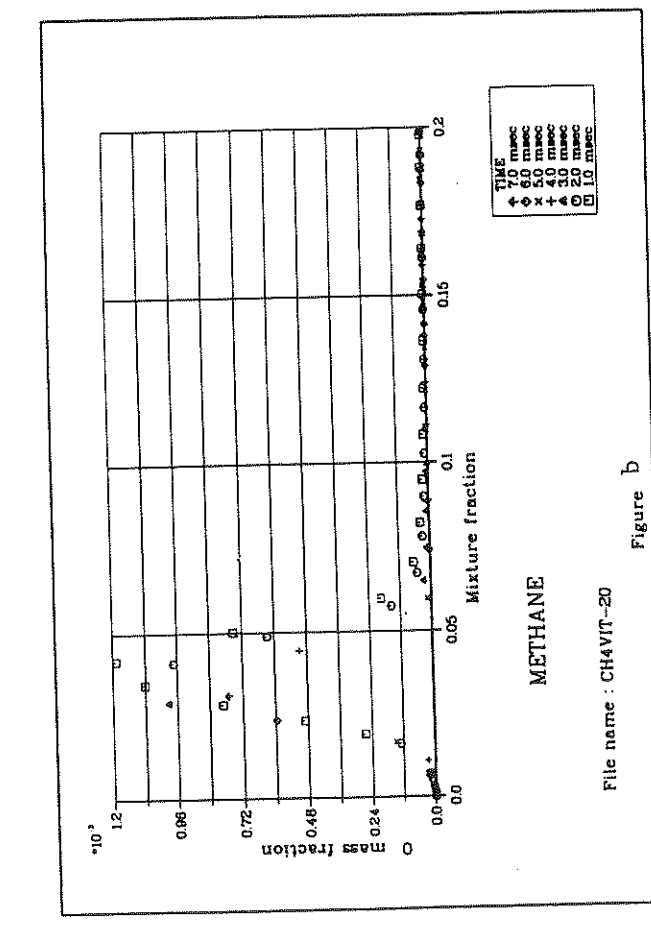


Figure d

Figure E34

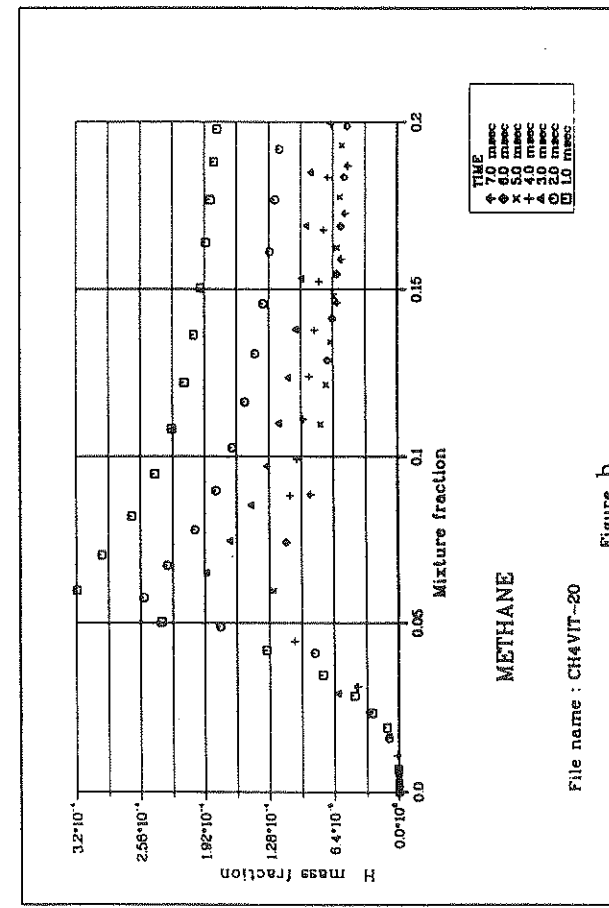
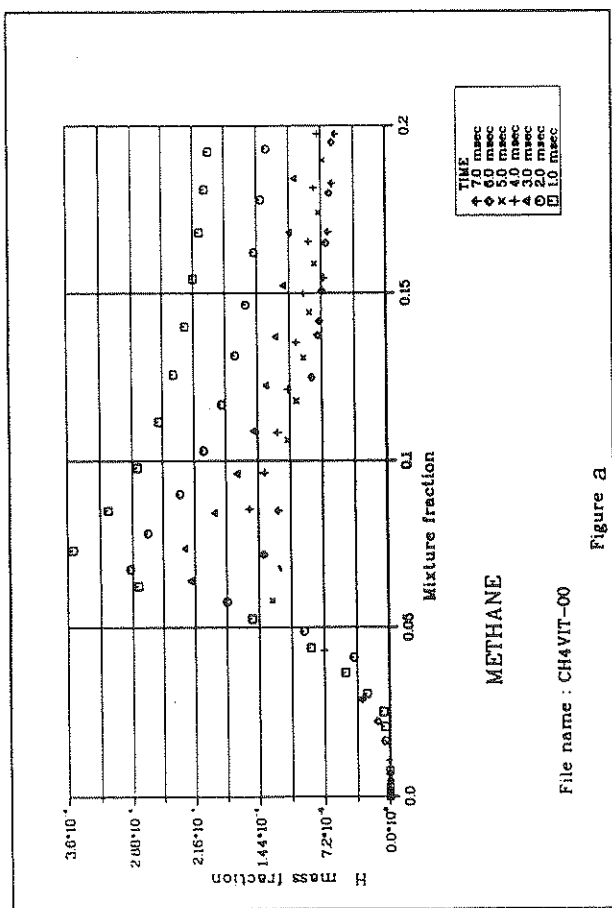
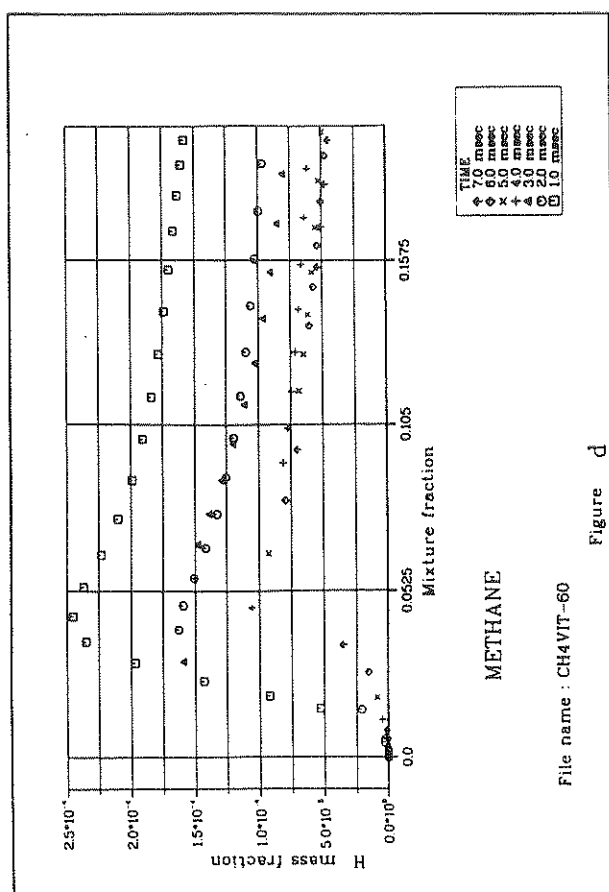
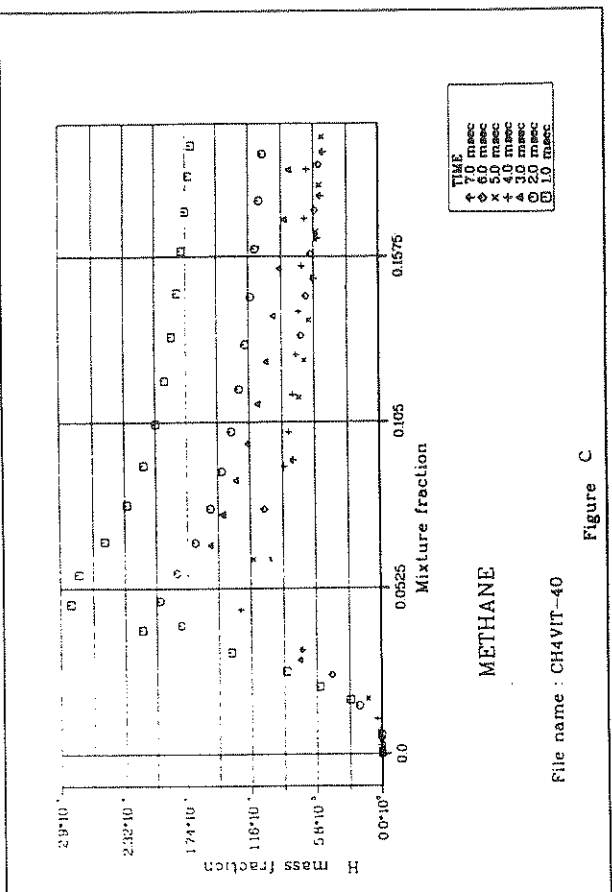


Figure E35

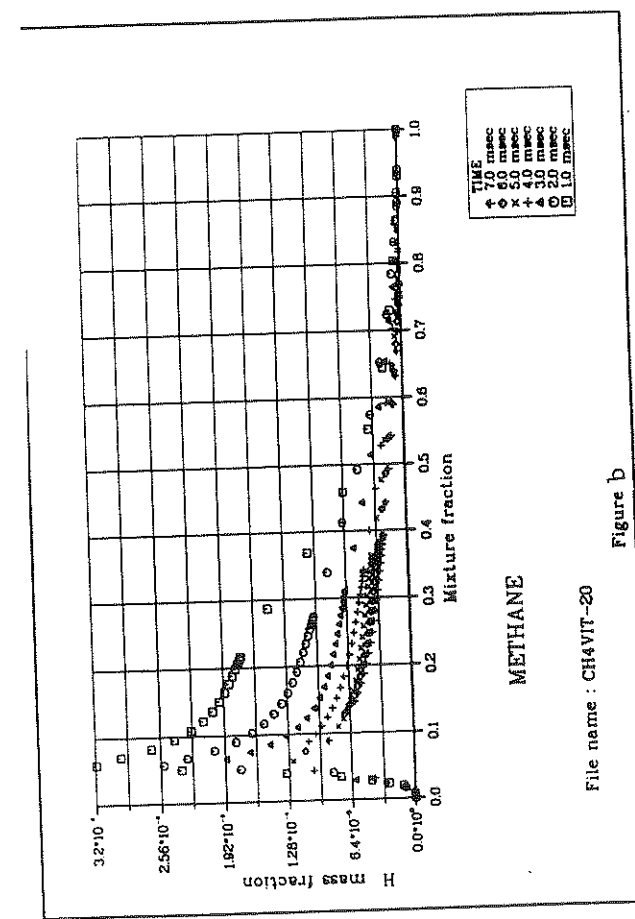
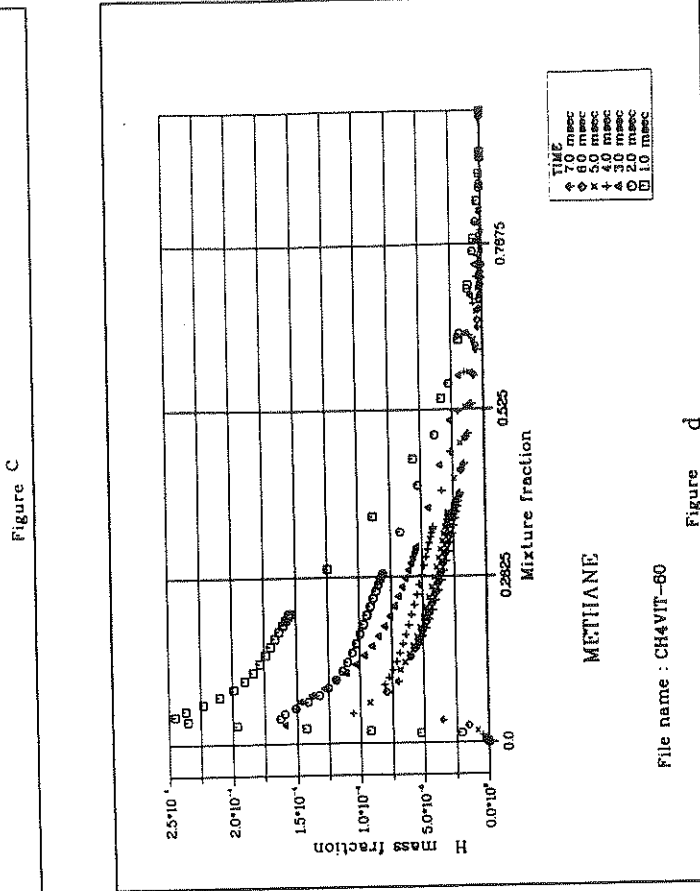
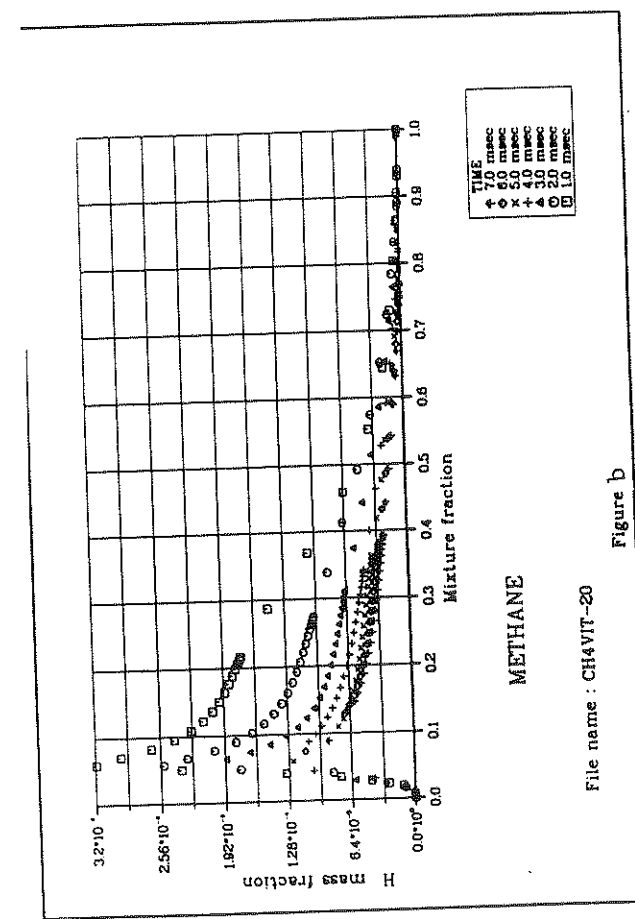
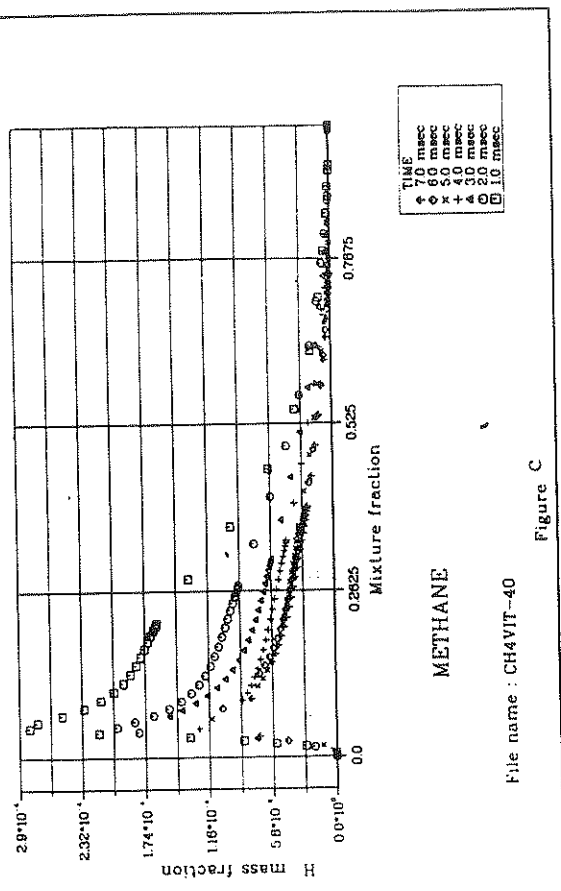


Figure E36

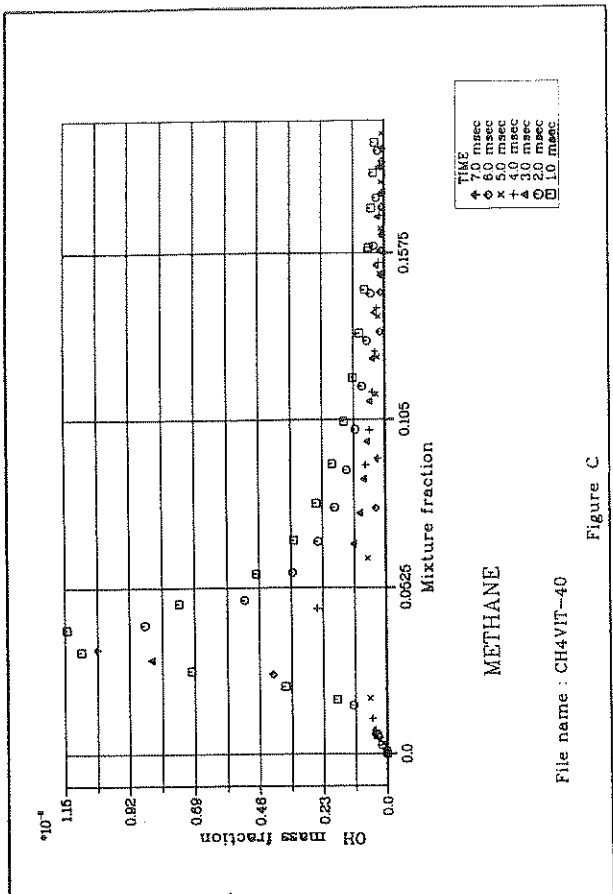


Figure C

File name : CH4VIT-40

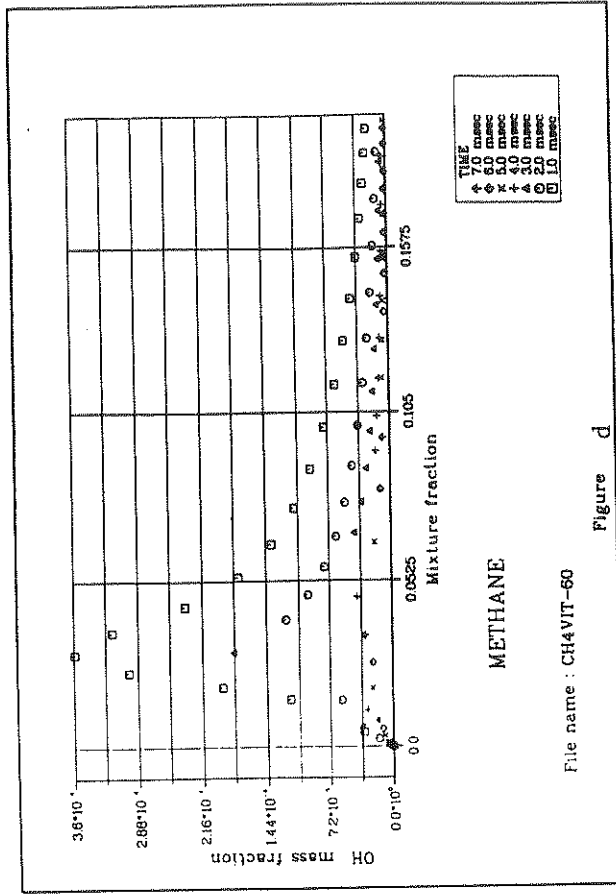


Figure d

File name : CH4VIT-50

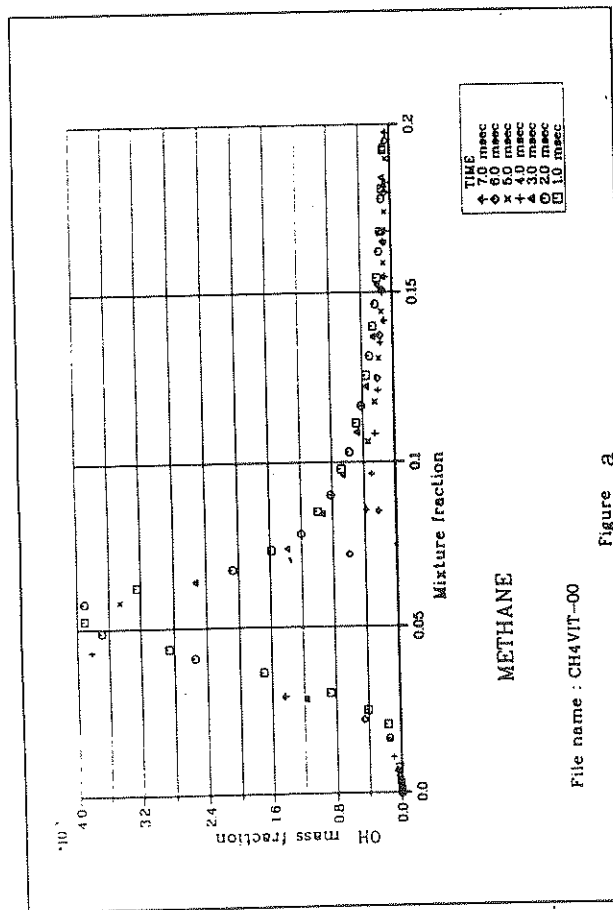


Figure a

File name : CH4VIT-00

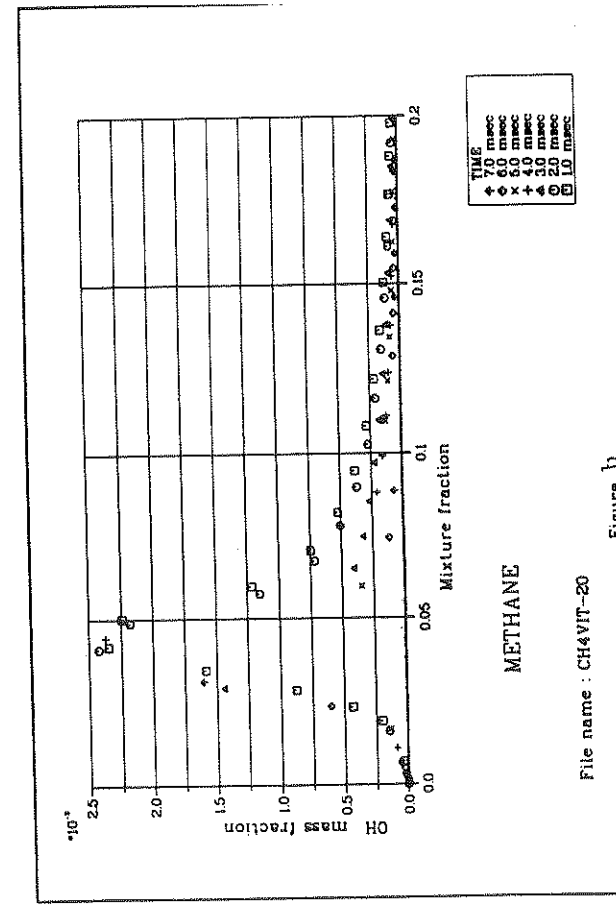


Figure b

File name : CH4VIT-10

Figure E37

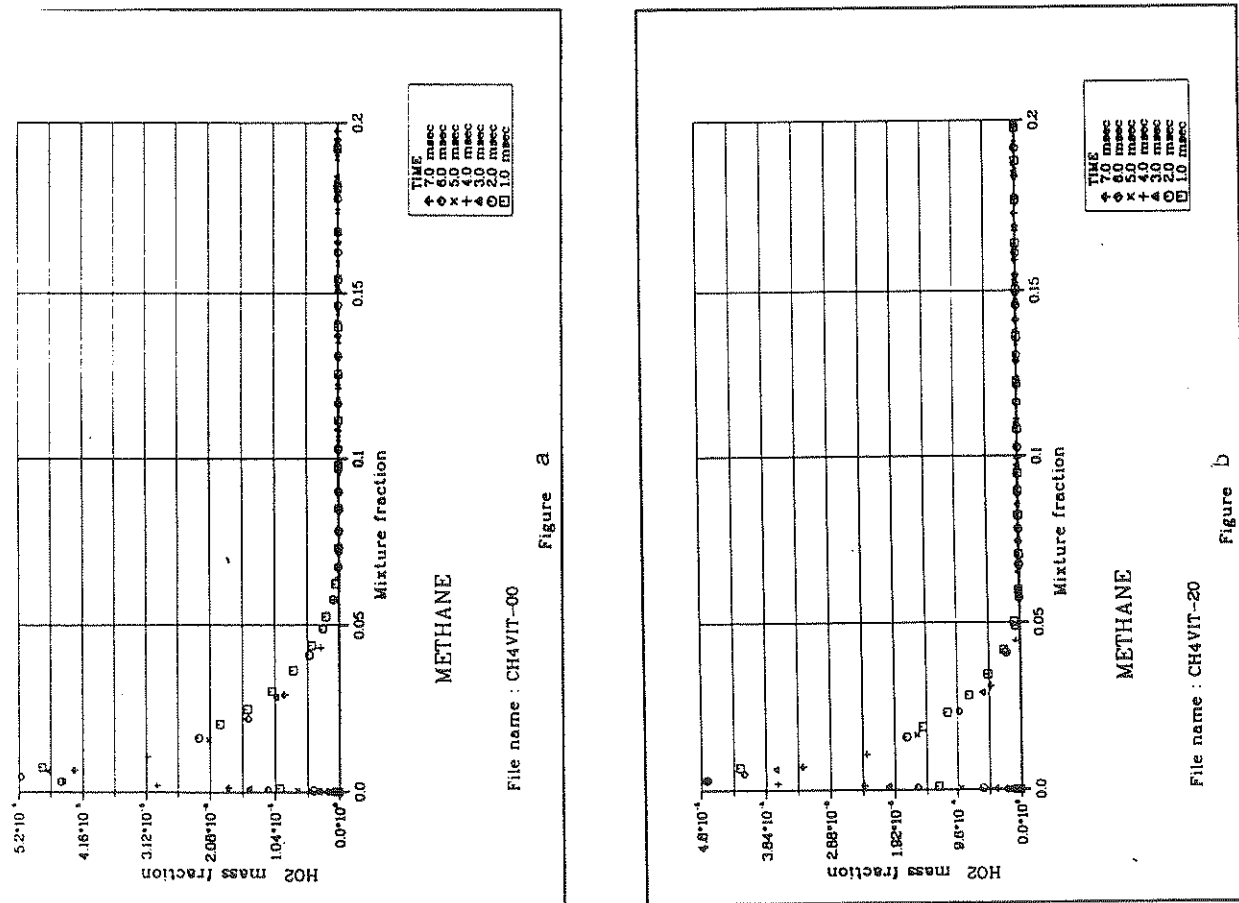
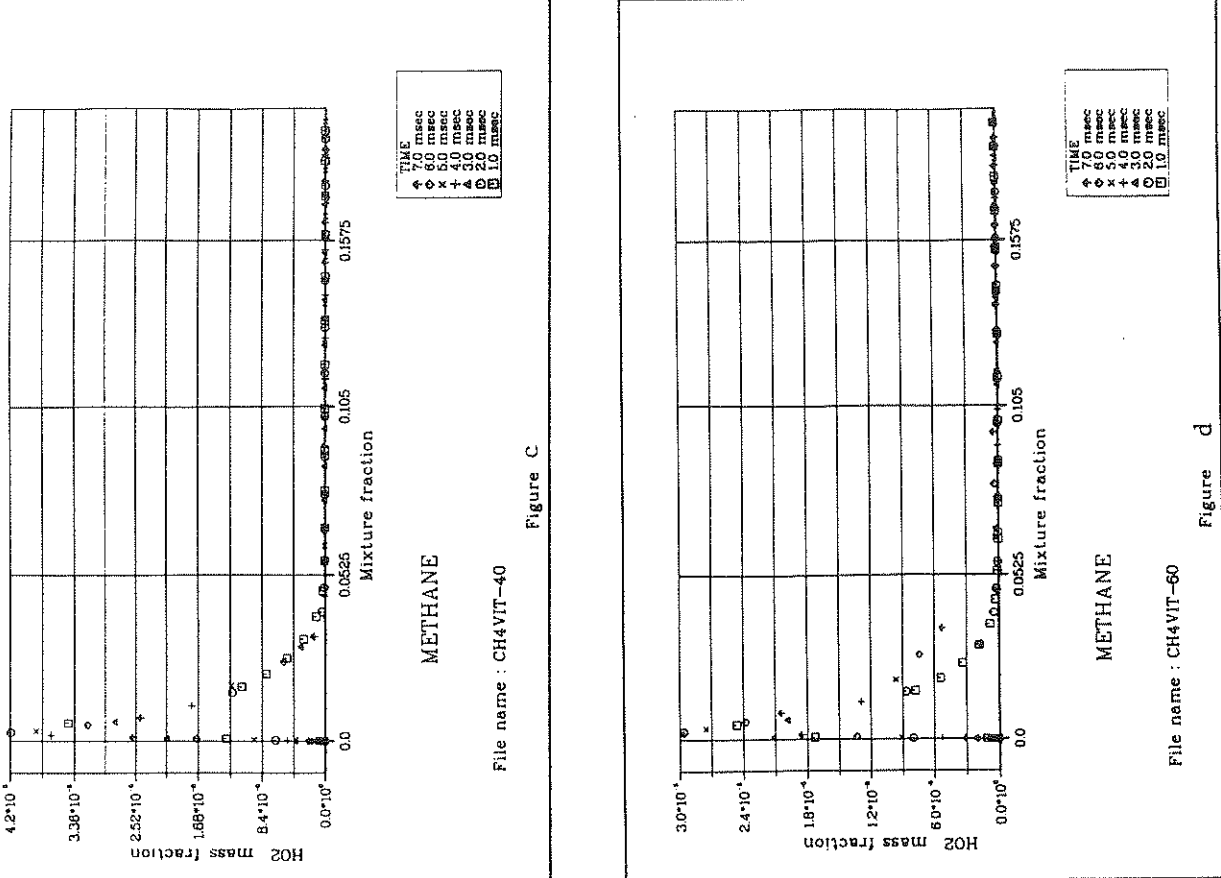
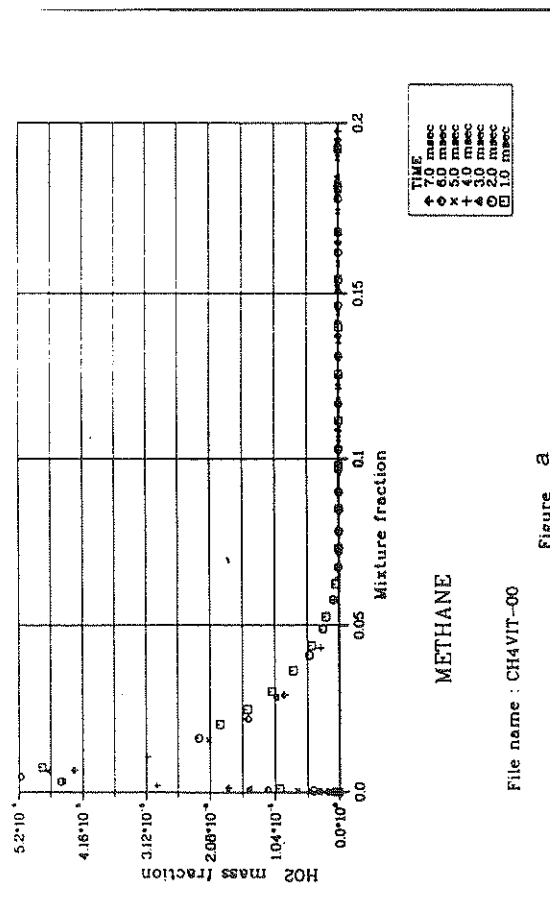
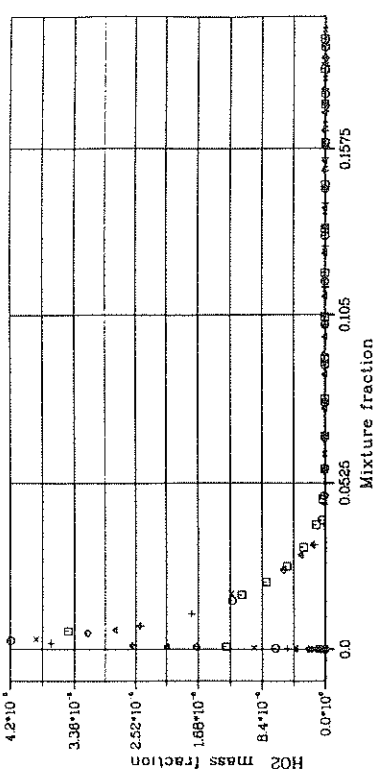


Figure E38

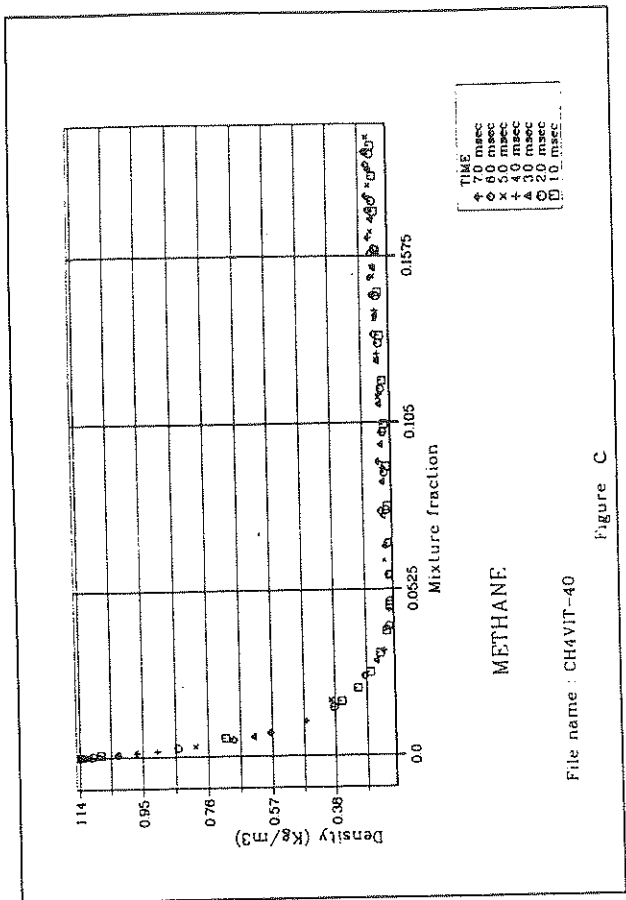


Figure C

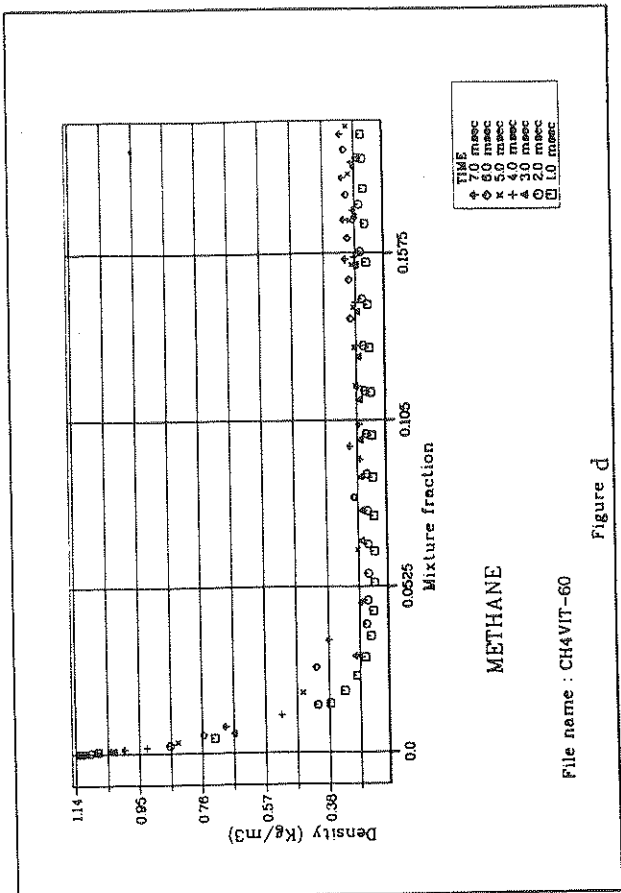


Figure d

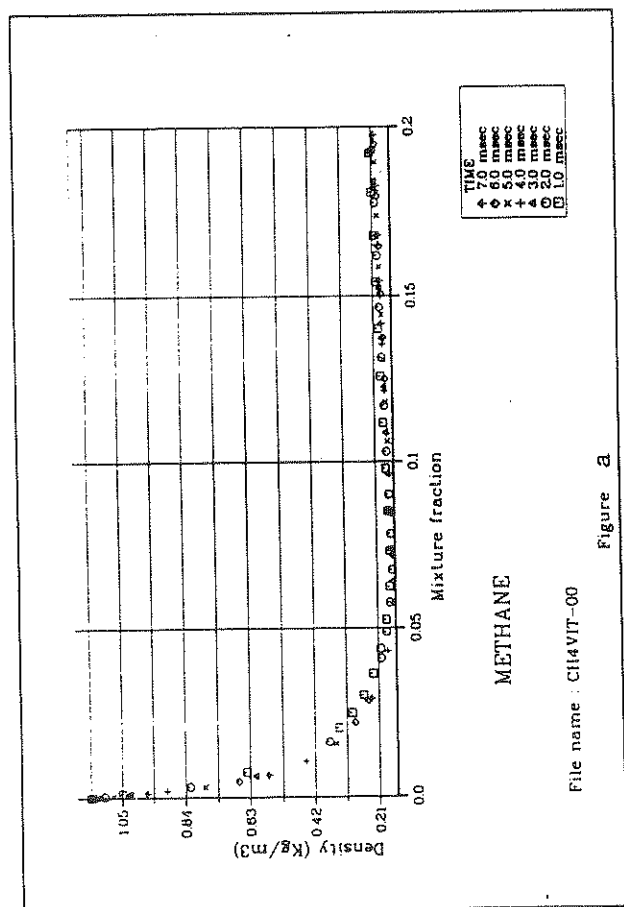


Figure a

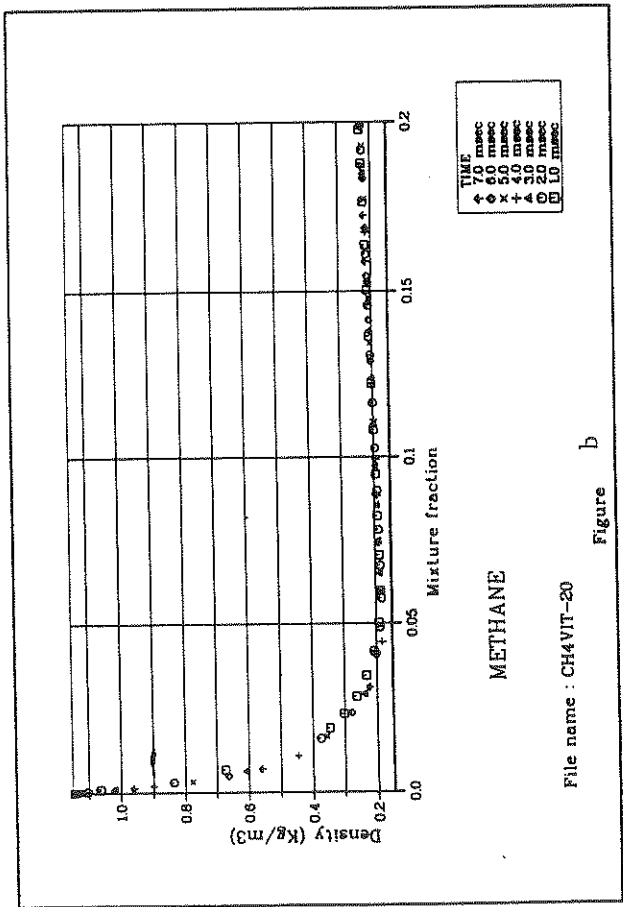


Figure b

Figure E39

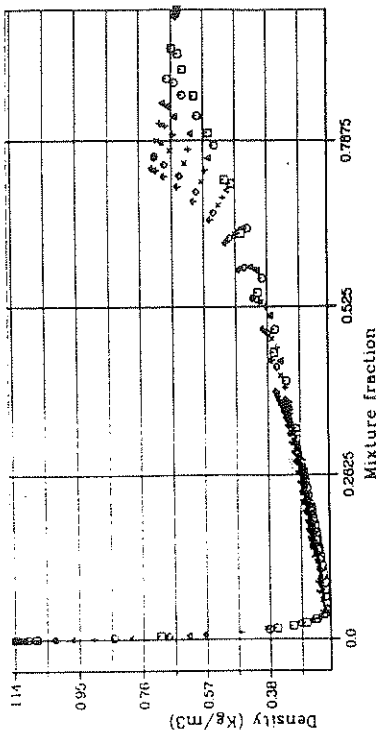


Figure C

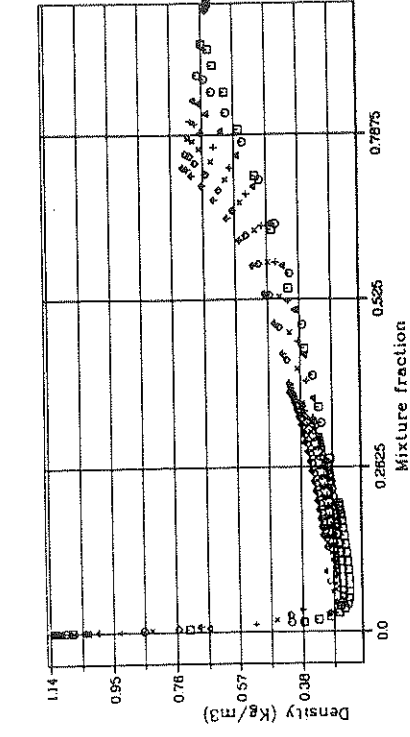


Figure d

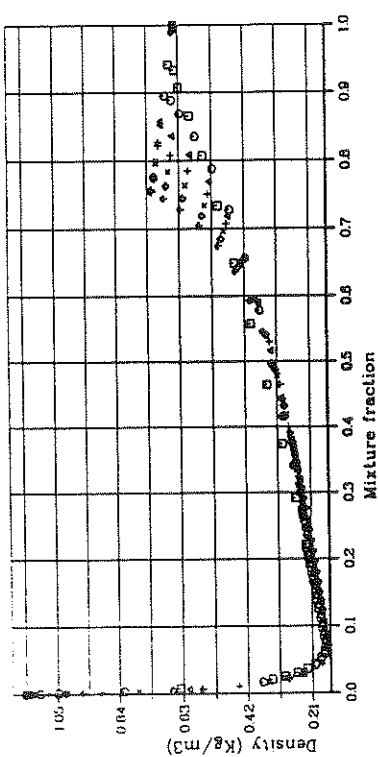


Figure a

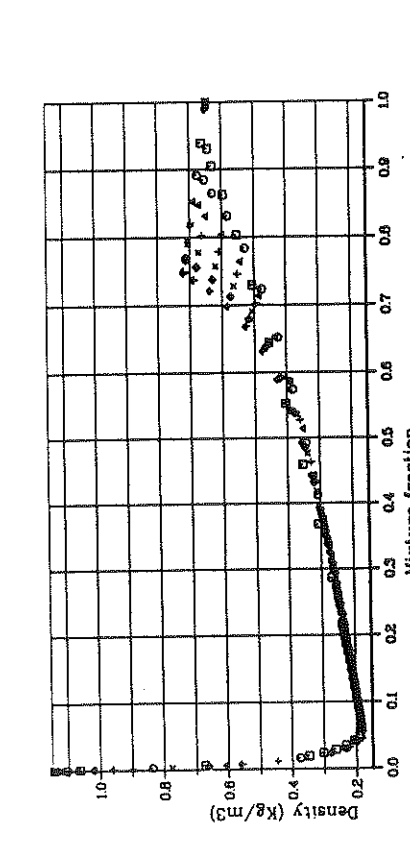


Figure b

Figure E40

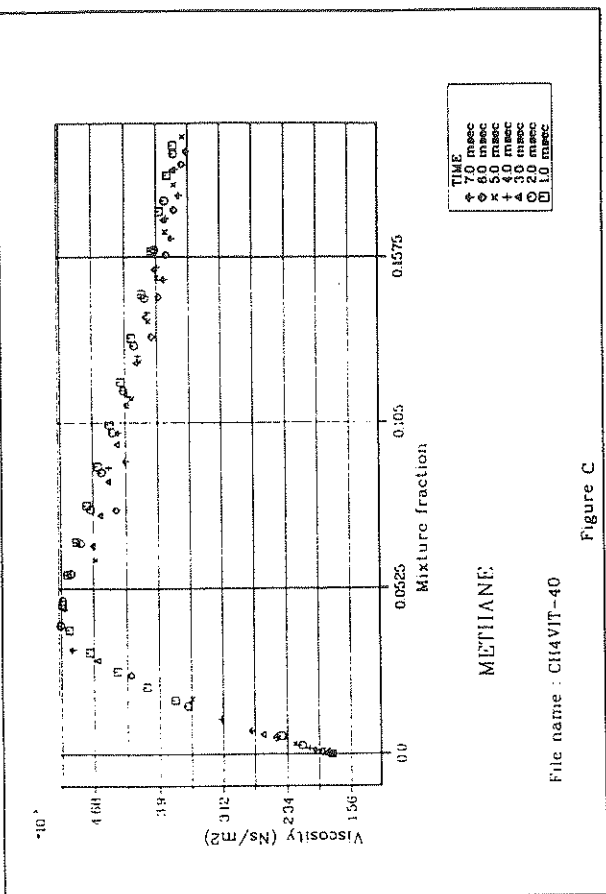


Figure C

File name : CH4VIT-40

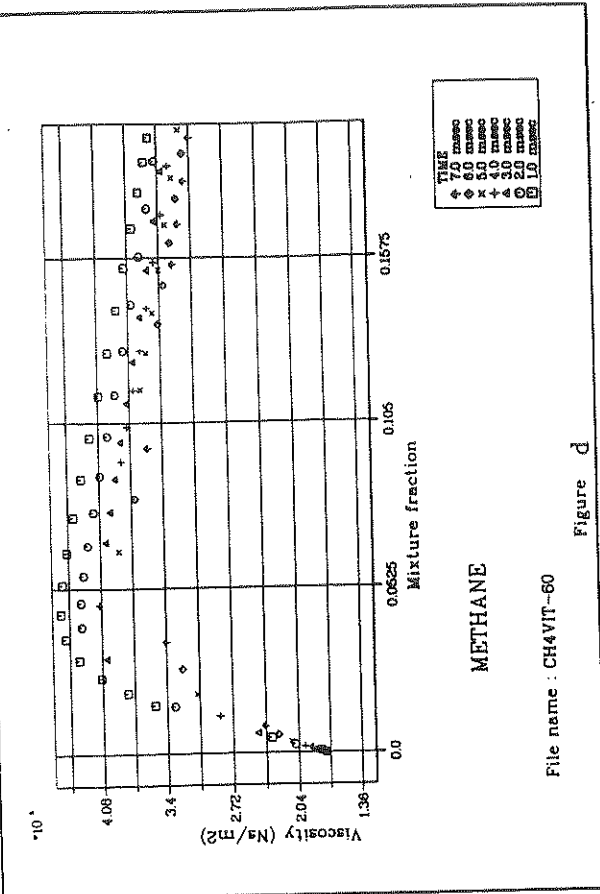


Figure d

File name : CH4VIT-60

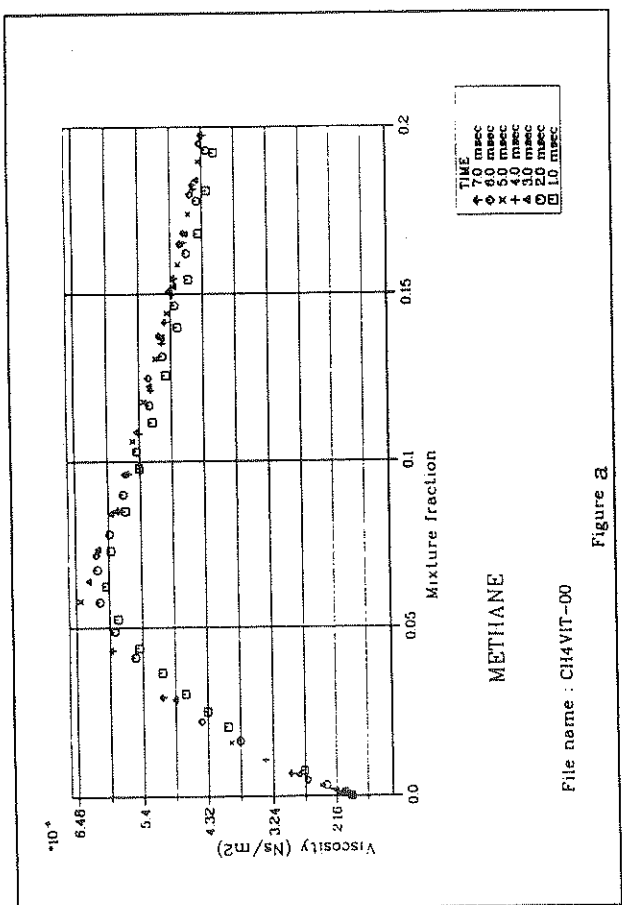


Figure b

File name : CH4VIT-00

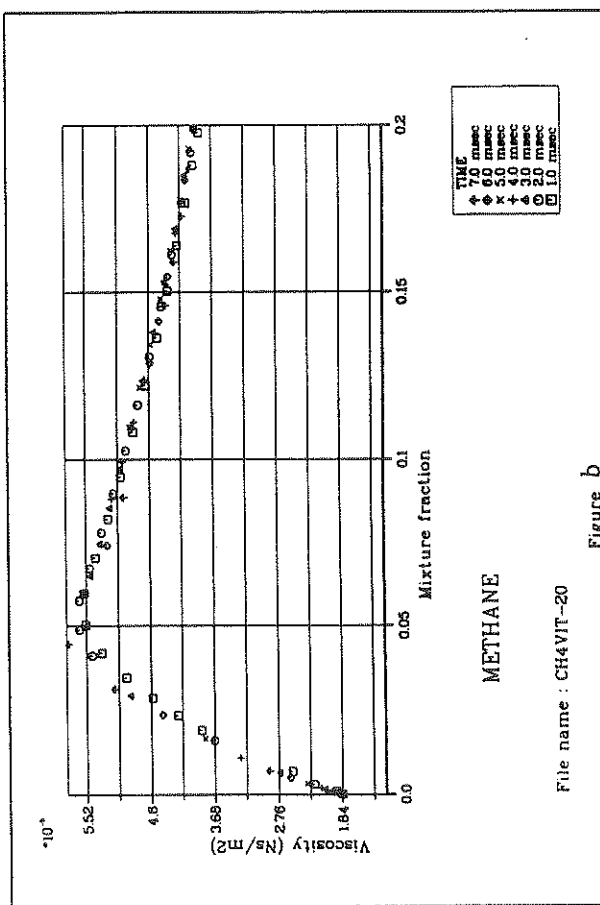


Figure a

File name : CH4VIT-20

Figure E41

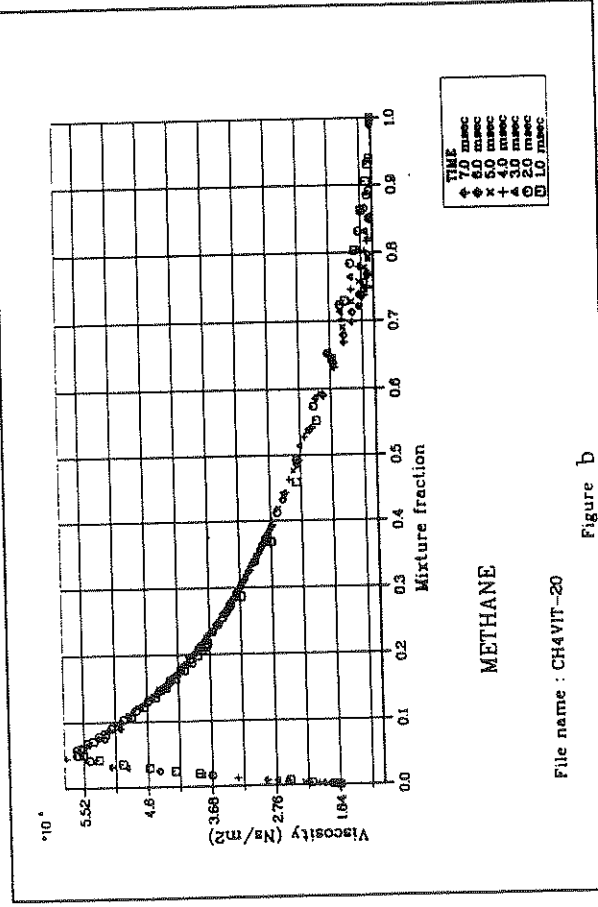
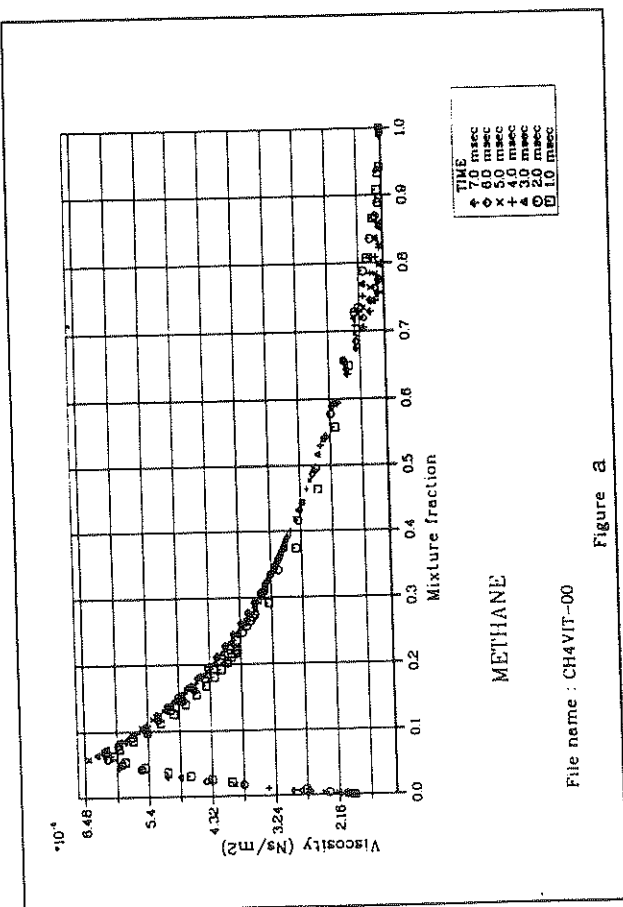
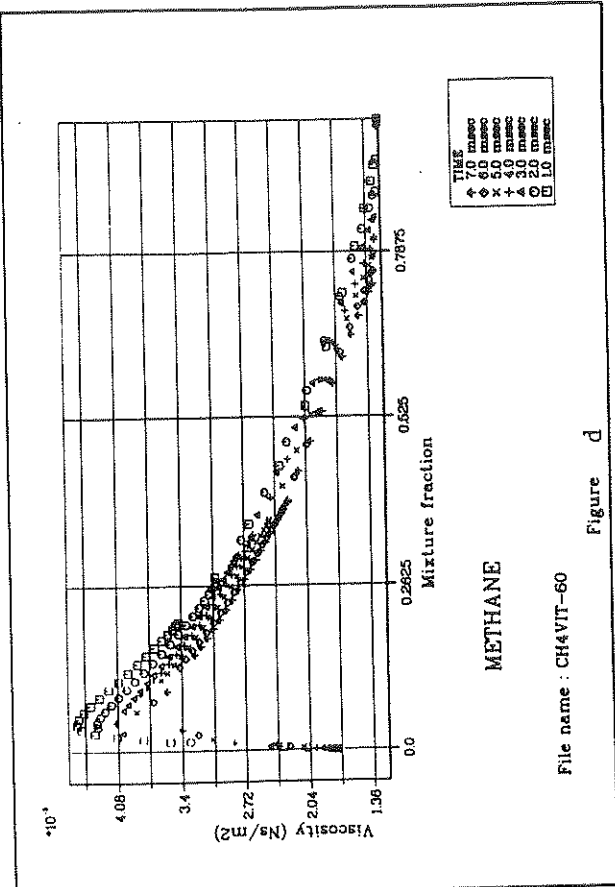
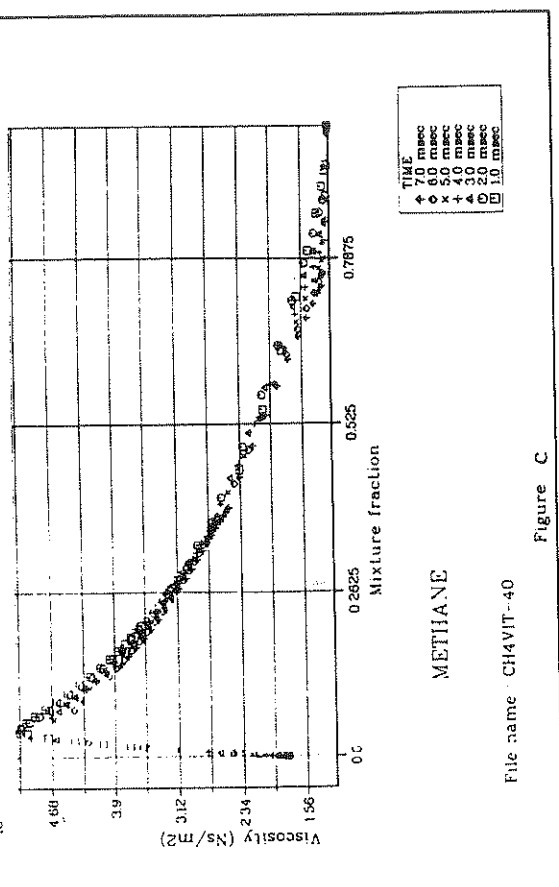


Figure E42

